University of Cagliari
University of Sassari

PhD Degree

in Chemical Science and Technology

Cycle XXXIII

PhD Thesis

# Hydroxycinnamate-based Ionic liquids as bioactive compounds: physico-chemical characterization, biological activity and NMR insights into the effects on mutated cells metabolome

**SSD**

Chim/02 (Physical-Chemistry)

**Grant funded by UNICA**

Presented by Dr. Monica Demurtas

Supervisor Prof. Flaminia Cesare Marincola
Co Supervisor Prof. Francesca Mocci

PhD Coordinator Prof. Stefano Enzo

Final exam Academic Year 2019– 2020
Thesis defence: May 2021

# Abstract

Nowadays, there is a strong collaboration between the research in drug discovery and drug delivery to improve pharmacokinetic and pharmacodynamic properties of new or use-consolidated drugs. With this purpose, several approaches have been proven to be fundamental for the developing of commercial drugs which are still in use. In this context, natural compounds such as Hydroxycinnamic acids (HCAs) are gaining increasing attention in pharmaceutical research due to their well-estabilished wide ranging benefits on health.

HCAs are a group of phenolic products of plant secondary metabolism widely studied for their numerous biological properties, such as antioxidant, anti-inflammatory, anti-microbial, anti-collagenase, and anti-melanogenic activity. These features have made HCAs very attractive compounds for medicinal and pharmaceutical applications. However, their low water solubility represents a major drawback for their incorporation in hydrophilic topical formulations and thus, the search for new formulations with enhanced water solubility is of high priority in current research.

The conversion of drugs or bioactive molecules into ionic liquids (ILs) rapresents a strategy to improve some issues related to solubility, polymorphism and bioavalibility. Indeed, by choosing an appropriate benign counterion, it is possible to obtain biocompatible and environmentally friendly ILs. In particular, ILs containing cholinium cation combined with hydroxycinnamic acid-based anion ([Cho][HCA] ILs) are promising compounds that are themselves components in active pharmaceutical ingredients (APIs) with potential applications in the formulation of pharmaceutical and cosmetic products due to the higher water solubility and antioxidant properties compared to their acidic precursors.

In the present PhD thesis, I have synthesized six new derivatives of HCAs as [Cho][HCA] ILs. Several physico-chemical and biological properties of these compounds, considered important for their potential use in the pharmaceutical field, were studied: aqueous solubility, thermal stability, anti-oxidant activity, citotoxicity. To rationalize the experimental antioxidant activities, density functional theory (DFT) calculations were performed. Furthermore, some [Cho][HCA] ILs were also tested for their activity on mushroom tyrosinase, melanine production in human MNT-1 melanome cells and their impact of the cellular metabolome. Overall, this work successfully shows that [Cho][HCA] ILs may be good candidates as an alternative to HCAs in pharmaceutical field.

# Acknowledgments

I would like to express my gratitude to my supervisors Prof. Flaminia Cesare Marincola and Professor Francesca Mocci for their support and guidance throughout this PhD work.

I would also like to thank Prof Valentina Onnis for her constant advices and the other lab groups I have worked with during the course of this PhD. In particular, thanks to Dr Joanna Lachowicz, Dr Leon de Villiers Engelbrecht, Prof Paolo Zucca, Prof Antonio Rescigno and Prof Guido Ennas for their precious collaboration.

I am grateful for the Erasmus+ programme experience which has enabled me to undertake a huge part of this project and for funding my traineeship at the University of Aveiro.
This project has been a transformative experience for me and has allowed me to look at my life in surprising and new prospectives that I would have never considered before. Thanks to Prof Iola Duarte and to Dr Luis Mendes for their fundamental contribute to my PhD work.

Thanks to my gorgeous portuguese family: Eleonora, Antonio, Renato e Giovanni, who has cared about me during my stay in Aveiro.

Thanks to my parents Barbara and Luigi for their support and love.
Many thanks to my brother Gabriele and my sister in law Alessandra for being my safe haven.
To my “besties” Fabiana and Martina who have always cheered me.

Luca, who only recently entered my life but has already taken a special place in my heart.

# CONTENT

## Abbreviations

**Ala**: Alanine
**ADA**: 4-amino-N,N-diethylaniline
**APIs**: Active Pharmaceutical Ingredients
**BCCA**: Branched-chain aminoacids
**BDE**: Bonding dissociaton enthlapy
**[$C_2$ mim][$BF_4$]**: 1-ethyl-3-methylimidazolium bromide
***o*-CA**: *orto* Coumaric Acid
***m*-CA**: *meta* Coumaric Acid
***p*-CA**: *para* Coumaric Acid
**CAFA**: Caffeic acid
**ChoCl**: Choline Cloride
**[Cho][*o*-Coum]**: Cholinium *orto* Coumarate
**[Cho][*m*-Coum]**: Cholinium *meta* Coumarate
**[Cho][*p*-Coum]**: Cholinium *para* Coumarate
**[Cho][Fer]**: Cholinium Ferulate
**[Cho][HCA]** Cholinium Hydroxycinnamate
**[Cho][$HCO_3$]:** Choline bicarbonate
**Cho-ILs**: Cholinium Ionic Liquids
**[Cho][OH]:** Choline hydroxide
**[Chol][Sal]**: Cholinium Salycilate
**[Cho][Sinapate]**: Cholinium Sinapate
**DG**:Diacilglicerol
**DFT:** Density functional theory
**DPPH**: 2,2-diphenyl-2-picrylhydrazyl hydrate
**DSC**: Differential scan calorimetry
**E-factor**: Environmental factor
**ETE**: Electron transfer enthalpy
**[$EtNH_3$] [$NO_3$]**: ethyl ammonium nitrate
**FA**: Ferulic acid
**HAT**: Hydrogen atom transfer
**HCAs**: Hydroxicinnamic Acids
**ILs**: Ionic Liquids
**Gln**: Glutamine
**Glu**: Glucose
**IP**: Ionization potential
**KA**: Kojic acid
**MI**: Myo inositol
**MT**: Mushroom Tyrosinase
**MTT**: 3-(4,5-dimethylthiazol-2-yl)-2,5-diphenyltetrazolium bromide
**PA**: Proton affinity
**PC**: Phosphocoline
**PCA**: Principal component analysis

**PCM**: Polarizable continuum model
**PCr**:Phosphocreatine
**PDE**: Proton dissociation enthalpy
**PILs:** Protic Ionic Liquids
**PLS-DA**: Partial least squares discriminant analysis**PTE**: Phosphatidilethanolamine
**PTC**: PhosphatidilCholine
**QM**: Quantum mechanics
**ROS**: Reactive oxygen species
**SA**: Sinapic acid
**SET-PT**: Sequential electron tranfer proton transfer
**SM**: Sphingomielin
**SPLET**: Single proton loss electron transfer
**Tau**: Taurine
**TBC**: 4-tert-butyl-1,2-benzoquinone
**TGA**: Thermogravimetric Analysis
**Tyr**: Tyrosine
**Val**: Valine
**VIP**: Variable importance in the Project

# 1

# History, Development and Applications of Ionic Liquids

## 1.1 Ionic Liquids

Ionic liquids (ILs) are defined generally as organic salts with melting points below 100 °C (many are liquid at ambient temperature).[1] ILs *per se* have been known for over a century. Ethyl ammonium nitrate, [$EtNH_3$] [$NO_3$], (m.p. 12 °C) was the first room temperature IL known, reported by Paul Walden in 1914.[2] Initially proposed as alternatives to the common organic solvents,[3] ILs have only recently been the subject of intense worldwide interest due to their remarkable properties, including extremely low vapor pressure, high thermal stability, wide temperature range as liquids, and tunable physicochemical characteristics.[4,5] In particular, the report of Wilkes and Zaworotko on air- and moisture-stable room-temperature liquid salts in 1992 has initiated their use in many chemistry research areas such as organic synthesis, catalysis, electrochemistry, biomass conversion, fuel production and processing, liquid crystal development, biotransformation, and biotechnology.[6]

Traditionally, ILs are classified into three generations based on their chemical structure and properties.[7] (Figure 1.1). The *first generation* includes water- and air-sensitive ILs prepared basically by combaining dialkylimidazolium and alkylpyridinium cations with chloroaluminate or other metal halide anions. This generation of ILs can only be handled under inert-gas atmosphere due to the hygroscopic nature of $AlCl_3$. The *second generation* is air- and water-stable; the most common cations include dialkylimidazolium, alkylpyridinium, ammonium, and phosphonium, whereas halides, tetrafluoroborate, and hexafluorophosphate are among the most common anions. These ILs present interesting properties such as lower melting points, different solubilities in classic organic solvents, viscosities that make the second generation of great interest in various fields. Disadvantages of these ILs are the the high cost and toxicity. The *third generation* of ILs employs biodegradable and natural ions, such as choline and aminoacids, or ions with known biological activities.[7] Furthermore, this third generation is readily available, presents lower toxicities, lower costs (similar to organic solvents), is simple to prepare and does not require purification (the purity of the starting materials determines the final purity). These ILs are subject of interest not only in chemistry, but also in biology, ecology, and pharmaceutical sciences.[6]

ILs have been investigated for an extensive range of applications and their intrinsical worth for advancing science is finding nowaday its way into a wide variety of industrial applications.[5] In this context, it is noteworthy that ILs are already used at industrial scale in companies such as BASF (Bar Association of San Francisco) or IFP (Institut Français du Pétrole). For instance, BASF has proposed ionic liquids as entrainers, or separation enhancers,[8] to break common

azeotropes such as water–ethanol and water–tetrahydrofuran[9] with a significant reduction in costs of separation and recycling of the entrainer. BASF has demonstrated also that hydrogen chloride in ionic liquids can act in chlorination reactions as a phosgene substitute.[10]

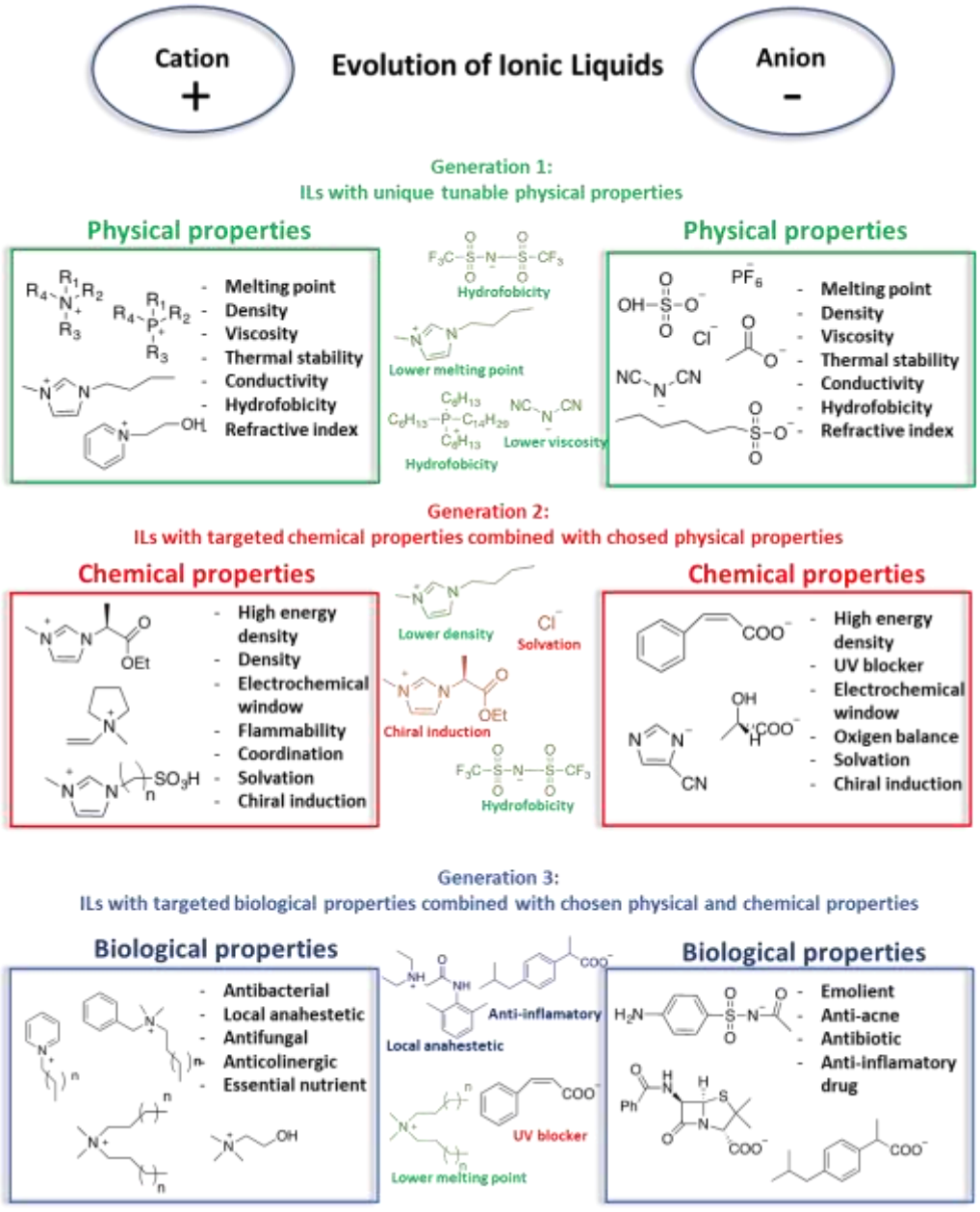


**Figure 1.1** Classification of ILs. Figure adapted from ref.7

IFP has been the first to operate an ionic liquid pilot plant. In IFP, the Nobel laureate Yves Chauvin and Helene Olivier-Bourbigou[11,12] developed and pioneered the use of chloroaluminate (III) ionic liquids as solvents for the Dimersol process wich consist in a traditional technology of the dimerisation of alkenes, typically propene (Dimersol-G) and butenes (Dimersol-X) and for

the more valuable branched hexenes and octenes.[5] This reaction can be performed as a biphasic system between -15 °C and 5 °C, as the products form a second layer that can be easily separated and the catalysts remains selectively dissolved in the ionic liquid phase. The activity of the catalyst is much higher than in both solvent-free and conventional solvent systems, and the selectivity for desirable dimers is enhanced. This process has been patented as the Difasol process and is described in Chauvin's Nobel lecture.[13]

Like BASF, the chemical company Degussa is pursuing ILs in many different directions, such as additives to a new range of paints, for improved finish, appearance and drying properties.[14] The range is marketed under the name TEGO1 Dispers, and added to the Pliolite1 paint range.[15] By using these ionic liquids as secondary dispersing agents, universal, water-based pigment pastes can be used for all types of paints and coatings. This will allow a reduction in the use of volatile organic substances in paints and coatings in the future.

## 1.2 Green aspects of ionic liquids

Due to the increase of environmental consciousness in chemical research and industry, the challenge for a sustainable environment calls for clean procedures that avoid the use of harmful organic solvents. One of the most important principles of the *Green Chemistry* is the elimination of hazardous solvents in chemical synthesis and reduction or prevention of pollution at the laboratory and industrial scales.[2] It also deeply supports the development of economical and eco-friendly techniques that not only make the process more efficient , but decrease also the generation of waste.[16]

ILs are often addressed as green solvents due to their negligible volatility and non-flammability. These properties make ILs safer and environmentally more benign solvents than conventional volatile organic compounds (VOCs). Nevertheless, the assessment of how green a solvent is, requires the consideration of various factors, such as environmental impact arising from the industrial production, recycling and disposal processes, as well as EHS (environmental, health and safety) characteristics. More rigorously, the term 'green' should be used for an IL if all twelve principles of green chemistry apply,[17] formalised and extensively promoted since the 1990s by Prof. Paul Anastas (Figure 1.2).

Assessing the greenness of ILs is mainly based on the atom economy[18] and environmental factor (E-factor).[19] The atom economy is defined as the ratio between the mass of the atoms making up the final product(s) and the mass of the atoms that are incorporated in all the reagents. It is reported as a percentage value whereas those values closest to 100% reflecting superior

atom economies.[20] The E-factor term has been introduced to assess the greenness of ILs. The process is considered truly green, and E-factor is zero or close to zero, if all materials used (and not just the reagents) are contained in the final product.[20]

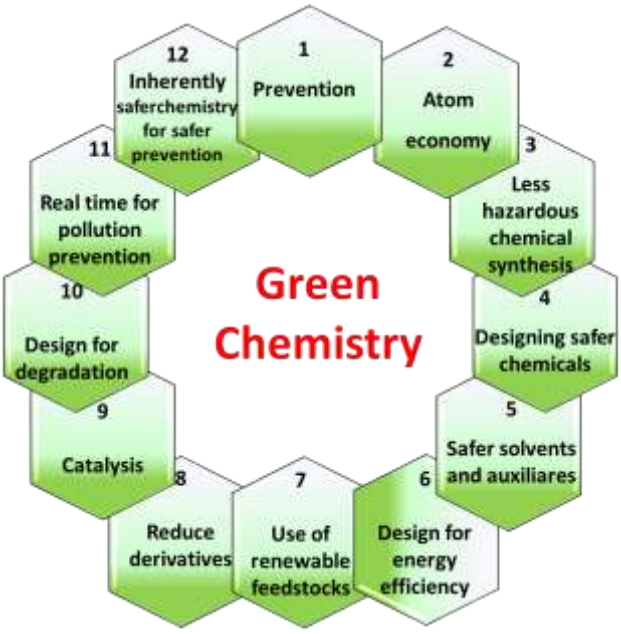


**Figure 1.2.** The Twelve Principles of Green Chemistry

Energy utilization and purification are a couple of research topics that need to be considered for improvement of the E-factor. To promote the greenness in terms of energy efficiency, methods such as microwave irradiation[21,22] and ultrasound-assisted reactions[23] are reasonable choices for ILs synthesis. Microwave irradiation method requires low energy, promotes faster reactions rates, induces higher selectivity of desire product, and requires smaller quantities of reagents compared to traditional conductive heating procedure. Whenever possible, performing the solvent-free synthesis of ILs generates less harmful waste and is easier to dispose of.[20] Other "greener approaches" in ILs synthesis might include using benign solvents,[24] solvent recovery,[25] or the creation of safer chemical products such as biobased derived ILs.[26,27] It is important to note that although many ILs have various industrial and commercial applications, the environmental fate and any potential toxicity issues for most of them are yet to be fully understood. One of the problems concernes their water solubility. Indeed, even though the ILs cannot contribute to the air pollution, being non-volatile, the water solubility of many ILs is not negligible. The potential release of ILs into aquatic and terrestrial environment may lead to water and soil pollution, and related risks. In particular, some ILs have been proven to be even more toxic for aquatic organisms than the classical organic solvents that they are aiming to replace. Although some experimental evidences have pointed out systematic trends of ILs ecotoxicity, the

nature of this ecotoxicity is not totally understood. For example, it is widely accepted that the cation is the main driver of toxicity.[28,29,30] ILs containing quaternary ammonium and alicyclic cations (morpholium, piperidinium and pyrroliudinium) generally display much lower toxicity than those derived from imidazolium and pyridinium with long side chain substituents.[31] Furthermore, ILs with longer cation alkyl side chains tend to be more ecotoxic until a certain threshold. Also the anion is known to contribute to the overall toxicity,[32] but its effect is usually neglected.

However, as the study of ILs became more widespread and the characterization of their green nature grew, the constant synthesis of new ILs offers an opportunity for the design of ILs with less and less toxic and more biodegradable ions which can comply the most demanding technical requisites.[33]A good example of this is the new familiy of ILs based on cholinium cation.

## 1.3 Cholinium-based Ionic Liquids

Choline (common name for 2-hydroxyethyltrimethyl ammonium) is a biologically widespread molecule that occurs in human and animals as a cation that forms various quaternary ammonium salts and is always associated with undefined counteranion (chloride, hydroxide, tartrate).[34] Choline was first isolated by Adolph Strecker from bile in 1862[35] and in 1865 it was synthesized in form of chloride salt (ChoCl) by Oscar Liebreich through a simple and efficient gas phase reaction between ethylene oxide, trimethylamine, and HCl.[34] ChoCl is one of the most important, biodegradable, inexpensive and water-soluble organic salt.

In human body, choline serves as a precursor molecule for the neurotransmitter acetylcholine, which is involved in many functions including memory and muscle control. The choline cation is a constituent of cell membranes being the head groups of two classes of phospholipid: phosphatidylcholine and sphingomyelin.[36] Due to its importance for many physiological processes, in 1998 it was added as essential nutrient to the list of human vitamins by the National Academy of Sciences (NAS)[37] and it is commercialized in form of ChoCl as an ingredient in common food supplements.[38]

The use of cholinium as the cationic moiety in the structure of ILs has attracted interest throughout the scientific community as an effective approach towards the development of bio-based ILs composed of ions derived from natural sources. Cholinium-based ILs (Cho-ILs) can be generated by anion exchange with environmentally friendly materials such as commercially available choline chloride or choline hydroxide and selecting suitable anion species (alkylcarboxylates, aminoacids and organic acids-derived anions).[39] The improved

biodegradability and toxic character compared to other common ILs (for instance, pyridinium and imidazolium-based ILs),[40] has encouraged the scientific and industrial communities to expand and intensify the use of Cho-ILs in a broader range of fields such as the development of bio-based IL composites with catalycit ability,[34] the conversion of biomass into valuable chemicals and fuels,[41] polimerization and gas absorption processes.[34]

The green nature of this third evolution of ILs has aroused great interest for Cho-ILs also in pharmaceutical research. Indeed, the tunable chemical and physical properties of Cho-ILs used in drug formulations both as a solvent and components in active pharmaceutical ingredients (APIs)[6] offers multiple opportunities to improve the solubility and permability of poorly water-soluble drugs,[42,43] both decisive for the druggability and bioavailability of a drug substance. In particular, the use of API-ILs has emerged as an excellent tool to help solving problems related not only to the solubility, but also to the polymorphism, delivery, release rates, handling, therapeutic efficacy, and adverse reactions during administration.[44,45] It is worth mentioning the pioneering conversion of salicylic acid into choline salicylate ([Chol][Sal])[46] that allowed a better dissolution rate and enhanced absorption by the gastrointestinal tract whereas the anti-inflammatory, antipyretic, and analgesic effects of salicylic acid were maintened.[47] Choline salicylate is already marketed as a drug against mouth ulcer and a pain-relieving agent in teething children under the brand name Bonjelas and Bucagel.[48] Since then, an increasing number of cholinium salts has been reported coupled with a wide range of anions with anti-inflammatory,[49] antimicrobials, antibacterial[27,7] and antioxidant activities.[48]

## 1.4 Hydroxycinnamic acid-based ILs as suitable bioactive compounds

Hydroxycinnamic acids (HCAs) and their derivatives are a group of phenolic products of plant secondary metabolism. They all originate from phenylalanine and tyrosine and are present in nature as six molecules: ferulic acid, sinapic acid, caffeic acid, *o*-coumaric, *m*-coumaric, and *p*-coumaric acid [50-52] (Figure 1.3).

HCAs have been intensively studied for their numerous biological properties, such as antioxidant, anti-inflammatory, anti-microbial, anti-collagenase, and anti-melanogenic activity.[51,52] The beneficial effects displayed by these compounds have been mainly attributed to the presence of multiple hydroxyl groups and an extended pattern of conjugated double bonds between the phenolic moiety and the carboxylic group.[53] Due to their ability in scavenge free radicals and in pro-oxidating metals, several studies have attributed a remarkable role of

these compounds in the prevention of various diseases associated with oxidative stress, such as cardiovascular disease, cancer and other chronic diseases.[54]

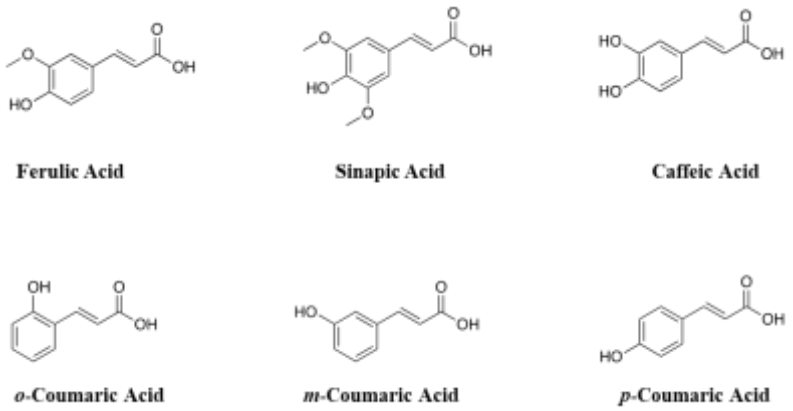


**Figure 1.3** Chemical structure of the six natural hydroxycinnamic acids.

*p*-Coumaric acid (4-hydroxycinnamic acid, *p*-CA) is a phenolic acid synthesized mainly from tyrosine and phenylalanine. It is a major precursor in the synthesis of other phenolic acids and is classified as a nutraceutical and phytochemical agent.[50] It is widely distributed in fruits (e.g. apples, pears, grapes, oranges, tomatoes and berries), vegetables (e.g. beans, potatoes and onions) and cereals (e.g. maize, oats and wheat, particularly in the cell walls of Graminea family members).[55] Extensive investigations have shown that *p*-CA exhibits a huge bioactivity range including antioxidant, anti-inflammatory, antimutagenic, anti-ulcer, antiplatelet, and anti-cancer activities. In addition, it is reported as preventive agent for stomach cancer by reducing the formation of carcinogenic nitrosamines, for diabetes and for mitigating oxidative cardiac damage.[56]

Caffeic acid (3,4-dihydroxycinnamic acid, CAFA) is one of the most common hydroxycinnamics present in wine.[57] As a key precursor for lignin formation, CAFA is widely found in plants. It is biosynthesized mainly from tyrosine through a two-step pathway in which tyrosine is converted to *p*-CA and then to CAFA by tyrosine ammonia lyase and 4-coumarate 3-hydroxylase.[58] CAFA is an intriguing compound because it possesses various pharmacological activities, including antioxidant,[51] antitumor,[59] antiviral,[60] antidepressive,[61] antidiabetic activities,[62] and has been shown to be a α-tocopherol protectant in low-density lipoprotein (LDL).[63]

Ferulic acid (3-methoxy-4-hydroxycinnamic acid, FA), is a ubiquitous plant constituent. As well as to the other HCAs, it arises from the plant metabolism of phenylalanine and tyrosine. It occurs primarily in seeds and leaves both in its free form and covalently linked to

lignin and other biopolymers.[64] FA has therapeutic effects on many diseases, such as cardiovascular disease, cancer, Alzheimer's disease, diabetes mellitus and skin disease.[65] By virtue of its properties, FA has been encapsulated into nanoplatforms or other formulations. For instance, FA and gallic acid have been coencapsulated into hydroxypropyl-β-cyclodextrin for antioxidant application or encapsulated into electrospun nanofibers to observe the effects against HepG2 cells.[66] Being an effective scavenger of free radicals, FA has been approved in certain countries as food additive to prevent lipid peroxidation[67] and for its strong capability in UV absorbtion[64] is currently employed as photoprotective ingredient in many skin lotions and sunscreens.[68]

Sinapic acid (3,5-dimethoxy-4-hydroxycinnamic acid, SA) is a frequent phytochemical compound in the human diet and is widespread in the plant kingdom. Although SA has not received as much attention from the scientific community as other HCAs such as CAFA or FA, its antioxidant effectiveness is considered superior to that of FA and comparable to that of CAFA. Indeed, as CAFA and FA, some studies suggested that SA could be considered for potential uses as preservatives in foods, cosmetics, and in the pharmaceutical industry.[69] The biological effects of SA comprehend antimicrobial,[70] anti-inflammatory,[71] anticancer,[72] and anti-anxiety activities.[71] Moreover, it is reported that SA is the most efficient among *p*-hydroxycinnamic acids in terms of absorbance[73] and recent studies on some sinapic acid esters has highlighted their great potential as UV filters.[74]

The attractive features of HCAs have made them very popular as ingredients also in cosmetic and pharmaceutical development[75] due to their interaction with several biochemical processes in the skin, namely antioxidant augmentation, UV filtering, melanin inhibition, promotion of collagen synthesis, suppression of collagenase, photoprotection and anti-elastase activity. The human skin is constantly exposed to both endogenous and environmental pro-oxidant agents. Reactive oxygen (ROS) and nitrogen (NOS) species produced by metabolism of the substances are responsible of oxidative damage comprising DNA modification, lipid peroxidation, as well as the activation of inflammatory pathways.[76] ROS can be also generated by UVB and UVA radiations producing protein oxidative modification and thus skin photoaging.[77] To minimize these deleterious effects, mammalian skin cells are equipped with antioxidant defense mechanisms, which comprise enzymatic and non-enzymatic antioxidant agents.[78] Nevertheless, these systems may not be enough to preserve the skin barrier integrity.[79] For this reason, the research in this field is focused to the search for natural antioxidants, such as HCAs, to serve as an exogenous source to compensate the high level of free radical generation in the body.

Despite the benefic activities attributed to HCAs, their low water solubility represents a major drawback for their incorporation in hydrophilic topical formulations[52,80] and thus, the search of new formulation to enhance water solubility is one of the priority in current pharmaceutical research. Recently, some ILs containing cholinium cation combined with phenolic acid-based anion have been proposed as promising compounds that are themselves APIs with potential applications in the formulation of pharmaceutical and cosmetic products due to the higher water solubility and antioxidant properties compared to their acidic precursors.[48] Moreover, the coupling to the cholinium cation has been also proposed as a source of essential nutrients within the vitamin B complex. These features are certainly a great advantage afforded by these salts making them suitable to be incorporated into more formulations and for a widespread range of applications for which their high water solubility is relevant.

## 1.5 Aim and Outline of this thesis

The present PhD thesis was focused on the development of new cholinium-based ILs using hydroxycinnamates as anions [Cho][HCA] ILs in the final goal to obtain compounds with improved physico-chemical and biological properties compared to the parent acids (i.e. HCA).
The main body of the experimental part of the thesis is structured into four chapters.

- Chapter 2 reports the synthesis and physicochemical characterizzation of six [Cho][HCA] ILs derived from CAFA, FA, SA, *o*-CA, *m*-CA and *p*-CA, respectively. By using a very easy synthetic procedure, all compounds were obtained in quantitative yields. The structure and purity of ILs was confirmed by $^{1}H$ and $^{13}C$ NMR, IR spectroscopy and elemental analysis. Their solubility and themal stability were evaluated and compared with those of their parent acids.
- Chapter 3 describes the antioxidant activity of [Cho][HCA] ILs evaluated by the combined use of experimental and computational approaches. To rationalize the antioxidant activities observed with 2,2-diphenyl-1-picrylhydrazyl (DPPH) assay, density functional theory (DFT) calculations were performed. The theoretical approach allowed for identification of the most likely radical scavenging mechanisms involving HCAs and the corresponding ionic forms under the studied experimental conditions and to rationalize the observed activity differences between salts and acids.
- Chapther 4 contains the evaluation of biological activity of the [Cho][HCA] ILs prepared from CA, FA and *p*-CA. Compounds were tested for their effects on mushroom tyrosinase and for their cytotoxicity on human MNT-1 melanoma cell lines. In order to gain insights

into their tyrosinase activity, a test on melanin production was also performed on the same cell line.

- Chapter 5 is dedicated to cell metabolomics experiments. The effect of the [Cho][HCA]ILs prepared from CAFA, FA, and *p*-CA on the metabolome of human MNT-1 melanoma cells was investigated by $^{1}$H NMR spectroscopy with the aim of exploring, at the molecular level, the impact of exposure to these compounds on cell metabolism.

## References


1. Sun, P. and Armstrong, D. W. (2010). Ionic liquids in analytical chemistry. Analitica Chimica Acta, **661**, 1–16.
2. Singh, S. K. and Savoy, A. W. (2020). Ionic liquids synthesis and applications: An overview. Journal of Molecular Liquids, **297**, 112038.
3. Welton, T. (1999). Room-Temperature Ionic Liquids. Solvents for Synthesis and Catalysis. Chemical Review, **99**, 2071–2083.
4. Pandey, S. (2006). Analytical applications of room-temperature ionic liquids: A review of recent efforts. Analitica Chimica Acta, **556**, 38–45.
5. Plechkova, N. V. and Seddon, K. R. Applications of ionic liquids in the chemical industry. Chemical Society Review, **37**, 123–150 (2008).
6. Egorova, K. S., Gordeev, E. G. and Ananikov, V. P. (2017). Biological Activity of Ionic Liquids and Their Application in Pharmaceutics and Medicine. Chemical Review, **117**, 7132–7189.
7. Hough, W. L., Smiglak, M., Rodríguez, H., Swatloski, R. P., Spear, S. K., Daly, D. T. and Rogers, R. D. (2007). The third evolution of ionic liquids: active pharmaceutical ingredients. New Journal of Chemistry, **31**, 1429.
8. Y. Beste, M. E. and H. S. (2004). Einsatz ionischer Flüssigkeiten zur Entschwefelung von Produktströmen bei der Erdölverarbeitung Alternative Lösungsmittel Ionische Flüssigkeiten als Entrainer in der Extraktivdestillation. Chemie Ingeniur Technik, 67056
9. W. Arlt, M. Seiler, C. Jork, T. Scheiner. (2002). Ionic Liquids as Selective Additives fort he Separation of Close-Boiling or Azeotropic Mixtures, Patent: PCT Int. Appl. WO 0274718 A2.
10. Stegmann V, Massonne K. (2005). Method for producing haloalkanes from alcohols. World Patent no. WO 2005026089, Canadian Patent no. CAN 142:338152.
11. Olivier-Bourbigou H., Hugues F. (2003) Applications of Ionic Liquids to Biphasic

Catalysis. In: Rogers R.D., Seddon K.R., Volkov S. (eds) Green Industrial Applications of Ionic Liquids. NATO Science Series (Series II: Mathematics, Physics and Chemistry), vol 92.

12. Breuil, PA.R., Magna, L. and Olivier-Bourbigou, H. (2015). Role of Homogeneous Catalysis in Oligomerization of Olefins : Focus on Selected Examples Based on Group 4 to Group 10 Transition Metal Complexes. Catalysis Letters. **145**, 173–192.
13. Chauvin, Y. (2006). Nobel Lectures Olefin Metathesis : The Early Days ( Nobel Lecture ). 3740–3747.
14. Weyershausen, B. and Lehmann, K. (2007). Industrial application of ionic liquids as performance additives. Green Chemistry, **7**, 15–19.
15. A. Hoff, C. Jost, A. Prodi-Schwab, F. G. Schmidt and B. Weyershausen. (2004). Ionic Liquids: New designer compounds for more efficient chemistry, Elements: Degussa Science Newsletter, 10–15
16. Vert, M., Doi, Y., Hellwich, K., Hess, M., Hodge, P., Kubisa, P., Rinaudo, M., & Schué, F. (2012). Terminology for biorelated polymers and applications (IUPAC Recommendations 2012), Pure and Applied Chemistry, 84(2), 377-410.
17. Anastas, P. and Eghbali, N. (2010). Green Chemistry: Principles and Practice. Chemical Society Review **39**, 301–312.
18. Trost, B. (1991). The atom economy: a search for synthetic efficiency. Science, **254** (5037), 1471–1477.
19. Sheldon, R. A. (2007).The E Factor: Fifteen years on. Green Chemistry **9**, 1273–1283
20. Deetlefs, M. and Seddon, K. R. (2010). Assessing the greenness of some typical laboratory ionic liquid preparations. Green Chemistry, **12**, 17–30.
21. Hoffmann, J., Nüchter, M., Ondruschka, B. and Wasserscheid, P. (2003). Ionic liquids and their heating behaviour during microwave irradiation - A state of the art report and challenge to assessment. Green Chemistry, **5**, 296–299
22. Wang, Z. (2008). Green Chemistry: Recent Advances in Developing Catalytic Processes in Environmentally-Benign Solvent Systems.http://ccc.chem.pitt.edu/wipf/frontiers/zhiyong.pdf
23. Ameta, G., Pathak, A. K., Ameta, C., Ameta, R. and Punjabi, P. B. (2015).Sonochemical synthesis and characterization of imidazolium based ionic liquids: A green pathway. Journal of Molecular Liquids, **211**, 934–937.
24. Horváth, I. T. (2008).Solvents from nature. Green Chemistry **10**, 1024–1028
25. Kim, J. F., Székely, G., Valtcheva, I. B. and Livingston, A. G. (2014). Increasing the

sustainability of membrane processes through cascade approach and solvent recovery - Pharmaceutical purification case study. Green Chemistry **16**, 133–145.

26. Petkovic, M., Ferguson, J. L., Gunaratne, H. Q. N., Ferreira, R., Leitão, M. C., Seddon, K. R., Rebelo, L.P.N. and Pereira, C. S. (2010). Novel biocompatible cholinium-based ionic liquids—toxicity and biodegradability. Green Chemistry, **12**, 643.
27. Hough-Troutman, W. L., Smiglak, M., Griffin, S., Matthew Reichert, W., Mirska, I., Jodynis-Liebert, J., Adamska, T., Nawrot, J., Stasiewicz, M., Rogers, Robin D. and Pernak, J. (2009). Ionic liquids with dual biological function: sweet and anti-microbial, hydrophobic quaternary ammonium-based salts. New Journal of Chemistry, **33**, 26–33.
28. Ventura, Sónia P.M.; de Barros, Rafael L.F.; Sintra, Tânia; Soares, Cleide M.F.; Lima, Álvaro S. and Coutinho, João A.P. (2012). Simple screening method to identify toxic/non-toxic ionic liquids: Agar diffusion test adaptation. Ecotoxicology and Environmental Safety, **83**, 55–62.
29. Couling, D. J., Bernot, R. J., Docherty, K. M., Dixon, J. N. K. and Maginn, E. J. (2006). Assessing the factors responsible for ionic liquid toxicity to aquatic organisms via quantitative structure–property relationship modeling. Green Chemistry **8**, 82–90.
30. Ranke, J., Mölter, K., Stock, F., Bottin-Weber, U., Poczobutt, J., Hoffmann, J., Ondruschka, B., Filser, J. and Jastorff, B. (2004). Biological effects of imidazolium ionic liquids with varying chain lengths in acute Vibrio fischeri and WST-1 cell viability assays. Ecotoxicology and Environmental Safety, **58**, 396–404.
31. Petkovic, M., Seddon, K. R., Rebelo, L. P. N. and Pereira, C. S. (2011). Ionic liquids: A pathway to environmental acceptability. Chemical Society Review, **40**, 1383–1403.
32. Stolte, S., Arning, J., Bottin-Weber, U., Matzke, M., Stock, F., Thiele, K., Uerdingen, M., Welz-Biermann, U., Jastorff, B. and Ranke, J. (2006). Anion effects on the cytotoxicity of ionic liquids. Green Chemistry, **8**, 621.
33. Smiglak, M., Pringle, J. M., Lu, X., Han, L., Zhang, S., Gao, H. MacFarlane, D.R. and Rogers, R. D. (2014). Ionic liquids for energy, materials, and medicine. Chem. Commun., 50(66), 9228–9250.
34. Gadilohar, B. L. and Shankarling, G. S. (2017). Choline based ionic liquids and their applications in organic transformation. Journal of Molecular Liquids, **227**, 234–261.
35. Zeisel, S. H. (2012). A Brief History of Choline. Annals of Nutrition and Metabolism, 254–258.
36. Blusztajn, J. K. (1998). Choline, a vital amine. Science, **281**, 794–795
37. Zeisel, S. H. and Da Costa, K. A. (2009). Choline: An essential nutrient for public health.

Nutrition Review, **67**, 615–623

38. Zeisel, S. H., Klatt, K. C. and Caudill, M. A. (2018). Choline. Advances in Nutrition, **9**, 58–60.
39. Rengstl, D., Fischer, V. and Kunz, W. (2014). Low-melting mixtures based on choline ionic liquids. Physical Chemistry Chemical Physics, **16**, 22815–22822.
40. Ventura, S. P. M., e Silva, F. A., Gonçalves, A. M. M., Pereira, J. L., Gonçalves, F., and Coutinho, J. A. P. (2014). Ecotoxicity analysis of cholinium-based ionic liquids to Vibrio fischeri marine bacteria. Ecotoxicology and Environmental Safety, 102, 48–54.
41. Zhang, Z., Song, J. and Han, B. (2017). Catalytic Transformation of Lignocellulose into Chemicals and Fuel Products in Ionic Liquids. Chemical Reviews, **117**, 6834–6880.
42. Caldwell, G. W., Ritchie, D. M., Masucci, J. A., Hageman, W. and Yan, Z. (2001). The New Pre-Preclinical Paradigm : Compound Optimization in Early and Late Phase Drug Discovery. Current Topics in Medicinal Chemistry, 353–366
43. Hartmann, T., Schmitt, J., Rohring, C., Nimptsch, D., Noller, J., Mohr, C., (2006). ADME Related Profiling in 96 and 384 Well Plate Format - A Novel and Robust HT-Assay for the Determination of Lipophilicity and Serum Albumin Binding. Current Drug Delivery, 3(2), 181–192.
44. Araújo, João M. M.; Florindo, Catarina; Pereiro, Ana B.; Vieira, Nicole S. M.; Matias, Ana A.; Duarte, Catarina M. M.; Rebelo, Luís P. N and Marrucho, Isabel M. (2014). Cholinium-based ionic liquids with pharmaceutically active anions. RSC Advances, 4(53), 28126
45. Ferraz, R., Branco, Luís C., Marrucho, Isabel M., Araújo, João M. M., Rebelo, Luis Paulo N., da Ponte, Manuel N., Prudêncio, C., Noronha, João. and Petrovski, Ž. (2012). Development of novel ionic liquids based on ampicillin. Medicinal Chemistry Communication, 3(4), 494
46. Sasmor, R. H. B.-K. J. (1957). United States Patent Office 3,069,32. **52**, 415–417.
47. Bica, K., Rijksen, C., Nieuwenhuyzen, M. and Rogers, Robin D. (2010). In search of pure liquid salt forms of aspirin: ionic liquid approaches with acetylsalicylic acid and salicylic acid. Physical Chemistry Chemical Physics, 12(8), 2011.
48. Sintra, T., Luís, A., Rocha, S., Lobo Ferreira, A. I. M. C., Gonçalves, F., Santos, L. M. N. B. F., Neves, B. M., Freire, M. G., Ventura, S. P.M. and Coutinho, J. A.P. (2015). Enhancing the antioxidant characteristics of phenolic acids by their conversion into cholinium salts. ACS Sustainable Chemistry & Engineering, **3**, 2558–2565.
49. Santos, Miguel M.; Raposo, Luís R.; Costa, Alexandra; Dionísio, Madalena; Baptista,

Pedro V.; Fernandes, Alexandra R.; Branco, Luis C. (2019). Ionic Liquids and salts from Ibuprofen as promising innovative formulations of an old drug. ChemMedChem, **14**, 907-911.

50. El-Seedi, Hesham R.; El-Said, Asmaa M. A.; Khalifa, Shaden A. M.; Göransson, Ulf; Bohlin, Lars; Borg-Karlson, Anna-Karin; Verpoorte, Rob (2012). Biosynthesis, Natural Sources, Dietary Intake, Pharmacokinetic Properties, and Biological Activities of Hydroxycinnamic Acids. Journal of Agricultural and Food Chemistry, **60**, 10877–10895.
51. Maurya, D. K., Paul, T. and Devasagayam, A. (2010). Antioxidant and prooxidant nature of hydroxycinnamic acid derivatives ferulic and caffeic acids. Food and Chemical Toxicology, **48**, 3369–3373.
52. Taofiq, O., González-Paramás, A. M., Barreiro, M. F., Ferreira, I. C. F. R. and McPhee, D. J. (2017). Hydroxycinnamic acids and their derivatives: Cosmeceutical significance, challenges and future perspectives, a review. Molecules, **22**,
53. Bendary, E., Francis, R. R., Ali, H. M. G., Sarwat, M. I. and Hady, S. El. (2013). Antioxidant and structure – activity relationships ( SARs ) of some phenolic and anilines compounds. Annals of Agriculture Science, **58**, 173–181
54. Rocha, L. D., Monteiro, M. C. & Teodoro, A. J. (2012). Anticancer Properties of Hydroxycinnamic Acids -A Review. Cancer and Clinical Oncology, **1**, 109–121.
55. Pei, K., Ou, J., Huang, J. and Ou, S. (2016). p-Coumaric acid and its conjugates: Dietary sources, pharmacokinetic properties and biological activities. Journal of the Science and Food Agriculture, **96**, 2952–2962.
56. Pragasam, S. J., Venkatesan, V. and Rasool, M. (2013). Immunomodulatory and anti-inflammatory effect of p-coumaric acid, a common dietary polyphenol on experimental inflammation in rats. Inflammation **36**, 169–176.
57. Gülçin, I. (2006). Antioxidant activity of caffeic acid (3,4-dihydroxycinnamic acid). Toxicology, **217**, 213–220
58. Zhang, H. and Stephanopoulos, G. (2013). Engineering E. coli for caffeic acid biosynthesis from renewable sugars. Applied Microbiology and Biotechnology, **97**, 3333–3341.
59. Rajendra Prasad, N., Karthikeyan, A., Karthikeyan, S. and Venkata Reddy, B. (2011). Inhibitory effect of caffeic acid on cancer cell proliferation by oxidative mechanism in human HT-1080 fibrosarcoma cell line. Molecular and Cellular Biochemistry, **349**, 11–19.
60. Ikeda, K., Tsujimoto, K., Uozaki, M., Nishide, M., Suzuki, Y., Koyama, A.H., and Yamasaki, H. (2011). Inhibition of multiplication of herpes simplex virus by caffeic acid .

International Journal of Molecular Medicine, **28**, 595-598.

61. Takeda, H., Tsuji, M., Miyamoto, J., Masuya, J., Iimori, M. and Matsumiya, T. (2003). Caffeic acid produces antidepressive- and/or anxiolytic-like effects through indirect modulation of the α1A-adrenoceptor system in mice. NeuroReport, **14**, 1067–1070.
62. Celik, S., Erdogan, S. and Tuzcu, M. (2009). Caffeic acid phenethyl ester (CAPE) exhibits significant potential as an antidiabetic and liver-protective agent in streptozotocin-induced diabetic rats. Pharmacological Research, **60**, 270–276.
63. Laranjinha, J., Vieira, O., Madeira, V. and Almeida, L. (1995). Two related phenolic antioxidants with opposite effects on vitamin E content in low density lipoproteins oxidized by ferrylmyoglobin: Consumption vs regeneration. Archive of Biochemistry and Biophysics, **323**, 373–381.
64. Graf, E. (2012). Antioxidant potential of ferulic acid. Free Radical and Biology and Medicine, **13**, 19–2
65. Ghosh, S., Basak, P., Dutta, S., Chowdhury, S. and Sil, P. C. (2017). New insights into the ameliorative effects of ferulic acid in pathophysiological conditions. Food and Chemical Toxicology, **103**, 41–55
66. Zheng, Y., You, X., Guan, S., Huang, J., Wang, L., Zhang, J. and Wu, J. (2019). Poly(Ferulic Acid) with an Anticancer Effect as a Drug Nanocarrier for Enhanced Colon Cancer Therapy. Advanced Functional Materials, 1808646.
67. Srinivasan, M., Sudheer, A. R. and Menon, V. P. (2007). Ferulic acid: Therapeutic potential through its antioxidant property. Journal of Clinic Biochemichal Nutrition, **40**, 92–100.
68. Saija, A., Tomaino, A., Cascio, Rossella Lo; Trombetta, Domenico; Proteggente, Anna; De Pasquale, Anna; Uccella, Nicola; Bonina, Francesco (1999). Ferulic and caffeic acids as potential protective agents against photooxidative skin damage. Journal of the Science of Food and Agriculture, **79**, 476–480.
69. Nićiforović, N. and Abramovič, H. (2014). Sinapic Acid and Its Derivatives : Natural Sources and Bioactivity. Comprehensive Review in Food Science and Food Safety, **13**, 34–51.
70. Barber, M. S., Mcconnell, V. S. and Decaux, B. S. (2000). Antimicrobial intermediates of the general phenylpropanoid and lignin specific pathways. Phytochemistry **54**, 54–57.
71. Yun KJ., Koh DJ., Kim SH., Park SJ., Ryu JH., Kim DG., Lee JY. and L. K. (2008). Anti-Inflammatory Effects of Sinapic Acid through the Suppression of Inducible Nitric Oxide Synthase , Cyclooxygenase-2 , and Proinflammatory Cytokines Expressions via Nuclear

Factor- K B Inactivation. Journal of Agricultural and Food Chemistry, **56**, 10265–10272.

72. Hudson, E. A., Dinh, P. A., Kokubun, T., Simmonds, M. S. J. and Gescher, A. (2000). Characterization of Potentially Chemopreventive Phenols in Extracts of Brown Rice That Inhibit the Growth of Human Breast and Colon Cancer Cells 1. Cancer Epidemiology and Biomarkers Prevention, **9**, 1163–1170
73. Peyrot, C., Mention, M. M. and Brunissen, Fanny and Allais, F. Sinapic Acid Esters : Octinoxate Substitutes Combining Suitable UV Protection and Antioxidant Activity. Antioxidants, **9**, 782 (2020).
74. Mention, M. M., Flourat, A. L., Peyrot, C. and Allais, F. (2020). Biomimetic regioselective and high-yielding Cu(I)-catalyzed dimerization of sinapate esters in green solvent Cyrene™. Green Chemistry, 2077–2085.
75. Taofiq, O., González-Paramás, A. M., Barreiro, M. F., Ferreira, I. C. F. R. and McPhee, D. J. (2017). Hydroxycinnamic acids and their derivatives: Cosmeceutical significance, challenges and future perspectives, a review. Molecules, **22**, 281.
76. Nathan, C. and Cunningham-bussel, A. (2013). Beyond oxidative stress : an immunologist ' s guide to reactive oxygen species. Nature Reviews Immunology, **13**, 349–361.
77. Baldisserotto, A., Demurtas, M., Lampronti, I., Moi, Davide., Balboni, G.,Vertuani, S., Manfredini, S., and Onnis, V. (2018). Benzofuran hydrazones as potential scaffold in the development of multifunctional drugs: Synthesis and evaluation of antioxidant, photoprotective and antiproliferative activity. European Journal of Medicinal Chemistry, **156**, 188-125.
78. Kovacic, P. and Somanathan, R. (2010). Dermal Toxicity and Environmental Contamination : Electron Transfer , Reactive Oxygen Species , Oxidative Stress , Cell Signaling , and Protection by Antioxidants. Reviews of Environmental Contamination and Toxicology, **23**, 119–138.
79. Briganti, S. and Picardo, M. (2003), Antioxidant activity, lipid peroxidation and skin diseases. What's new. Journal of the European Academy of Dermatology and Venereology, **17**, 663-669.
80. Mukherjee, P. K., Maity, N., Nema, N. K. and Sarkar, B. K. (2011). Bioactive compounds from natural resources against skin aging. Phytomedicine, **19**, 64–73.

# 2

# Synthesis and Physico-Chemical Characterization of Cholinium Hydroxycinnamate-based Ionic Liquids

## 2.1 Solubility and thermal stability of [Cho][HCA]ILs

Pharmaceutical industries face a series of challenges in the delivery of drug molecules concerning their bioavailability, stability and polymorphic conversion. These features are further exacerbated when drug molecules are insoluble or sparingly soluble in water and most pharmaceutically accepted organic solvents. Solubility is indeed the most important physical characteristic of a drug for its formulation, oral bioavailability, and therapeutic efficacy. To overcome limitations in drug bioavailability and absorption, innovation is required in the pharmaceutical research for the formulation of drugs, solvents or systems for effective drug delivery.

For non-ionizable drugs, the solubility is a fixed physical property, although it may be advantageously modified by derivatization (esterification or prodrug formation). For ionizable drugs, salt formation is the simplest, most cost-effective strategy to address poor aqueous solubility and enhance bioavailability.[1] Nevertheless, even when a salt is formed, bioavailability of drugs might not be enhanced adequately. Thus, in alternative, other approaches can be used to overcome the challenge of solubility and absorption such as particle size reduction, nanonization, pH adjustment, solid dispersion, and inclusion complexation.[2]

The extent of solubility in a specific solvent is expressed as the concentration of the solute in a saturated solution at a given temperature. Most pharmaceutical compounds are weakly ionizable acids or bases, or combinations of these two ionization types. Since the extent of drug ionization varies with the solvent pH, the measured solubility has to be viewed in the context of the pH of the solution at equilibrium and the pKa values of the compound. Thus, for an ionizable compound, solubility without reference to pH and pKa is meaningless. Dissociation constants of polyprotic substances, such as HCAs can be determined by several different methods. When drug compounds are sparingly soluble in water, a precise determination of their pKa values poses a challenging problem for potentiometric titration. This technique is commonly used due its accuracy and the commercial availability of fast, automated instruments.[3] However, to detect a significant change in shape of the titration curve, this method is restricted by its detection limit of about $10^{-4}$ M.[3] To prevent errors for measurements at neutral-to-high pH, another mandatory condition is the laboriously preparation of fresh carbonate-free solutions.[4] Spectroscopic titration can be utilized as an alternative to determine pKa values of substances with large molar absorptivities because of its high sensitivity at concentrations of substance as low as $10^{-6}$ M.[5] However, the compound under investigation must possess chromophore(s) in proximity to the ionization center(s) so that the protonated and deprotonated species exhibit sufficient spectral

dissimilarity.[5] During the course of titration, spectral data are recorded continuously by a diode-array spectrometer following the changes of the UV-vis absorption spectra of the samples due to the variations of the concentration of neutral and ionized species present. The largest change in absorbance occurs at the pH corresponding to pKa value. The determination of pKa values by UV–vis spectroscopy assumes that the solute of interest is pure or that its impurities do not absorb in this spectral range, to avoid the overlap of the relative spectra.[3]

Information on the polymorphism of a candidate pharmaceutical product is fundamental for processing and solubility considerations. Furthermore, the nature and characteristics of polymorphism are important to guarantee physicochemical stability for the entire shelf life of the pharmaceutical substance. Thermogravimetry (TG) and differential scanning calorimetry (DSC) are techniques successfully applied in the pharmaceutical industry to reveal important information regarding the physicochemical properties of drug. DSC is a thermal analytical tool that can be used for characterizing the melting behavior, crystallization, polymorphism and solid state transitions.[6] It provides quantitative and qualitative information about physical and chemical changes occurring during endothermic or exothermic processes, or changes in heat capacity. Basically, during a DSC experiment, a substance and a reference material (thermally stable) are subjected to an identical controlled temperature program. The difference in the energy between sample and reference would be the amount of excess heat absorbed or released by the molecule in the sample during an endothermic or exothermic process, respectively. These events are expressed in the form of peaks: upward peaks represent exothermic events, while downward peaks are characteristic of endothermic events. In the case of second-order transitions, there are changes in the baseline without peaks.

TG analysis (TGA) uses change in mass upon increasing temperature to identify and measure the physical and chemical processes that take place when heating the sample. It is used in pharmaceutical sciences for the characterization of hydrates and the determination of vaporization, decomposition, or sublimation temperatures. It gives information about the composition and thermal stability of the sample, the intermediate products and end residue. Furthermore, it is useful to determine the effects of water vapor on the stability of crystalline drugs and excipients, and the water content, both free and bound, of a wide variety of materials.[7]

In the present PhD thesis, I have synthesized new derivatives of HCAs by conversion of caffeic, ferulic, sinapic, *o*-coumaric, *m*-coumaric, and *p*-coumaric acids into cholinium-based ionic liquids ([Cho][HCA] ILs). The choice of using cholinium as cation is due to the intent of preparing bio-based ILs with pharmaceutical applications. The chemical structures of synthetized [Cho][HCA] ILs were characterized by using FT-IR, $^{1}H$ and $^{13}C$ NMR spectroscopy. The extent

of the improvement in water solubility of ILs (in comparison with the acidic precursors) was measured by combined potentiometric-spectrophotometric methods, while thermal analysis was performed by using both DSC and TGA.

## 2.2 Synthesis and structure of [Cho][HCA]ILs

Two basic methods are employed for the synthesis of ILs: metathesis of a halide salt and acid-base neutralization reactions.[8] The metathesis process occurs in presence of halide salts with sodium, potassium or silver salts of $CH_3COO^-$, $NO_2^-$, $NO_3^-$, $BF_4^-$, $SO_4^{2-}$, $PF_6^-$ and many more free acids of corresponding anions.[9]

A general metathesis mechanism is shown in Scheme 2.1, while an example of a metathesis reaction which regard the synthesis of 1-ethyl-3-methylimidazolium bromide [$C_2$mim][$BF_4$] is shown in Scheme 2.2[10]

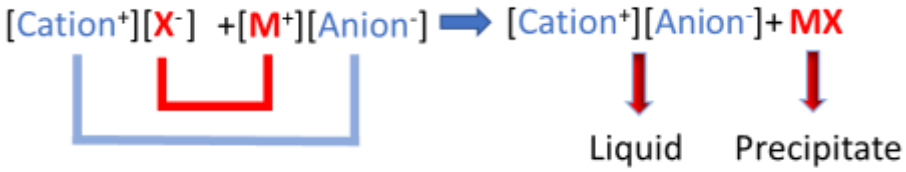


**Scheme 2.1.** Generalized metathesis reaction for the synthesis of ILs.

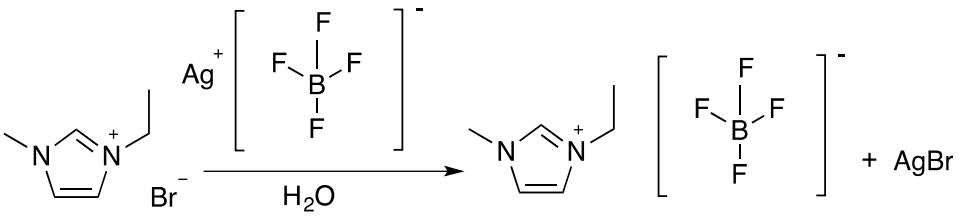


**Scheme 2.2** Synthesis of [$C_2$mim][$BF_4$] via metathesis.

The other above-mentioned synthetic method is a neutralization reaction. Among the many neutralized salts prepared in this way, some amines are excellent candidates. There are few anions suitable for the preparation of ILs, and their acids can be used to neutralize the selected amines.[11] This method is useful also for the synthesis of protic ionic liquids (PILs) which involves the transfer of a proton from a Bronsted acid to a Bronsted base.[12] By using bio-ILs such as aminoacids, or pharmaceutical active organic acids, can be easily prepared.[13,14] Since this method has no problem of contamination by undesirable by-product salts, it is useful for

preparing pure ILs and their models.[15] In the development of bio-ILs family, there is a clear dominance of cholinium-based ILs.[16,17] Several publications have reported the synthesis of cholinium ILs using choline chloride.[18–20] Nowadays, the most common and straightforward procedure for [Cho]ILs synthesis is conducted using a neutralization reaction between the commercially available choline hydroxyde [Cho][OH] or choline bicarbonate [Cho][$HCO_3$] solutions, and a slight equimolar excess of the desired carboxylic acid.[21] Commonly, the reaction involves mixing for 12–24 h at room temperature. To remove the acid excess, the mixture is subjected to purification by extraction with a suitable organic solvent followed by filtration. The crude product is further dried *in vacuo*. Representative examples of [Cho]ILs synthetic processes using [Cho][OH] and [Cho][$HCO_3$] are shown in Scheme 2.3 A and B, respectively.[22]

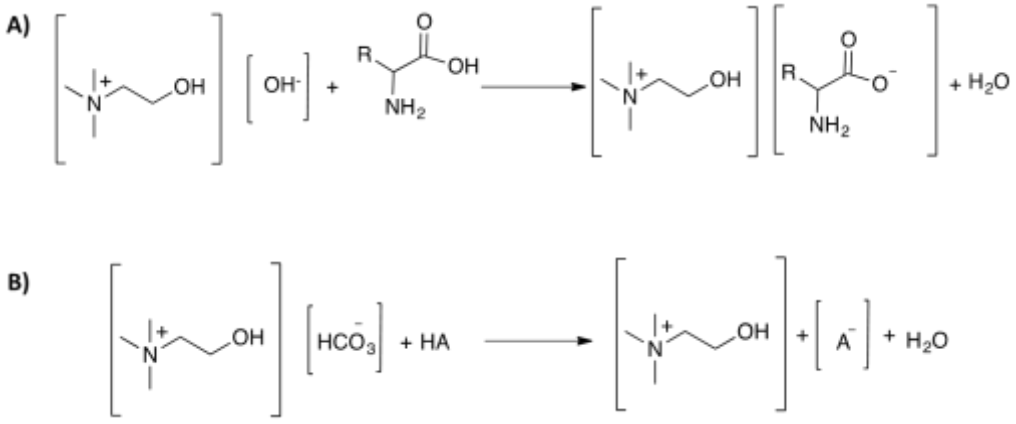


**Scheme 2.3** Synthetic pathway of ILs by neutralization reaction toward A) cholinium-amino acid based ILs and B) cholinium carboxylate ILs.

The method used in the present study to synthetize [Cho][HCA] ILs is shown in Scheme 2.4. It consisted of neutralizing an aqueous solution of choline hydroxide with the appropriate hydroxycinnamic acid: ferulic acid (FA), sinapic acid (SA), caffeic acid (CAFA), *o*-Coumaric acid (*o*-CA), *m*-Coumaric acid (*m*-CA) and *p*-Coumaric acid (*p*-CA). The methanolic solution of each HCA (1.1 equivalents) was cooled in an ice bath, then [Cho][OH] (1 equivalent 46 wt % in a water solution) was added dropwise. The resulting mixture was stirred for 3 hours in the dark at room temperature. The solvent was evaporated under vacuum. In order to remove the unreacted acid, the solid [Cho][Caff] was further washed with acetone and filtered, while the others [Cho][HCA] ILs were subjected to extraction with ethyl acetate.[19] The residual solvents were evaporated at reduced pressure at 60 °C and the residual water was removed by freeze drying for 12 hours before each utilization or characterization. The structure of the six

synthesized cholinium-based ionic liquids, [Cho][Fer], [Cho][Sin], [Cho][Caf], [Cho][*o*-Coum], [Cho][*m*-Coum], [Cho][*p*-Coum], were characterized by $^{1}H$ and $^{13}C$ NMR, IR and elemental analysis, providing indication of high level of purity for all compounds.

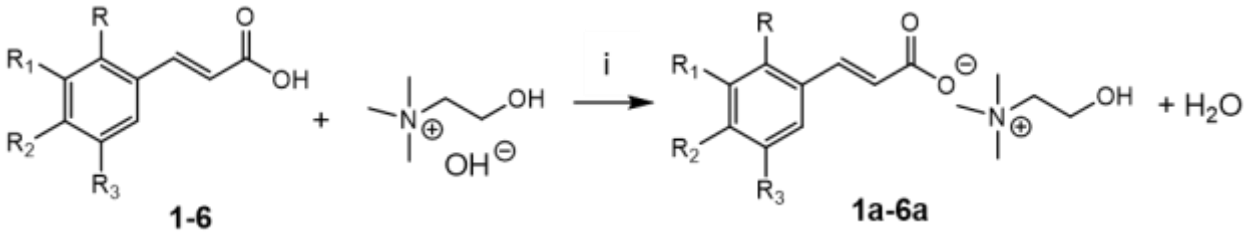


**1-6** **1a-6a**

| R | $R_1$ | $R_2$ | $R_3$ | HCA | [Cho][HCA] IL |
|---|---|---|---|---|---|
| H | OMe | OH | H | 1 Ferulic acid (FA) | 1a Cholinium ferulate ([Cho][Fer]) |
| H | OMe | OH | OMe | 2 Sinapic acid (SA) | 2a Cholinium sinapate ([Cho][Sin]) |
| H | OH | OH | H | 3 Caffeic acid (CAFA) | 3a Cholinium caffeate ([Cho][Caff]) |
| OH | H | H | H | 4 *o*-Coumaric acid (*o*-CA) | 4a Cholinium *o*-coumarate ([Cho][*o*-Coum]) |
| H | OH | H | H | 5 *m*-Coumaric acid (*m*-CA) | 5a Cholinium *m*-coumarate ([Cho][*m*-Coum]) |
| H | H | OH | H | 6 *p*-Coumaric acid (*p*-CA) | 6a Cholinium *p*-coumarate ([Cho][*p*-Coum]) |

**Scheme 2.4** Reagents and conditions for the synthesis of [Cho][HCA] ILs (**1-6a**): (i) methanol, 0 °C then, r.t. 3 h.

**1a. (2-Hydroxyethyl) trimethylammonium (E)-3-(4-hydroxy-3-methoxyphenyl) acrylate: Cholinium ferulate, [Cho][Fer].**

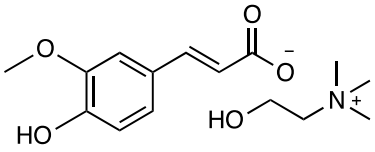


Viscous and bright yellow liquid (98% yield). **$^{1}$H NMR** (DMSO-$d_6$, 500 MHz) δ (ppm): 6.98 (d, 1H, $J_{HH}$ = 1.8 Hz, H-2) ; 6.97 (d, 1H, $J_{HH}$ = 15 Hz, C<u>H</u>CHCOO), 6.81 (dd, 1H, $J_{HH}$ =1.8 Hz, H-6) 6.78 (d, 1H, $J_{HH}$ =8.1 Hz, H-5), 6.15 (d, 1H, $J_{HH}$ = 15 Hz, CHC<u>H</u>COO), 3.86 (m, 2H, $NCH_2C\underline{H}_2OH$), 3.76 (s, 3H, $OCH_3$), 3.46 (m, 2H, $NC\underline{H}_2CH_2OH$), 3.13 (s, 9H, $(N(CH_3)_3)$). **$^{13}$C NMR** (DMSO-$d_6$, 125.72 MHz), δ (ppm): 170.15 (COO), 148.25 (<u>C</u>$OCH_3$), 147.91 (COH-4), 136.00 (<u>C</u>HCHCOO), 127.21 (C-1), 126.53 (C-6), 120.66 (CH<u>C</u>HCOO), 116.17 (C-5), 110.30 (C-2), 67.23 ($N\underline{C}H_2CH_2OH$), 55.47 ($OCH_3$), 55.0 ($NCH_2\underline{C}H_2OH$), 53.07 ($(N(CH_3)_3)$). **IR** (Wavenumber, $cm^{-1}$): 3028 (OH), 1635, 1592 (COO), 1517 (CH), 1379 (COO), 1275, 1158(CN), 987, 862, 817. **Elemental analysis** (%): calculated for $C_{15}H_{23}NO_5$: C, 60.59; H, 7.80; N, 4.71;

found: C, 60.65; H, 7.68; N, 4.65.

**2a. (2-Hydroxyethyl) trimethylammonium (E)-3-(3-hydroxy-2,4-dimethoxyphenyl) acrylate: Cholinium sinapate, [Cho][Sin].**

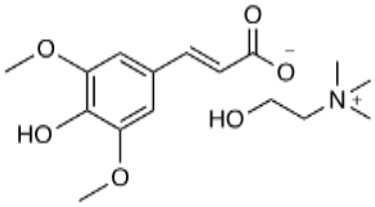

Viscous and light orange liquid (97% yield), **$^{1}$H NMR** (DMSO-$d_6$, 500 MHz) δ (ppm): 6.94 (d, 1H, $J_{HH}$= 15.8 Hz, C<u>H</u>CHCOO), 6.71 (s, 2H, H-2,6), 6.18 (d, 1H, $J_{HH}$= 15.8 Hz, CHC<u>H</u>COO), 3.86 (m, 2H, $NCH_2C\underline{H_2}OH$), 3.75 (s, 6H, $OCH_3$ x2), 3.42 (t, OH, $NC\underline{H_2}CH_2OH$), 3.13 (s, 9H, $(N(CH_3)_3)$. **$^{13}$C NMR** (DMSO-$d_6$, 125.72 MHz), δ (ppm): 169.87 (COO), 148.10 (C-3,5), 144.71 (<u>C</u>HCHCOO), 135.60 (COH-4), 126.8 (C-1), 109.37 (CH<u>C</u>HCOO), 104.57 (C-2,6), 67.21 ($N\underline{C}H_2CH_2OH$), 55.97 (2 x $O\underline{C}H_3$), 55.06 (m, $N(CH_3)_3$), 53.19 ($NCH_2\underline{C}H_2OH$). **IR** (Wavenumber, $cm^{-1}$): 3029 (OH), 1634, 1594 (COO), 1517 (CH), 1378 (COO), 1275, 1156(CN), 957, 917, 836. **Elemental analysis** (%): calculated for $C_{16}H_{25}NO_6$: C, 58.70; H, 7.70; N, 4.28; found: C, 58.61; H, 7.66; N, 4.15.

**3a. (2-Hydroxyethyl) trimethylammonium (E)-3-(3,4-dihydroxyphenyl) acrylate: Cholinium caffeate, [Cho][Caf].**

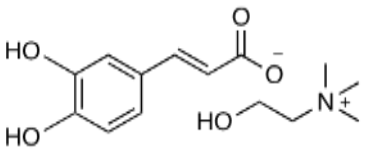

White solid (99% yield) **$^{1}$H NMR** (DMSO-$d_6$, 500 MHz) δ (ppm): 7.07 (d, 1H, $J_{HH}$ = 15.8 Hz, C<u>H</u>CHCOO), 6.89 (d, 1H, $J_{HH}$ = 2.1, H-2), 6.74 (dd, 1H, $J_{HH}$ = 8.1 Hz and $J_{HH}$ = 2.1 Hz, H-6), 6.67 (d, 1H, $J_{HH}$ = 8.1 Hz, H-5), 6.11 (d, 1H, $J_{HH}$ = 15.8 Hz, CHC<u>H</u>COO), 3.85 (m, 2H, $NCH_2C\underline{H_2}OH$), 3.41 (m, 2H, $NC\underline{H_2}CH_2OH$), 3.11 (s, 9H, $(N(CH_3)_3)$. **$^{13}$C NMR** (DMSO-$d_6$, 125.72 MHz), δ (ppm): 170.97 (COO), 148.67 (COH-4), 146.48 (COH-3), 139.04 (<u>C</u>HCHCOO), 126.90 (C-1), 123.50 (CH<u>C</u>HCOO), 119.96 (C-6), 117.19 (C-5), 114.63 (C-2), 66.57 ($N\underline{C}H_2CH_2OH$), 55.59 ($NCH_2\underline{C}H_2OH$), 53.21 ($N(CH_3)_3$). **IR** (Wavenumber, $cm^{-1}$): 3024 (OH), 1635, 1589 (COO), 1512 (CH), 1373 (COO), 1265, 1157 (CN), 987, 864, 817, 694, 586. **Elemental analysis** (%): calculated for $C_{14}H_{21}NO_5$: C, 59.35; H, 7.47; N, 4.94; found: C 59.35, H 7.47, N 4.94; found: C 60.61, H 7.40, N 4.89.

**4a. (2-Hydroxyethyl) trimethylammonium (*E*)-3-(2-hydroxyphenyl) acrylate: Cholinium *o*-Coumarate, ([Cho][*o*-Coum]).**

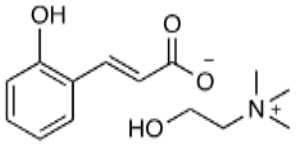

Obtained from *o*-coumaric acid. Viscous and light yellow liquid (99% yield) **$^{1}$H NMR** (DMSO-$d_6$, 500 MHz) δ (ppm): 7.47 (d, 1H, $J_{HH}$ = 15.8 Hz, C<u>H</u>CHCOO), 7.29 (dd, 1H, $J_{HH}$ = 7.7 Hz and $J_{HH}$ =1.8 Hz, H-6), 6.96 (ddd, 1H, $J_{HH}$ = 8.5 Hz, $J_{HH}$ =7.2, $J_{HH}$ =1.7 Hz, H-4), 6.80 (m, 1H, H-3), 6.55 (m, 1H, H-5), 6.37 (d, 1H, $J_{HH}$= 15.8 Hz, CHC<u>H</u>COO), 3.86 (m, 2H, $NCH_2C\underline{H}_2OH$), 3.42 (m, 2H, $NC\underline{H}_2CH_2OH$), 3.19 (s, 9H, $(N(CH3)_3)$). **$^{13}$C NMR** (DMSO-$d_6$, 125.72 MHz), δ (ppm): 171.51 (COO), 159.17 (COH-2), 132.7 (C<u>H</u>CHCOO), 128.69 (C-4), 127.50 (CH<u>C</u>HCOO), 126.92 (C-6), 123.63 (C-2), 116.90 (C-3), 116.42 (C-5), 116.40 (C-1), 67.16 ($N\underline{C}H_2CH_2OH$), 55.07 ($NCH_2\underline{C}H_2OH$), 53.15 ($N(CH_3)_3$). **IR** (Wavenumber, $cm^{-1}$): 3024 (OH), 1633, 1609 (COO), 1515 (CH), 1384 (COO), 1298, 1153(CN), 996, 957, 885. **Elemental analysis** (%): calculated for $C_{14}H_{21}NO_4$: C, 62.90; H, 7.92; N, 5.24; found: C, 62.41; H, 7.84; N, 5.18.

**5a. (2-Hydroxyethyl) trimethylammonium (*E*)-3-(3-hydroxyphenyl) acrylate: Cholinium *m*-Coumarate ([Cho][*m*-Coum]).**

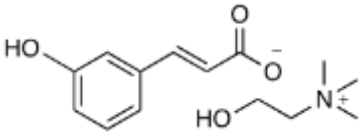

Obtained from *m*-coumaric acid. Viscous and light yellow liquid (99% yield) **$^{1}$H NMR** (DMSO-$d_6$, 500 MHz) δ (ppm): 7.08 (t, 1H, H-6, $J_{HH}$ = 7.8 Hz), 7.03 (d, 1H, C<u>H</u>CHCOO $J_{HH}$= 15.8 Hz), 6.93 (t, 1H, H-2, $J_{HH}$= 2.1 Hz), 6.81 (dt, 1H, H-5, $J_{HH}$ =7.7 Hz, $J_{HH}$ =1.2 Hz) 6.70 (ddd, 1H, H-4, $J_{HH}$ =7.8 Hz, $J_{HH}$ =2.4 Hz, $J_{HH}$ =1.2 Hz), 6.28 (d, 1H, CHC<u>H</u>COO $J_{HH}$= 15.8 Hz), 3.86 (m, 2H, $NCH_2CH_2OH$), 3.43 (m, 2H, $NCH_2CH_2OH$), 3.11 (s, 9H, $(N(CH3)_3)$). **$^{13}$C NMR** (DMSO-$d_6$, 125.72 MHz), δ (ppm): 170.08 (COO), 156.67 (COH-3), 137.71 (C<u>H</u>CHCOO), 136.17 (C-1), 129.38 (C-6), 129.36 (CH<u>C</u>HCOO), 117.22 (C-5), 115.60 (C-4), 113.71 (C-2), 67.21 ($N\underline{C}H_2CH_2OH$), 55.08 ($NCH_2\underline{C}H_2OH$), 53.15 ($N(CH_3)_3$). I**R** (Wavenumber, $cm^{-1}$): (OH), 1640 (COO), 1556 (CH), 1478 (COO), 1283, 1158(CN), 969, 957, 866. **Elemental analysis** (%): calculated for $C_{14}H_{21}NO_4$: C, 62.90; H, 7.92; N, 5.24; found: C, 63.21; H, 7.88; N, 5.20.

**6a. (2-Hydroxyethyl) trimethylammonium (*E*)-3-(4-hydroxyphenyl) acrylate: Cholinium *p*-Coumarate, ([Cho][*p*-Coum]).**

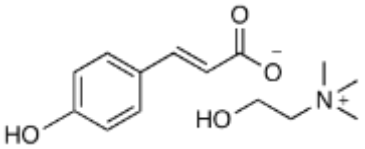

Obtained from *p*-coumaric acid. Viscous and light yellow liquid (99% yield) **$^{1}$H NMR** (DMSO-$d_6$, 500 MHz) δ (ppm): 7.26 (m, 2H, H-2,6), 7.07 (d, 1H, $J_{HH}$ = 15.6 Hz, CHCHCOO), 6.78 (m, 2H, H-3,5), 6.17 (d, 1H, CHCHCOO, $J_{HH}$ = 15.6 Hz), 3.87 (m, 2H, $NCH_2CH_2OH$), 3.47 (m, 2H, $NCH_2CH_2OH$), 3.13 (s, 9H, $(N(CH_3)_3)$. **$^{13}$C NMR** (DMSO-$d_6$, 125.72 MHz), δ (ppm): 170.57 (COO), 159.27 (COH-4), 136.5 (CHCHCOO), 128.23 (C-2,6), 126.3 (C-1), 125.23 (CHCHCOO), 115.83 (C-3,5), 67.20 ($NCH_2CH_2OH$), 55.04 ($NCH_2CH_2OH$), 53.19 ($N(CH_3)_3$). **IR** (Wavenumber, $cm^{-1}$): 3029 (OH), 1638, 1609 (COO), 1515 (CH), 1378 (COO), 1275, 1156(CN), 968, 957, 835. **Elemental analysis** (%): calculated for $C_{14}H_{21}NO_4$: C, 62.90; H, 7.92; N, 5.24; found: C, 63.18; H, 7.97; N, 5.17.

## 2.3 Physico-chemical characterization

### *2.3.1 Protonation equilibria and water solubility*

In the present study, the protonation equilibria of the six HCAs precursors of the cholinium-based ILs under investigation were studied by combined potentiometric-spectrophotometric measurements. Experiments were performed over a pH range of 3-11. The UV spectra of the titration analyte solutions were characterised by different bands and distinct isosbestic points (Figure 2.1).

Based on the analysis of absorptivity bands (calculated with the HypSpec program) (Figure 2.2), we propose a common equilibrium model for all studied acids

$$H^2L \leftrightarrow [HL]^- \leftrightarrow [L]^{2-}$$

which takes into account two dissociations: the proton dissociation of the carboxylic group, leading to the spectral changes in the acidic pH range, and the dissociation of the phenolic group shifting the absorbance bands in the basic pH range. The third dissociation constant of caffeic acid, associated to the second hydroxyl group, was not observed, being outside the pH range under investigation (i.e. at pH > 11).[23]

CAFA, FA, SA, and *p*-CA acids shared common spectral changes (Figures 2.1A-D). Their acidic dissociation was characterized by ipso- and ipochromic shift, while the basic dissociation led to the bato- and iperchromic shift of the bands. The absorbance bands of *o*-CA and *m*-CA acids were less intense than those of the other acids. The proton dissociation of both compounds was characterized by the ipsochromic shifts of the bands at acidic pH and ipso- and batochromic shifts at basic pH (Figures 2.1E-F).

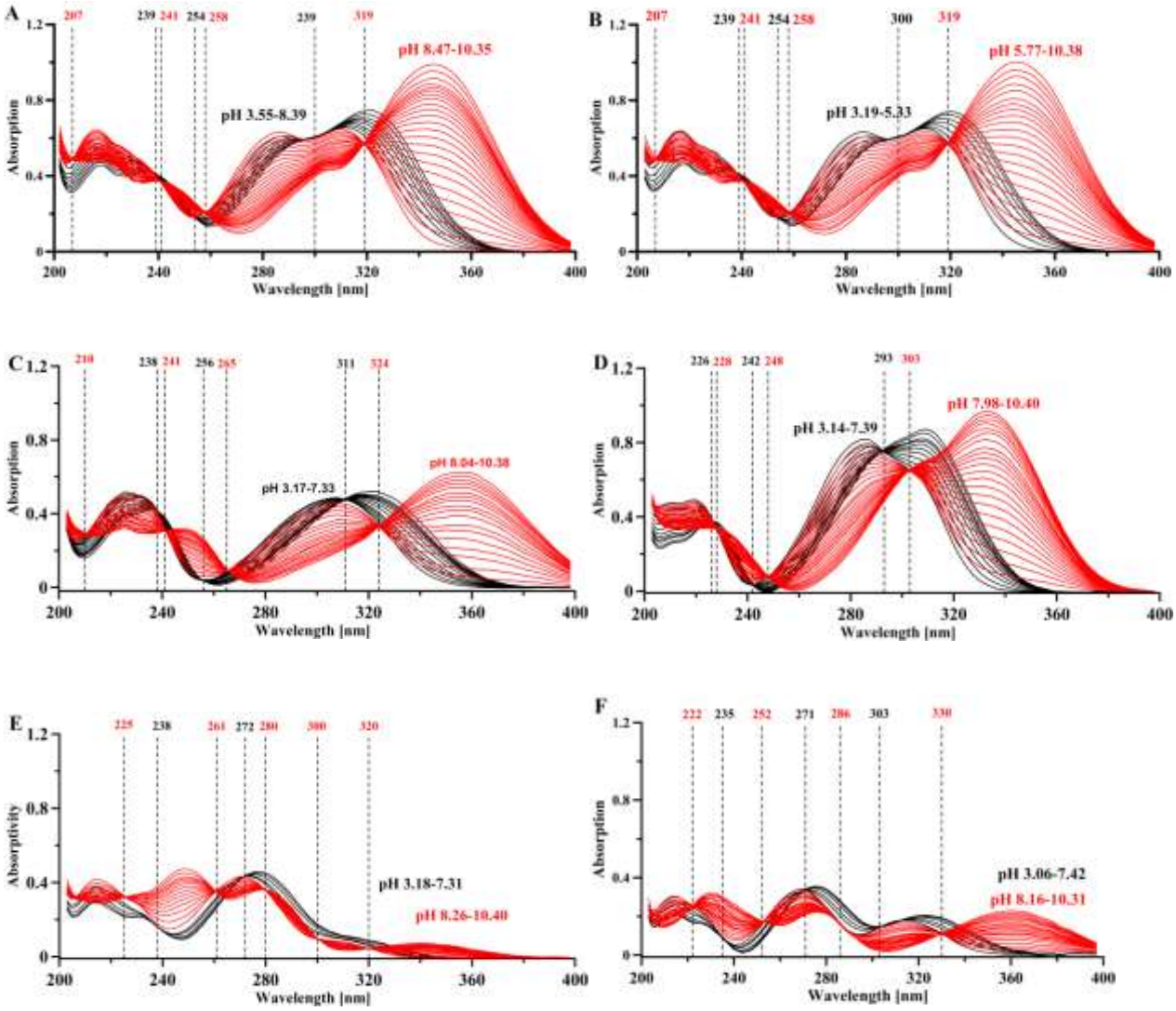


**Figure 2.1** UV spectra of caffeic CAFA (A), FA (B), SA (C), *p*-CA (D), *m*-CA (E), and *o*-CA (F) acids. Isosbestic points are signed as a dashed line.

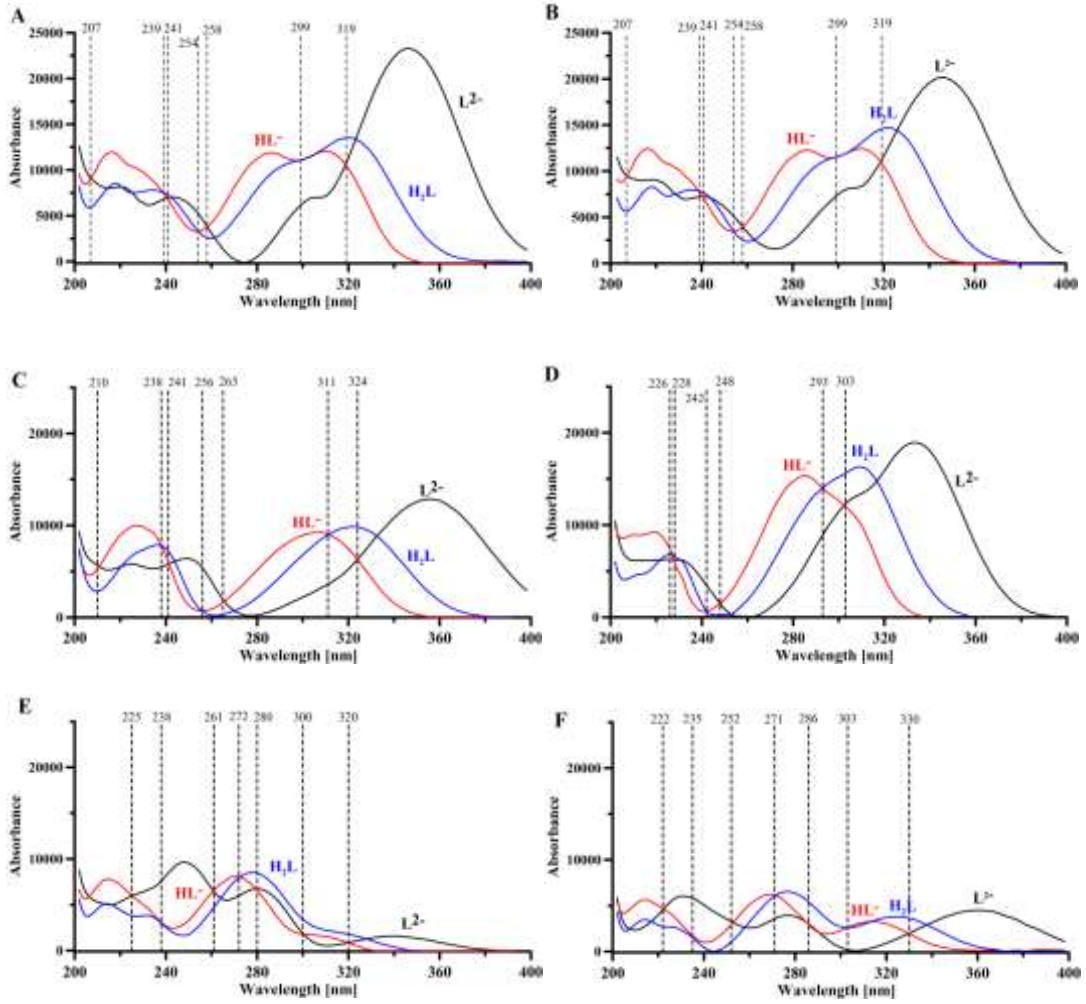


**Figure 2.2** Absorptivity spectra of CAFA (A), FA (B), SA (C), *p*-CA (D), *m*-CA (E), and *o*-CA (F) acids calculated with HypSpec2014 program. Isosbestic points are signed as a dashed line.

Compared to the literature data, our experiments provided satisfactory values of the protonation constants (Table 2.1), despite the different experimental conditions of temperature and ionic strength. Furthermore, it can be noted that that the acidic and basic dissociation constants are inversely correlated (R=0.97) (Figure 2.3). Such a relation can be associated to the formation of intramolecular hydrogen bonds, as previously observed for caffeic acid derivatives[24,25] and other small molecules.[26]

The solubilities of [Cho][HCA] ILs and their parent acids were measured by UV spectroscopy. Since the absorbance at the isosbestic point is independent of the pH value of solutions, the solubility was estimated at isosbestic wavelengths. Table 2.2 shows the solubility values of both salts and acidic precursors, expressed as the average of three independent

experiments, and the experimental pH of aqueous solutions. The values are in good agreement with those reported in the literature.[27,28]

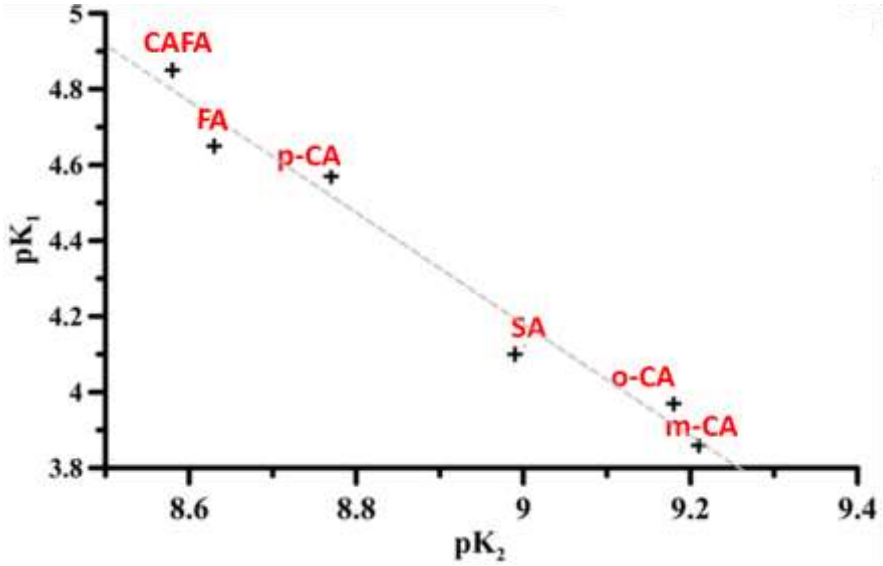


**Figure 2.3** $pK_1$ vs $pK_2$ plot for HCAs.

**Table 2.1** Comparison of the obtained protonation constants for HCAs (at 25 °C evaluated from combined potentiometric-UV-vis data with Hyperquad2013 and HypSPec2014 programs) with literature data. Standard deviations are given in brackets.

| **Name** | **Potentiometry-UV-vis** | | **Potentiometry*** | | **UV-vis**** | |
|---|---|---|---|---|---|---|
| **HCAs** | **$pK_1$** | **$pK_2$** | **$pK_1$** | **$pK_2$** | **$pK_1$** | **$pK_2$** |
| FA | 4.65 (0.05) | 8.63 (0.03) | 4.56 (0.05) | 8.65 (0.02) | | |
| SA | 4.10 (0.03) | 8.99 (0.02) | | | 4.19 (0.01) | 9.40 (0.03) |
| CAFA | 4.85 (0.05) | 8.58 (0.01) | 4.47 (0.04) | 8.32 (0.01) | | |
| *p*-CA | 4.57 (0.04) | 8.77 (0.04) | 4.39 (0.04) | 8.37 (0.02) | 4.360 (0.003) | 8.982 (0.001) |
| *m*-CA | 3.86 (0.04) | 9.21 (0.04) | | | | |
| *o*-CA | 3.97 (0.04) | 9.18 (0.03) | | | | |

* $H_2O$, 0.1 M ionic strength (salt unknown), T= 25°C [29] (F.Z. Erdemgil, S. Şanli, N. Şanli, G. Özkan, J. Barbosa, J. Guiteras, J.L. Beltrán Determination of pKa values of some hydroxylated benzoic acids in methanol–water binary mixtures by LC methodology and potentiometry, *Talanta*, 72 (2007) 489-496).
** $H_2O$; 0.1 M KCl, T= ambient temperature[30] (J.L. Beltrán, N. Sanli, G. Fonrodona, D. Barrón, G. Özkan, J. Barbosa, Spectrophotometric, potentiometric and chromatographic pKa values of polyphenolic acids in water and acetonitrile–water media, *Analytica Chimica Acta* 484 (2003) 253–264).

For the phenolic acids, the following order of decreasing solubility was found: *m*-CA > *o*-CA ≈ *p*-CA > FEA ≈ CAFA > SA. It is noteworthy that this solubility trend correlates linearly with the pK values of the acids (Figure 2.4). Acids with only one hydroxyl group in the aromatic ring have the highest solubility, while addition of other functional groups (-OH and/or -$OCH_3$) lowers the overall solubility of the molecule. Addition of different functional groups leads to the electron-withdrawing or electron-donating effects, as well as resonance effects, which in turn influence the values of protonation constants.[31,32] The change of protonation state of the molecule influences the extend of hydrogen bonding of the molecule with water. Moreover, the special proximity of different dissociation groups in the same molecule (e.g. caffeic acid) leads to the formation of intramolecular hydrogen bonds, which not only changes significantly the protonation constant of the neighbouring group[26,33] but also lowers the overall number of hydrogen bonds of the molecule with solvent.

**Table 2.2** Solubility ([M]) of HCAs and the corresponding [Cho][HCA] ILs, and pH of the water solutions under UV-vis solubility analysis.

| Compound | Solubility[a] [M] | pH |
|---|---|---|
| FA | 0.0047 ± 0.0007 | 5.0 |
| [Cho][Fer] | 0.6 ± 0.1 | 6.6 |
| SA | 0.0028 ± 0.0002 | 5.4 |
| [Cho][Sin] | 0.2 ± 0.1 | 7.5 |
| CAFA | 0.0040 ± 0.0006 | 5.2 |
| [Cho][Caf] | 1.3 ± 0.1 | 5.7 |
| *p*-CA | 0.007 ± 0.002 | 5.1 |
| [Cho][*p*-Coum] | 1.4 ± 0.1 | 6.4 |
| *m*-CA | 0.013 ± 0.002 | 4.7 |
| [Cho][*m*-Coum] | 2.8 ± 0.5 | 6.4 |
| *o*-CA | 0.008 ± 0.001 | 5.5 |
| [Cho][*o*-Coum] | 2.9 ± 0.8 | 6.3 |

[a] Values are means of three determinations ± standard deviation.

The conversion of HCAs into cholinium-based ILs notably increased the solubility by two/three orders of magnitude. This finding agrees with previously literature data.[34] Data in

Table 2.2 show that the strongest variation was recorded for the *o*-CA/[Cho][*o*-Coum] pair. Respect to the acids, the trend of solubility of salts was slightly different, following the order: [Cho][*m*-Coum] ≈ [Cho][*o*-Coum] > [Cho][*p*-Coum] ≈ [Cho][Caf] > [Cho][Fer] > [Cho][Sin]. Considering that both acids and salts have the same mono-protonated state at the pH of the solubility analysis, it is likely that the basic counterpart of the salt influences the overall solubility of the salt.

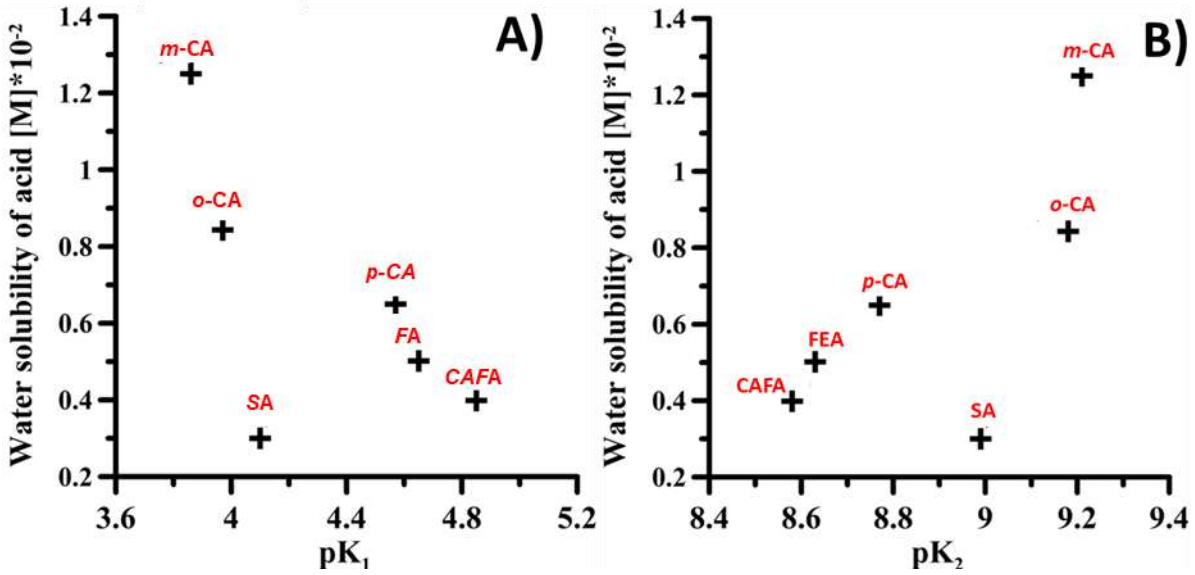


**Figure 2.4** The correlation of acids solubility and respective $pK_1$ (A) and $pK_2$ (B) values for each HCA.

### *2.3.2 Thermal characterization*

The thermal stability of [Cho][HCA] ILs and their acidic precursors was investigated by simultaneous thermogravimetric analysis (TGA) and differential scanning calorimetry (DSC). TGA is a useful technique to investigate the mass loss of a sample upon heating at a given heating rate, while DSC investigates the thermal effect so that differentiating between phase transformation and decomposition. The reproducible extrapolated melting ($T_M$) and decomposition ($T_D$) onset temperatures were calculated. The experimental curves are reported in Figures 2.5-2.7, while the results are depicted in Tables 2.3 and 2.4 for HCAs and [Cho][HCA] ILs, respectively.

Two different endotherm effects were evidenced by the DSC thermograms of HCAs, a first endothermic signal, due to melting, followed by a second large endothermic signal (2nd TD) (Figure 2.5). Only the DSC thermogram of sinapic acid showed two net endothermic DSC

peaks, almost thirty degrees before decomposition, suggesting the presence of a polymorphic transition followed by melting. In the DSC curve of caffeic acid, the first endothermic peak is followed by a minor

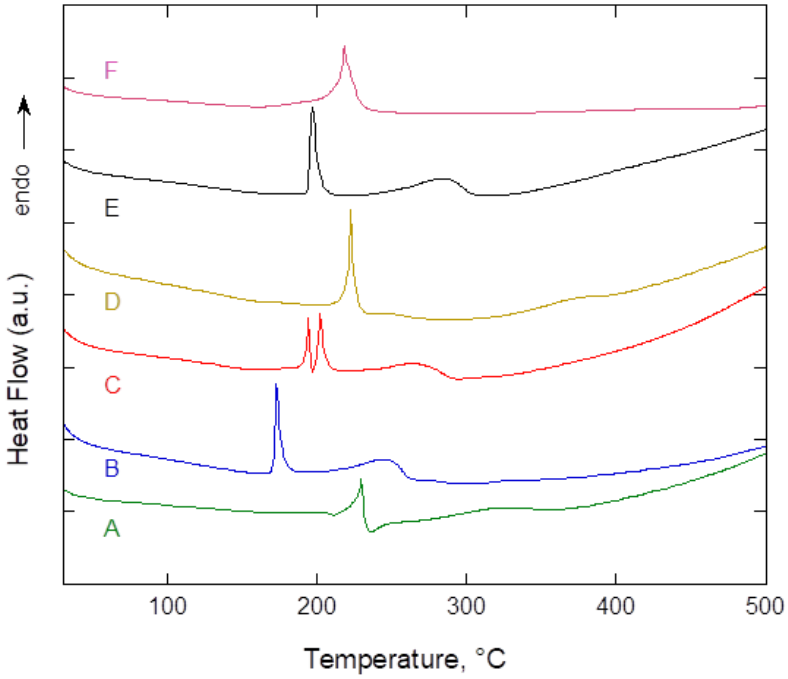


**Figure 2.5.** DSC thermograms of CAFA (A), FA (B), SA (C), *p*-CA (D), *m*-CA (E), and *o*-CA (F) acids.

exothermic tail, indicating that another phenomenon except from melting occurs either just after melting is complete or even simultaneously. It is noteworthy that in TG thermograms of CAFA, *o*-CA, and *p*-CA, the first significant step due to decomposition, characterized by the onset $T_D$ temperature, occurs very close to the melting of the samples observed in DSC thermograms (Table 2.3), indicating an incongruent melting, i.e. the decomposition occurs either just after melting is complete or even simultaneously. DSC results of HCAs samples are in agreement with literature.[34]

The conversion of HCAs into [Cho][HCA] ILs decreased the onset decomposition temperature (Table 2.4). Nevertheless, all cholinium salts kept exhibiting a good thermal stability with $T_D$ values higher than 100 °C. The most stable sample was [Cho][Caf] ($T_D$ = 148°C), while the lowest stability was shown by the two ILs containing methoxy groups in the aromatic ring i.e. [Cho][Sin] ($T_D$ = 103°C) and [Cho][Fer] ($T_D$ = 105°C). At temperatures higher than 150°C, the TG curves of all samples exhibited further steps indicating a complex decomposition (Figure 2.7). Only, [Cho][*o*-Coum] and [Cho][*m*-Coum] showed a slight weight loss at low temperature

due to solvent residual or moisture captured by the air during handling. DSC thermograms of [Cho][HCA] ILs confirmed the TGA results (Figure 2.7).

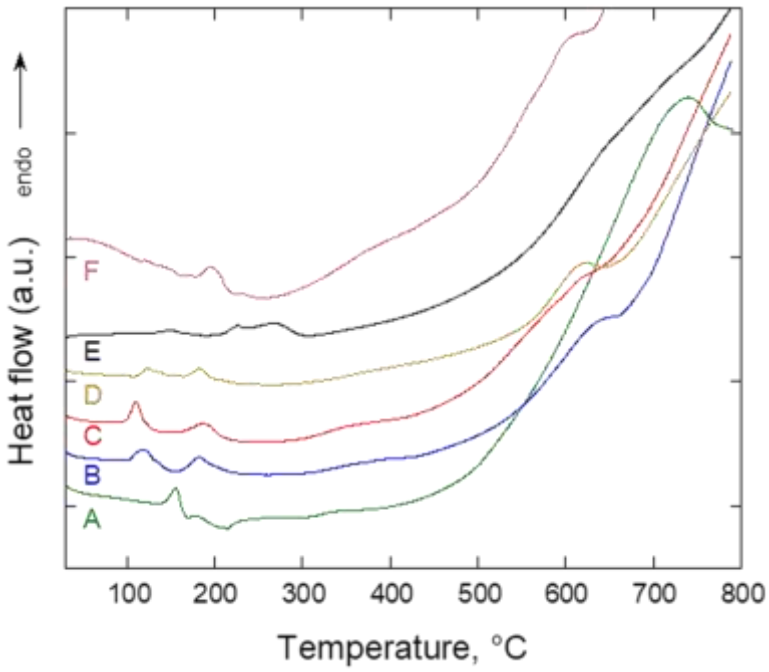


**Figure 2.6** DSC thermograms of [Cho][Caf] (A), [Cho][Fer] (B), [Cho][Sin] (C), [Cho][ *p*-Coum] (D), [Cho][ *m*-Coum] (E), and [Cho][ *o*-Coum] (F) ILs.

**Table 2.3** Onset Melting ($T_M$) and Decomposition ($T_D$) temperatures of HCAs.[a]

| **Compound** | **DSC** | | **TGA** |
|---|---|---|---|
| | **$T_M$, °C** | **2nd $T_D$, °C** | **$T_D$, °C** |
| FA | 172 | 208 | 211 |
| SA | 191 and 198[b] | 226 | 229 |
| CAFA | 217[c] | 269 | 216 |
| *p*-CA | 221[c] | 233 | 212 |
| *m*-CA | 194 | 242 | 245 |
| *o*-CA | 217[c] | 245 | 213 |

[a] Temperature accuracy of ± 1 °C.
[b] The first peak is due to phase transformation, the second to melting.
[c] Incongruent melting (the decomposition occurs either just after melting is complete or even simultaneously).

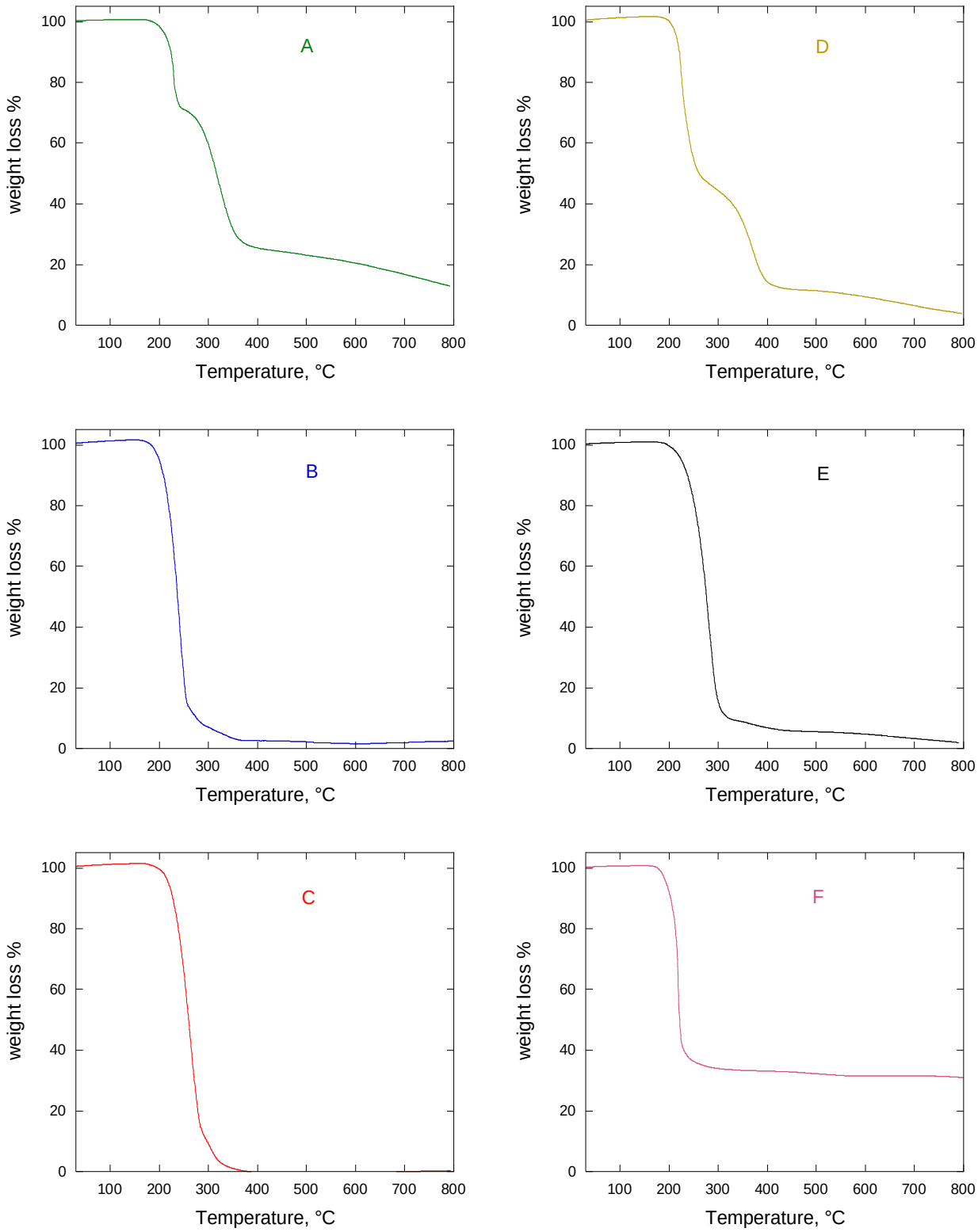


**Figure 2.7** TGA thermograms of (A) CAFA, (B) FA, (C) SA, (D) *p*-CA, (E) *m*-CA, and (F) *o*-CA acids.

**Table 2.4** Onset Melting ($T_M$) and Decomposition ($T_D$) temperatures of [Cho][HCA] ILs.[a]

| Compound | DSC $T_M$, °C | TGA $T_D$, °C |
|---|---|---|
| [Cho][Fer] | - | 105 |
| [Cho][Sin] | - | 103 |
| [Cho][Caf] | 141[b] | 148 |
| [Cho][*p*-Coum] | - | 118 |
| [Cho][*m*-Coum] | - | 132 |
| [Cho][*o*-Coum] | - | 180 |

[a] Temperature accuracy of ± 1 °C. [b] Incongruent melting (the decomposition occurs either just after melting is complete or even simultaneously)

## 2.4 Conclusions

Six hydroxycinnamic acids, poorly water-soluble antioxidant compounds, were converted into ionic liquids containing cholinium cation and hydroxycinnamic based anion ([Cho][HCA] ILs). The structures and purity of this new class of HCA derivatives were confirmed with FT-IR, $^{1}H$ and $^{13}C$ NMR spectroscopy. All the synthesized [Cho][HCA] ILs and the acidic precursors were evaluated for their solubility and thermal stability. The synthesized compounds exhibited water solubilities much higher than those of the corresponding hydroxycinnamic acids (on average, 3 orders of magnitude higher). Furthermore, ILs were found generally to display a good thermal stability (up to 100 °C) although lower than that of the corresponding HCAs. Thus, the present results suggest that synthesis of [Cho][HCA] ILs could be a useful method to overcome the solubility problems of parent acids. The improvement of solubility and the satisfactory stability of salts implies the possibility to develop HCA derivatives with higher bioavailability and good shelf-life.

## 2.5 Experimental section

### *2.5.1 Materials*

Cholinium hydroxide ([Cho]OH, in water solution at 46 wt %), trans-caffeic acid (98 wt % of purity), trans-ferulic acid (99 wt % of purity), methanol (99.8 wt % of purity), ethyl acetate (99.8 wt % of purity), acetone (99.9 wt % of purity) and reagents for potentiometric-

spectrophotometric titration (HCl, NaCl, KOH) were purchased from Sigma-Aldrich. Sinapic (98 wt % of purity), *p*-coumaric (98 wt % of purity), trans-*m*-coumaric (99 wt % of purity), and trans-*o*-coumaric (98 wt % of purity) acids were purchased from Alfa Aesar. Deuterated dimethyl sulphoxide (DMSO-$d_6$, 99.9 atom% D) was purchased from Cambridge Isotope Laboratories, Inc. Carbonate free potassium hydroxide solutions were prepared according to the literature[18].

### *2.5.2 NMR and IR spectroscopy and elemental analysis*

NMR spectra were acquired using a Bruker Advance III HD 600 spectrometer. The NMR chemical shifts (δ) are reported in part per million downfield from tetramethylsilane (TMS), which was used as internal standard, and the spectra were recorded in DMSO-$d_6$. IR spectra were recorded on a Vector 22 spectrometer (Bruker, Bremen, Germany) in Nujol mulls. The elemental analyses were performed by using a PerkinElmer series II-2400 CHNS/O analyzer.

### *2.5.3 Protonation equilibria*

Protonation equilibria of HCAs were investigated by a combination of potentiometric and spectrophotometric methods as previously described.[18,20] Briefly, the acid-base titrations were performed in 0.1 M NaCl at 298.1 ± 0.1 K using an automated Titrando 905 Metrohm titrator. The thermostated glass-cell was equipped with a magnetic stirrer system, a Metrohm LL 60234100 UNITRODE glass electrode, a microburet delivery tube, and an inlet–outlet tube for Argon. The combined Metrohm 6.0262.100 electrode was calibrated as a hydrogen-ion concentration probe by titrating previously standardized amounts of HCl with $CO_2$-free NaOH solutions and determining the equivalent point by Gran's method,[21] which gives the standard potential, E°, and the ionic product of water ($pK_w$ = 13.74(1) in 0.1 M NaCl at 298.1 K). The working molecule concentration was $3.0 \times 10^{-4}$ M. Measurements were done with the use of a Varian Cary 50 UV–vis spectrophotometer Dissolution System in the 200–400 nm spectral range, using 0.2 cm optical path length. Protonation data were analysed using HyperQuad2013 (http://www.hyperquad.co.uk/HQ2013.htm), Hyss and HypSpec (www.hyperquad.co.uk/HypSpec2014.htm) programs.

### *2.5.4 Water solubility*

The maximum water solubility of hydroxycinnamic acids and their corresponding cholinium

salts was determined by UV spectroscopy. The spectrophotometric measurements were performed by a Varian Cary 50 UV-vis spectrophotometer. The saturated aqueous solutions of acids/HCAs and corresponding salts were equilibrated at constant temperature (298.0 ± 0.5 K) and under agitation for 10 minutes. After the equilibration time, all samples were centrifuged at 298.0 ± 0.5 K for 10 min at 6000 rpm. Each solution was properly diluted before the analysis and the pH was measured (Table S2) with the Metrohm LL 60234100 UNITRODE glass electrode calibrated daily with Gran's Method.[21] The product concentrations were calculated on the base of Lambert-Beer equation ($A=c\cdot\varepsilon\cdot l$, where A is the absorption at proper wavelength, c corresponds to the molar concentration, ε is the molar absorptivity coefficient, and l is the path length expressed in cm). Due to variability of UV spectra of each studied molecule as a function of pH, the wavelength (λ [nm]) at isosbestic point was chosen for the analysis. The isosbestic point corresponds to the wavelength at which the total absorbance of the samples is constant. Since each protonation state of the molecule had different isosbestic points, the proper isosbestic points were chosen on the base of the pH of the analyzed solution (properly diluted before the measurement in order to obtain absorption values in the 0-1 range). Triplicate measurements were performed.

### *2.5.5 Thermal Characterization*

A Perkin Elmer STA6000 instrument was used to carry out simultaneous thermogravimetric (TG) and Differential Scanning Calorimetry (DSC) analysis at atmospheric pressure and under a nitrogen flow of 60 mL $min^{-1}$. A total of 5 mg of each compound was placed in an alumina crucible, and measurements were performed in the temperature range of 30÷800 °C (heating rate of 10 °C $min^{-1}$). Standard samples were used to calibrate the instrument (temperature accuracy of ± 1 °C).

## References


1. Serajuddin, A. T. M. (2007). Salt formation to improve drug solubility. Advanced drug delivery reviews. **59**, 603–616.
2. Zhi Hui, L., Asim Kumar, S. and Paul Wan, S. H. (2015). ScienceDirect Overview of milling techniques for improving the solubility of poorly water-soluble drugs. Asian Journal of Pharmaceutical Sciences **10**, 255–274.
3. Babić, S., Horvat, A. J. M., Mutavdžić Pavlović, D. and Kaštelan-Macan, M. (2007). Determination of pKa values of active pharmaceutical ingredients. TrAC - Trends in Analytical Chemistry **26**, 1043–1061.
4. Qiang, Z. and Adams, C. (2004). Potentiometric determination of acid dissociation constants ( p K a ) for human and veterinary antibiotics. Water Research. **38**, 2874–2890.
5. Albert, A. and Serjeant, E. P. (1984). The Determination of Ionization Constants doi:10.1007/978-94-009-5548-6
6. Basu, P., Alexander, K. S. & Riga, A. T. (2006). A statistical model for the optimization of dsc performance in the evaluation of drugs for preformulation studies. Journal of Thermal Analysis and Calorimetry. **83**, 19–22.
7. Pyramides, G., Robinson, J. W. and Zito, S. W. (1995). Analysis of atenolol tablets. Journal of Pharmaceutical and Biomedical Analysis. **13**, 103–110.
8. Welton, T. Room-Temperature Ionic Liquids. Solvents for Synthesis and Catalysis. (1999). Chemical Review**. 99**, 2071–2083.
9. Vekariya, R. L. (2017). A review of ionic liquids: Applications towards catalytic organic transformations. Journal of Molecular Liquids. **227**, 40.
10. MacFarlane, D. R., Kar, M. and Pringle, J. M. (2017). Synthesis of Ionic Liquids. Fundamentals of Ionic Liquids (From Chemistry to applications) 81–102.
11. Ohno, H. (2006). Functional design of ionic liquids. Bulletin of the Chemical Society of Japan. **79**, 1665–1680.
12. Anouti, M., Caillon-Caravanier, M., Dridi, Y., Galiano, H. and Lemordant, D. (2008). Synthesis and characterization of new pyrrolidinium based protic ionic liquids. Good and superionic liquids. Journal of Physical Chemistry B. **112**, 13335–13343.
13. García-Suárez, E. J., Menéndez-Vázquez, C. and García, A. B. (2012). Chemical stability of choline-based ionic liquids supported on carbon materials. Journal of Molecular Liquids. **169**, 37–42.
14. Tao, G.H., He, L., Liu, W.S., Xu, L., Xiong, W., Wang, T., and Kou, Y. (2006).

Preparation, characterization and application of amino acid-based green ionic liquids. Green Chemistry. **8**, 639–646.

15. Ohno, H. and Yoshizawa, M. (2002). Ion conductive characteristics of ionic liquids prepared by neutralization of alkylimidazoles. Solid State Ionics. **154**–**155**, 303–309.
16. Petkovic, M., Ferguson, J. L., Gunaratne, H. Q. N., Ferreira, R., Seddon, K. R., Rebelo L. P. N. and Pereira, C. S. (2010). Novel biocompatible cholinium-based ionic liquids - Toxicity and biodegradability. Green Chemistry. **12**, 643–649.
17. Fukaya, Y., Iizuka, Y., Sekikawa, K. and Ohno, H. (2007). Bio ionic liquids: Room temperature ionic liquids composed wholly of biomaterials. Green Chemistry. **9**, 1155–1157.
18. Abbott, A. P., Capper, G., Davies, D.L., Munro, H.L., Rasheed, R.K. and Tambyrajah, V. (2001). Preparation of novel, moisture-stable, lewis-acidic ionic liquids containing quaternary ammonium salts with functional side chains. Chemical Communications. **1**, 2010–2011.
19. Gadilohar, B. L., Kumbhar, H. S. and Shankarling, G. S. (2014). Choline peroxydisulfate: Environmentally friendly biodegradable oxidizing TSIL for selective and rapid oxidation of alcohols. Industrial & Enginering Chemistry Research. **53**, 19010–19018.
20. Nockemann, P., Thijs, B., Driesen, K., Janssen, C. R., Van Hecke, K., Van Meervelt, L., Kossmann, S., Kirchner, B., and Binnemans K. (2007). Choline saccharinate and choline acesulfamate: Ionic liquids with low toxicities. Journal of Physical Chemistry B. **111**, 5254–5263.
21. Liu, Q. P., Hou, X. D., Li, N. (2012). and Zong, M. H. Ionic liquids from renewable biomaterials: Synthesis, characterization and application in the pretreatment of biomass. Green Chemistry. **14**, 304–307.
22. Gomes, J. M., Silva, S. S. and Reis, R. L. (2019). Biocompatible ionic liquids: Fundamental behaviours and applications. Chemical Society Reviews. **48**, 4317–4335.
23. Adams, M. L., O'Sullivan, B., Downard, A. J. and Powell, K. J. (2002). Stability constants for aluminum(III) complexes with the 1,2-dihydroxyaryl ligands caffeic acid, chlorogenic acid, DHB, and DASA in aqueous solution. Journal of Chemistry & Enginering Data. **47**, 289–296.
24. Matus, M. H., Domínguez, Z., Salas-Reyes, M., Hernández, J. and Cruz-Sánchez, S. (2010). Conformational study of caffeic acid derivatives. Journal of Molecular Structure. THEOCHEM **953**, 175–181.
25. Kontogianni, V. G. Charisiadis, P., Primikyri, A., Pappas, C.G., Exarchou, V., Tzakos,

A.G. and Gerothanassis, I.P. (2013). Hydrogen bonding probes of phenol -OH groups. Organic & Biomolecular Chemistry. **11**, 1013–1025.

26. Lachowicz, J. I., Nurchi, V. M., Crisponi, G., Pelaez, M. J., Rescigno, A., Stefanowicz, P., Cal, M. and Szewczuk, Z. (2015). Metal coordination and tyrosinase inhibition studies with Kojic-βAla-Kojic. Journal of Inorganic Biochemistry. **151**, 36–43.
27. Mota, F. L., Queimada, A. J., Pinho, S. P. and Macedo, E. A. (2008). Aqueous solubility of some natural phenolic compounds. Industrial & Enginering Chemistry Research. **47**, 5182–5189.
28. António, J. Q., Mota, F. L., Pinho, S. P. and Macedo, E. A. (2009). Solubilities of biologically active phenolic compounds: Measurements and modeling. Journal of Physical Chemistry B. **113**, 3469–3476.
29. Erdemgil, F. Z., Şanli. S., Şanli, N., Özkan, G., Barbosa, J., Guiteras, J. and J.L. Beltrán. (2007). Determination of pKa values of some hydroxylated benzoic acids in methanol-water binary mixtures by LC methodology and potentiometry. Talanta **72**, 489–496.
30. Beltrán, J. L., Sanli, N., Fonrodona, G., Barrón, D., Özkan, G. and Barbosa, J. (2003). Spectrophotometric, potentiometric and chromatographic pKa values of polyphenolic acids in water and acetonitrile-water media. Analytica Chimica Acta. **484**, 253–264.
31. Nurchi, V. M., Pivetta, T., Lachowicz, J. I. and Crisponi, G. (2009). Effect of substituents on complex stability aimed at designing new iron(III) and aluminum(III) chelators. Journal of Inorganic Biochemistry. **103**, 227–236.
32. Dalla Torre, G., Mujika, J. I., Lachowicz, J. I., Ramos, M. J. and Lopez, X. (2019). The interaction of aluminum with catecholamine-based neurotransmitters: Can the formation of these species be considered a potential risk factor for neurodegenerative diseases. Dalton Transition. **48**, 6003–6018.
33. Lachowicz, J. I., Nurchi, V. M., Crisponi, G., Jaraquemada-Pelaez, M.; Ostrowska, M., Jezierska, J., Gumienna-Kontecka, E., Peana, M., Zoroddu, M. A., Choquesillo-Lazarte, D., Niclós-Gutiérrez, J. and González-Pérez, J. M. (2015). Zinc(II) and copper(II) complexes with hydroxypyrone iron chelators. Journal of Inorganic Biochemistry. **151**, 94–106.
34. Sintra, T., Luís, A., Rocha, S., Lobo Ferreira, A. I. M. C., Gonçalves, F., Santos, L. M. N. B. F., Neves, B. M., Freire, M. G., Ventura, S. P.M. and Coutinho, J. A.P. (2015). Enhancing the antioxidant characteristics of phenolic acids by their conversion into cholinium salts. ACS Sustainable Chemistry Enginering. **3**, 2558–2565.

# 3

# Antioxidant activity and cytotoxicity of Cholinium Hydroxycinnamate-based Ionic Liquids

## 3.1 Introduction

Plants produce thousands of phenolic compounds as secondary metabolites that exert the role of free radical scavenger.[1] Their antioxidant action stem mainly by reacting with highly reactive species forming more stable and innocuous radicals for cells with respect to the inhibited ones, or turning off the radical chain reactions. Such action helps preventing the attack of radical species to biological macromolecules and thus limiting their damages.[2] HCAs derivatives have been found to have very good antioxidant properties.[3,4] It is widely established that the most essential structural characteristic of these metabolites which provide them an effective antioxidant activity is the presence of phenolic OH groups, which enhance the ability of such a molecules to quench the free radicals.[5] Despite the fact that many natural compounds display antioxidant activity, the list of authorized antioxidant additives it is still incredibly restricted, mainly due to solubility issues.[6]

In this thesis, the experimental antioxidant activity of the six [Cho][HCA] ILs, synthesised as described in the previous chapter, was evaluated by using the 2,2-diphenyl-2-picrylhydrazyl hydrate (DPPH) method[7] and their cytotoxicity was measured by 3-(4,5-dimethylthiazol-2-yl)-2,5-diphenyltetrazolium bromide (MTT) assay. For the sake of comparison, these assays were performed also on the parent acids. To gain an insight into the antioxidant mechanism of actions of cholinium salts and acids and on how the radical-scavenging activity is affected by the protonation state, the electronic properties of possible intermediates in their oxidation process were investigated by means of quantum mechanical (QM) calculations.

QM methods allow fairly accurate theoretical description of chemical reactions and other electronic processes, such as charge transfer or electronic excitation in molecular systems of up to a few hundred atoms.[8] Furthermore, with the development of the hybrid quantum-mechanics/molecular-mechanics (QM/MM) approach it is possible to understand and predict the chemical reactivity of extended chemical systems.[9] In a combined QM/MM computation, the system under study is partitioned in two or more regions in which the site of interest containing typically a few hundred atoms (a molecule or a fragment of a large molecular complex) can be modelled with high accuracy using QM methods, whereas the "environment" to the QM part is treated in a more approximate manner employing cheaper MM techniques.[9,10]

Among the main approximations used to solve the Schrödinger equation, that is, purely *ab initio* Hartree-Fock (HF), post HF methods based on the electronic wavefunctions (WFT), semiempirical methods and methods based on the Density Functional theory (DFT), the latter are by far the most used methods to study chemical systems of pharmaceutical interest. DFT methods can be applied to study both soft or hard matter, and generally allow accurate prediction

of the physical and chemical properties. The diffusion of DFT compared to WFT methods is due to the fact that DFT methods couple a relatively low computational cost with a reasonable accuracy. Compared to HF methods, DFT has the advantage of incorporating the correlation among electrons with a much lower computational cost than correlated wavefunction methods, such as Moller-Plesset perturbation theory, configuration interaction, multiconfiguration self-consistent field theory or coupled cluster theory.[11]

A quite large, and fastly increasing number of functionals are available nowadays. The most popular still being the B3LYP functional, even if its performance for a variety of systems have been questioned. By choosing the appropriate basis sets and functional for the study of the system of interest, DFT methods can be employed to predict relative conformational energies, binding energies, electron affinities, ionization energies, molecular geometries, transition barriers, metal-ligand bond strengths and transition metal reaction pathways readily.[12] Very importantly in the context of my study, DFT calculation are certainly the most popular and versatile to predict and rationalize the antioxidant properties of molecules.[13–16] Indeed, to investigate the mechanisms involved in the free radical–scavenging reactions and their likelihood in the studied process, DFT calculations of specific thermodynamical parameters are a key tool,[17,18] and their use will be further discussed in section 3.4.

## 3.2 Radical scavenging activity of [Cho][HCA] ILs

The radical scavenging capacity of HCAs and [Cho][HCA] ILs was measured *in vitro* by using the DPPH assay, one of the most commonly used antioxidant assays for plant extracts. This method is based on the scavenging of DPPH by antioxidants which decolorizes the DPPH methanol solution upon a reduction reaction (see Experimental section). Measuring the reducing ability of antioxidants toward the DPPH radical allows to built set-activity curves as a function of the concentration of the antioxidant agents to estimate the $EC_{50}$ (half maximum effective concentration) parameter. $EC_{50}$ essentially represents the required concentration for an antioxidant to reach 50% of scavenging free radical activity: the lower $EC_{50}$ value, the higher scavenging free radical activity of an antioxidant.

Table 3.1 shows the mean $EC_{50}$ values (± standard deviation) of three independent measurements for every compound under investigation with the exception of *o*-CA and *m*-CA and the corresponding cholinium salts. Indeed, the DPPH solutions of these latter samples reached discoloration levels lower than 50% at analyte concentrations higher than 25 mM, indicative of a very weak antioxidant activity (14 and 16 % for *m*-CA and [Cho][*m*-Coum],

respectively; 35 and 37 % for *o*-CA and [Cho][*o*-Coum] respectively).

Significant differences ($p < 0.05$) were observed among the scavenging activity of HCAs. The results showed the following decreasing order: CAFA > SA > FA > *p*-CA >> *o*-CA, *m*-CA. Thus, the most potent compound was caffeic acid, while the lowest antioxidant activity was exhibited by *o*-, *m*-, and *p*-coumaric acids. Investigations aimed at evaluating the antioxidant activities of cinnamic and benzoic acid derivatives have indicated a structure-activity relationship in the model systems.[19] As shown by the DFT results reported below, the structures of HCAs and [Cho][HCA] ILs under investigation are nearly planar in solution. Thus, any differences in activity among them should be ascribed to electronic phenomena rather than to steric hindrance effects. According to the literature,[19] the higher radical scavenging ability of CAFA in comparison to the other HCAs can be explained by the presence of an additional hydroxy group that increases the resonance stabilization, while SA and FA are more effective than *o*-, *m*- and *p*-CA due to the electron-donating methoxy group(s) which stabilize the phenoxy radical after hydrogen donation of the hydroxy group.

Interestingly, the conversion of HCAs into Cho-based ILs influenced positively the radical scavenging activity. Indeed, as can be seen in Table 3.1, all of the synthesized ILs were able to inhibit DPPH free radical scavenging at $EC_{50}$ values lower than that measured for the corresponding parent acids. As observed for HCAs, the most efficient cholinium salt was [Cho][Caf]. The possible mechanisms responsible of the antioxidant activities and their relationship with the DPPH experimental results are discussed in detail below, together with the finding of DFT calculations.

**Table 3.1** Antioxidant activity of HCAs and respective [Cho][HCA] ILs against DPPH

| **Compound** | **$EC_{50}$ (μM)[a]** |
|---|---|
| FA | 81.5 ± 1.1 |
| [Cho][Fer] | 76.4 ± 0.8 |
| SA | 62.9 ± 0.5 |
| [Cho][Sin] | 61.7 ± 0.3 |
| CAFA | 35.0 ± 0.6 |
| [Cho][Caf] | 33.4 ± 0.1 |
| *p*-CA | 25390 ± 741 |
| [Cho][*p*-Coum] | 22264 ± 1042 |

[a] $EC_{50}$ for concentration of antioxidant necessary to decrease the initial DPPH radical concentration by 50%. Values are means of three determinations ± standard deviation.

## 3.3 Cytotoxicity of [Cho][HCA] ILs

The influence of [Cho][HCA] ILs on the cell viability was determined on murine melanoma B16-F10 and murine fibroblast 3T3 cells with MTT assay. Compounds were tested at concentrations between 6.25 and 200 μmol/L. The dose–response cytotoxicity results are depicted in Figure 3.1 As can be seen, no one of the Cho-based ILs was found to have cytotoxic activity on both cell lines  in both cell lines at the concentration under investigation except for [Cho][Caff] that induced a significant reduction ($p < 0.001$) of B16-F10 tumoral cell viability (22,39 %) at the highest dose.

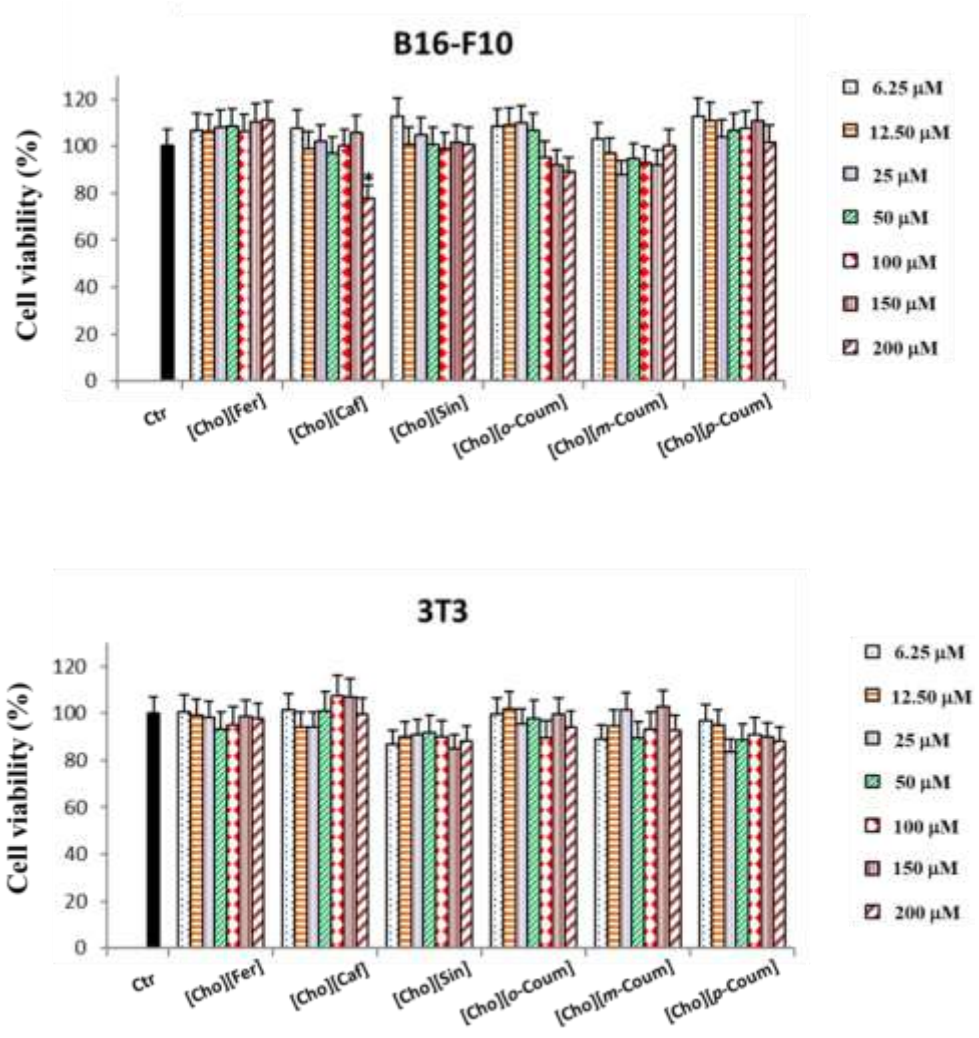


**Figure 3.1** Cell viability results (%) by MTT assay of melanoma B16F10 and fibroblast 3T3 cell lines exposed to different concentration of [Cho][HCA] ILs. Results are expressed as mean ± SD values of three observations; * significantly different from control ($p < 0.001$)

## 3.4 Computational study of antoxidant activity

### *3.4.1 Antioxidant mechanisms*

In this thesis, three well-known antioxidant mechanisms[20,21] were theorethically investigated with DFT method to elucidate the radical-scavenging processes of the hydroxycinnamates ($HCA^-$) and the corresponding acid precursors (HCA): the hydrogen atom transfer (HAT), single-electron transfer–proton transfer (SET–PT) and sequential proton loss electron transfer (SPLET). Table 3.2 schematizes the reaction mechanisms for HAT, SET-PT and SPLET and the equations of the related thermodynamic parameters. I note that the total energy of each reaction comprises the thermodynamic parameters of both the antioxidant and the particular radical species ($R^\bullet$) considered. Since in this thesis I have focused my attention on comparing the reactivity of the hydroxycinnamates with the corresponding hydroxycinnamic acids, and the reactivity between different species of the same class, I have limited my attention to the antioxidant species, following the procedure already applied on similar systems.[15,16,21,22]

**Table 3.2** Chemical equations of HAT, SPLET and SEPT mechanisms and the corresponding thermodynamic parameters calculated for the antioxidant species.

| **Reaction mechanisms** | **Chemical Equations** | **Thermodynamic Parameters** |
|---|---|---|
| | *Hydroxycinnamic Acid* | |
| HAT | $HCA + R^\bullet \rightarrow CA^\bullet + RH$ | $BDE = H(CA^\bullet) + H(H^\bullet) - H(HCA)$ |
| SET-PT (step 1) | $HCA^{\bullet+} + R^- \rightarrow CA^\bullet + RH$ | $IP = H(HCA^{+\bullet}) + H(e^-) - H(HCA)$ |
| SET-PT (step 2) | $HCA + R^\bullet \rightarrow HCA^{\bullet+} + R^-$ | $PDE = H(CA^\bullet) + H(H^+) - H(HCA^{\bullet+})$ |
| SPLET (step 1) | $HCA \rightarrow CA^- + H^+$ | $PA = H(CA^-) + H(H^+) - H(HCA)$ |
| SPLET (step 2) | $CA^- + R^\bullet \rightarrow CA^\bullet + R^-$ | $ETE = H(CA^\bullet) + H(e\text{-}) - H(CA^-)$ |
| | *Hydroxycinnamate* | |
| HAT | $HCA^- + R^\bullet \rightarrow CA^{-\bullet} + RH$ | $BDE = H(CA^{-\bullet}) + H(H^\bullet) - H(HCA^-)$ |
| SET-PT (step 1) | $HCA^\bullet + R^- \rightarrow (CA^{-\bullet}) + RH$ | $IP = H(HCA^\bullet) + H(e^-) - H(HCA^-)$ |
| SET-PT (step 2) | $HCA^- + R^\bullet \rightarrow HCA^\bullet + R^-$ | $PDE = H(CA^{-\bullet}) + H(H^+) - H(HCA^\bullet)$ |
| SPLET (step 1) | $HCA^- \rightarrow CA^{2-} + H^+$ | $PA = H(CA^{2-}) + H(H^+) - H(HCA^-)$ |
| SPLET (step 2) | $CA^{2-} + R^\bullet \rightarrow CA^{-\bullet} + R^-$ | $ETE = H(CA^{-\bullet}) + H(e\text{-}) - H(CA^{2-})$ |

As shown in Table 3.2, HAT is a single step mechanism involving the formal hydrogen atom transfer from the radical scavenger to a reactive radical ($R^{\bullet}$) and thus the formation of a radical by the loss of a phenolic hydrogen atom in HCA and $HCA^-$ (i.e. $CA^{\bullet}$ and $CA^{-\bullet}$, respectively in Table 3.1) and the formation of a radical by the loss of a phenolic hydrogen atom in HCA and $HCA^-$ (i.e. $CA^{\bullet}$ and $CA^{-\bullet}$, respectively, in Table 3.2).

An important parameter to evaluate the probability of the antioxidant action through the HAT mechanism is the bond dissociation enthalpy (BDE) of the phenolic O-H bond which releases the hydrogen. Compounds having the hydroxyl group(s) with lower BDE values are expected to be the most active with the HAT mechanism. Since the OH of carboxylic group is known to have BDE higher than that of phenolic OH,[23] the involvement of the carboxylic group in the radical scavenging has not be taken into account.

SET-PT is a double step mechanism (Table 3.2). The first step involves the loss of one electron and it is thus related to the ionization potential (IP). In the second and last step, the transfer of a proton from the radical formed in the first step occurs and it is thus correlated to the proton dissociation enthalpy (PDE).

SPLET is a multistep mechanism. The first step is the proton loss (step 1 in Table 3.1), and its energy depends on the proton affinity (PA) of the antioxidant. The second step involves the transfer of an electron, thus it is correlated to the electron transfer enthalpy (ETE). The third and final step is the protonation of the anion formed in the previous step.

To calculate the thermodynamic parameters related to the considered steps of the three mechanisms HAT, SEPT-PT and SPLET, I performed a full conformational search for all of the studied HCAs, HCAs-, and of all of the intermediate species involved. Vibrational analysis was performed for each species, and in all cases DFT method(s) were employed as better specified in the following.

### *3.4.2 Conformational analysis*

While many computational investigations on HCAs have been focused on the antioxidant activity of the undissociated carboxylic acids,[14,21,23,24 18,25–27] in the present study I have considered the corresponding carboxylate forms, and hydroxycinnamic acids were included mainly for comparative purposes. A full conformational analysis was performed *in vacuo* on all of the compounds and on all the intermediates involved in the radical scavenging activity. In Figure 3.2 the global minima structures obtained for all the species involved in the antioxidative process are

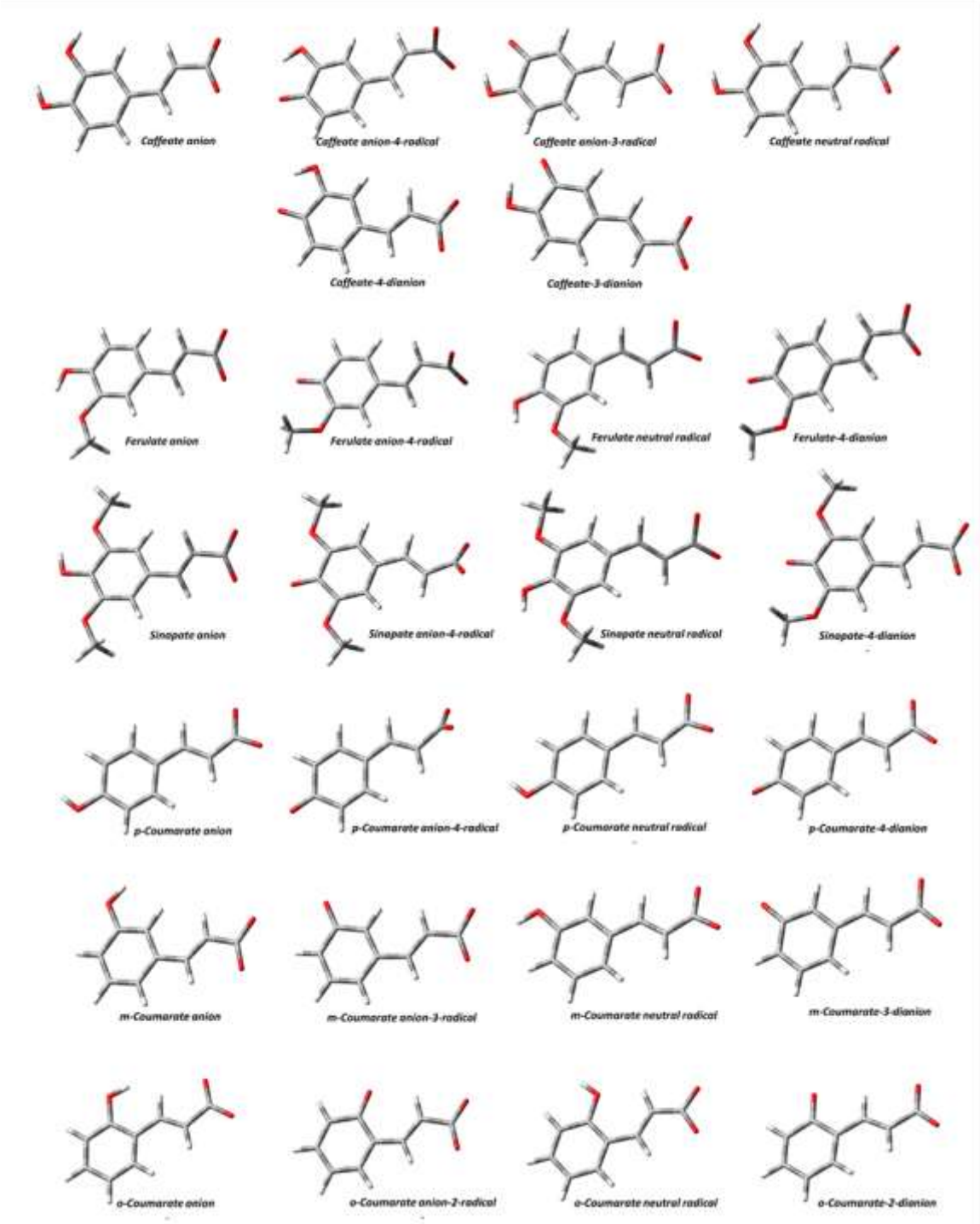


**Figure 3.2** Representation of the global minima of the studied hydroxycinnamates calculated *in vacuo* at the UB3LYP/6-311++G(d,p), and of all the intermediate species involved in the antioxidant process.

represented. Analogous calculations were carried out on the HCAs (see Experimental section).

The effects on the geometry and on the electronic properties of the two solvents used in the radical scavenging experiment, i.e. water and ethanol was estimated by further optimizing the *in vacuo* global minimum structure of each species using a polarizable continuum model (PCM) and the current implementation in Gaussian 16, performing a reaction field calculation using the integral equation formalism IEF-PCM.[28,29]

### *3.4.3 Proton, electron and hydrogen atom enthalpies in gas phase and in solution*

The calculated gas phase enthalpy of a proton and electron are 1.483 and 0.752 kcal/mol, respectively and were calculated at DFT B3LYP/6-311++G** theory level. Proton and electron solvation enthalpies were taken from Rimarcik et al.'s report[30] and references therein,[28,29,31] and are summarized in Table 3.3. The electron solvation enthalpy retrieved by Rimarcik et al.[30] was calculated using the integral equation formalism polarizable continuum model (IEF-PCM) at the B3LYP/6-311++G(d,p) theory level considering the reaction (1) where "Solvent(PCM-solv)" represents a single explicit solvent molecule embedded in the PCM solvent. The proton solvation energy was calculated using an analogous equation.

$$\text{Solvent(PCM-solv)} + e^-(g) \rightarrow \text{solvent-}e^- \text{ (PCM-solv)} \qquad (1)$$

**Table 3.3** Enthalpies in kcal mol$^{-1}$ of solvation ($\Delta_{solv}H$) and in gas phase ($H$) of proton ($H^+$), electron and hydrogen atom ($H^\bullet$).

| | $H$ | $\Delta_{solv}H$ | |
|---|---|---|---|
| | gas phase | water | ethanol |
| $H^\bullet$ | -313.690[a] | -0.0163[c] | -0.0157[c] |
| $e^-$ | 0.752[b] | -25.079[d] | - 18.152 [d] |
| $H^+$ | 1.483[b] | -244.10[d] | -249.594[d] |

[a] Calculated at DFT B3LYP/6-311++G** theory level in gas phase; [b] From ref. [31]; [c] Calculated at IEF/PCM B3LYP/6-311++G** theory level in water or ethanol.[28,29]; [d] From ref. [30]

Electron solvation values calculated with this approximation are known to vary largely not only with the solvent, but also with the solvent model and even more with the theory level. In detail, Markovic et al.[32] found that solvation model D (SMD)[33] produces values more

negative than IEF-PCM and, more importantly, that the solvation enthalpy of the electron with M062X both in ethanol and water is several kcal $mol^{-1}$ lower than that obtained with B3LYP. Data reported by Shameera et al.[34] are in agreement with this estimate. I note that the B3LYP values calculated for water with equation (1) are about 10 kcal $mol^{-1}$ lower than that estimated by Zhan et al.[8] with a more accurate supramolecular approach which takes into account the generally accepted view that the electron is solvated through a hydrogen bond network of several solvent molecules. The values obtained for the electron hydration enthalpy with M062X departs even more from the values obtained by Zhan.[8] Therefore, also for this functional, I used the values in Rimarcik report[4] as a more reliable reference, taking into consideration that underestimation of the absolute value of the solvation enthalpy of the electron would lead to a corresponding increase in the ETE and IP values.

### *3.4.4 Thermodynamic parameters-antioxidant mechanism relationship*

The thermodynamic parameters (TPs) in gas phase were calculated using exclusively the global minima structures. The calculation of the thermodynamical parameters in PCM solvent was performed after subjecting the *in vacuo* global minima to an optimization process in the selected solvating media. These indices calculated at the B3LYP/6-311++G(d,p) theory level are collected in Table 3.4 for both $HCA^-$ and HCA species, while those computed with M06-2X/6-311++G(d,p) are reported in Tables 3.5-3.7. Since the general trends of TPs obtained with the two theory levels are the same (Figures 3.3-3.6), in the following sections each mechanism is discussed in view of the results obtained with B3LYP/6-311++G(d,p), and the same conclusions hold also for M06-2X, unless otherwise specified. It is worth noting that the results for CAFA, FA, SA and *p*-CA are in agreement with those reported in the literature by Chen et al.[21] In the following sections, each mechanism is discussed in view of the obtained results.

### *3.4.5 BDE and HAT mechanism*

To assist with the analysis of the data in Table 3.4, the BDE values are also plotted in Figure 3.5 according to their radical scavenging capability as observed in the DPPH assay. In water, BDE values range from 71.03 to 81.87 kcal $mol^{-1}$ for $HCAs^-$ and from 74.42 to 83.42 kcal $mol^{-1}$ for HCAs. The BDE ranges observed in ethanol environment almost overlap with those in water, with values going from 71.73 to 81.77 kcal $mol^{-1}$ for the $HCA^-$ species and from 74.34 to 83.43 kcal $mol^{-1}$ for HCAs. Compared to the BDE values derived by B3LYP, those computed with M06-2X are slightly higher by about 3-4 kcal mol-1 (Tables 3.5-3.7). Nevertheless, the two

trends are the same (Figures 3.3-3.6). The BDEs obtained for the hydroxycinnamates in gas phase are lower than those obtained taking into account the solvent effects. Such a systematic difference cannot be discerned for the HCAs: for some compounds (CAFA, FA, *o*-CA) the solvent inclusion leads to BDE

**Table 3.4** Thermodynamic parameters (kcal $mol^{-1}$) of HCAs and $HCAs^-$ at the UB3LYP/6-311++G(d,p) level of theory obtained in gas phase, water, and ethanol at 298 K.

| **Medium** | **Site** | **$HCA^-$** | | | | | **HCA** | | | | |
|---|---|---|---|---|---|---|---|---|---|---|---|
| | | BDE | IP | PDE | PA | ETE | BDE | IP | PDE | PA | ETE |
| | | | | **[Caff]** | | | | | **CAFA** | | |
| Gas phase | 4-OH | 60.6 | 78.6 | 297.9 | 385.5 | -9.0 | 73.2 | 180.3 | 208.8 | 319.1 | 70.0 |
| | 3-OH | 66.7 | | 304.0 | 387.0 | -4.4 | 75.6 | | 211.2 | 324.7 | 66.8 |
| Water | 4-OH | 71.0 | 101.4 | 14.8 | 42.3 | 75.3 | 74.4 | 112.4 | 8.6 | 37.1 | 83.9 |
| | 3-OH | 74.1 | | 17.9 | 44.5 | 76.2 | 76.6 | | 10.8 | 40.8 | 82.4 |
| Ethanol | 4-OH | 70.7 | 107.2 | 11.6 | 39.4 | 79.4 | 74.3 | 121.1 | 1.2 | 32.7 | 89.7 |
| | 3-OH | 73.9 | | 14.8 | 41.6 | 80.3 | 76.5 | | 3.4 | 36.4 | 88.1 |
| | | | | **[Sin]** | | | | | **SA** | | |
| Gas phase | 4-OH | 67.9 | 77.5 | 306.3 | 395.0 | -11.1 | 77.2 | 170.2 | 222.9 | 328.2 | 65.0 |
| Water | 4-OH | 71.3 | 98.2 | 19.6 | 50.1 | 67.7 | 74.0 | 108.0 | 11.1 | 45.8 | 74.8 |
| Ethanol | 4-OH | 71.2 | 104.1 | 15.1 | 47.4 | 71.8 | 74.2 | 116.0 | 6.2 | 41.5 | 80.7 |
| | | | | **[Fer]** | | | | | **FA** | | |
| Gas phase | 4-OH | 69.3 | 76.9 | 308.3 | 394.6 | -9.3 | 80.7 | 176.4 | 219.5 | 331.3 | 65.4 |
| Water | 4-OH | 77.9 | 99.9 | 24.6 | 50.4 | 74.1 | 81.2 | 111.2 | 16.6 | 43.7 | 84.1 |
| Ethanol | 4-OH | 77.7 | 105.8 | 19.9 | 47.7 | 78.0 | 81.2 | 119.2 | 10.0 | 39.6 | 89.6 |
| | | | | **[*p*-Coum]** | | | | | ***p*-CA** | | |
| Gas phase | 4-OH | 67.2 | 78.1 | 305.0 | 394.2 | 0.7 | 81.2 | 184.4 | 212.8 | 396.4 | 70.4 |
| Water | 4-OH | 76.8 | 102.2 | 21.1 | 47.4 | 82.9 | 80.9 | 116.8 | 10.7 | 42.0 | 85.6 |
| Ethanol | 4-OH | 76.4 | 107.9 | 16.5 | 44.5 | 79.9 | 80.9 | 124.3 | 4.7 | 37.7 | 91.3 |
| | | | | **[*o*-Coum]** | | | | | **o-CA** | | |
| Gas phase | 2-OH | 76.1 | 81.7 | 310.4 | 405.7 | -13.7 | 80.8 | 187.5 | 209.3 | 328.7 | 68.1 |
| Water | 2-OH | 78.4 | 108.3 | 16.6 | 47.5 | 77.5 | 81.3 | 119.8 | 8.1 | 42.0 | 85.9 |
| Ethanol | 2-OH | 78.5 | 113.6 | 12.9 | 45.2 | 81.3 | 81.3 | 127.3 | 2.0 | 37.8 | 91.5 |
| | | | | **[*m*-Coum]** | | | | | ***m*-CA** | | |
| Gas phase | 3-OH | 78.4 | 80.7 | 313.6 | 398.2 | -3.9 | 84.1 | 190.1 | 210.0 | 336.3 | 63.8 |
| Water | 3-OH | 81.9 | 107.4 | 21.1 | 48.3 | 78.7 | 83.4 | 121.9 | 8.2 | 47.1 | 83.0 |
| Ethanol | 3-OH | 81.8 | 115.5 | 14.3 | 47.1 | 82.7 | 83.4 | 129.5 | 2.0 | 48.4 | 88.5 |

**Table 3.5** Thermodynamic parameters calculated in gas phase using M06-2X/6-311++G(d,p). For the sake of comparison between the two functionals, data obtained with B3LYP/6-311++G(d,p) are also reported.

| | B3LYP | | | | | M06-2X | | | | |
|---|---|---|---|---|---|---|---|---|---|---|
| | BDE | IP | PDE | PA | ETE | BDE | IP | PDE | PA | ETE |
| | (Kcal mol$^{-1}$) | | | | | (Kcal mol$^{-1}$) | | | | |
| [Caff] | 60.6 | 78.6 | 297.9 | 385.5 | -9.0 | 67.4 | 86.4 | 296.9 | 387.4 | -4.1 |
| [Sin] | 67.9 | 77.5 | 306.3 | 395.0 | -11.1 | 72.0 | 85.1 | 302.8 | 395.8 | -7.9 |
| [Fer] | 69.2 | 76.9 | 308.3 | 394.5 | -9.4 | 74.8 | 84.1 | 306.6 | 395.5 | -4.8 |
| [*p*-Coum] | 67.2 | 78.1 | 305.0 | 394.2 | -11.1 | 72.8 | 85.1 | 303.6 | 395.2 | -6.5 |
| [*o*-Coum] | 76.1 | 81.7 | 310.4 | 405.7 | -13.7 | 83.2 | 88.7 | 310.4 | 406.9 | -7.7 |
| [*m*-Coum] | 78.4 | 80.7 | 313.6 | 398.2 | -3.9 | 82.8 | 88.1 | 310.6 | 398.7 | 0.0 |
| CAFA | 73.2 | 180.3 | 208.8 | 319.1 | 70.0 | 76.3 | 185.9 | 206.4 | 321.7 | 70.5 |
| SA | 77.2 | 170.2 | 222.9 | 328.2 | 65.0 | 81.5 | 175.9 | 221.6 | 329.8 | 67.6 |
| FA | 80.7 | 176.4 | 219.5 | 331.3 | 65.4 | 83.8 | 182.2 | 216.8 | 333.4 | 66.4 |
| *p*-CA | 81.2 | 184.4 | 212.7 | 326.7 | 70.4 | 84.3 | 189.9 | 210.3 | 328.8 | 71.4 |
| *o*-CA | 80.8 | 187.4 | 209.3 | 328.7 | 68.1 | 83.9 | 193.3 | 206.6 | 330.1 | 69.8 |
| *m*-CA | 84.1 | 190.1 | 210.0 | 336.3 | 63.8 | 86.9 | 196.3 | 206.5 | 337.8 | 65.0 |

**Table 3.6** Thermodynamic parameters calculated using PCM water solvent and M06-2X/6-311++G(d,p). For the sake of comparison between the two functionals, data obtained with B3LYP/6-311++G(d,p) are also reported.

| | B3LYP | | | | | M06-2X | | | | |
|---|---|---|---|---|---|---|---|---|---|---|
| | BDE | IP | PDE | PA | ETE | BDE | IP | PDE | PA | ETE |
| | (Kcal mol$^{-1}$) | | | | | (Kcal mol$^{-1}$) | | | | |
| [Caff] | 71.0 | 101.4 | 16.3 | 42.3 | 75.3 | 74.9 | 110.2 | 11.3 | 43.0 | 78.5 |
| [Sin] | 71.3 | 98.2 | 19.6 | 50.1 | 67.7 | 74.6 | 106.7 | 14.5 | 50.0 | 71.1 |
| [Fer] | 77.9 | 99.9 | 24.5 | 50.4 | 74.1 | 81.6 | 108.8 | 19.4 | 50.4 | 77.8 |
| [*p*-Coum] | 76.8 | 102.2 | 21.1 | 47.4 | 75.9 | 80.6 | 111.8 | 10.8 | 47.8 | 79.4 |
| [*o*-Coum] | 78.4 | 108.3 | 16.6 | 47.5 | 77.5 | 82.3 | 115.7 | 13.1 | 47.8 | 81.1 |
| [*m*-Coum] | 81.9 | 107.4 | 21.1 | 49.8 | 78.7 | 85.2 | 119.7 | 12.0 | 49.1 | 82.7 |
| CAFA | 74.4 | 112.4 | 8.6 | 37.1 | 83.9 | 77.7 | 117.9 | 6.3 | 38.4 | 85.9 |
| SA | 74.0 | 108 | 12.5 | 45.8 | 74.8 | 76.8 | 113.9 | 9.5 | 45.9 | 77.5 |
| FA | 81.2 | 111.2 | 16.6 | 43.7 | 84.1 | 84.5 | 117 | 14.1 | 44.6 | 86.5 |
| *p*-CA | 80.9 | 116.8 | 10.7 | 42.0 | 85.6 | 84.2 | 121.9 | 8.9 | 42.9 | 87.9 |
| *o*-CA | 81.3 | 119.8 | 8.1 | 42.0 | 85.9 | 84.5 | 125 | 6.0 | 42.3 | 88.8 |
| *m*-CA | 83.4 | 121.9 | 8.2 | 47.0 | 83 | 85.8 | 126.3 | 6.1 | 47.2 | 85.2 |

**Table 3.7** Thermodynamic parameters calculated using PCM ethanol solvent and M06-2X/6-311++G(d.p). For the sake of comparison between the two functionals. data obtained with B3LYP/6-311++G(d.p) are also reported

| | B3LYP | | | | | M06-2X | | | | |
|---|---|---|---|---|---|---|---|---|---|---|
| | BDE | IP | PDE | PA | ETE | BDE | IP | PDE | PA | ETE |
| | (Kcal mol$^{-1}$) | | | | | (Kcal mol$^{-1}$) | | | | |
| [Caff] | 70.7 | 107.2 | 11.6 | 39.4 | 79.4 | 74.6 | 116.5 | 6.1 | 40.0 | 82.6 |
| [Sin] | 71.2 | 104.1 | 15.1 | 47.4 | 71.8 | 74.5 | 112.9 | 9.6 | 47.4 | 75.1 |
| [Fer] | 77.7 | 105.8 | 19.9 | 47.7 | 78.0 | 81.4 | 115 | 14.4 | 47.6 | 81.8 |
| [*p*-Coum] | 76.4 | 107.9 | 16.5 | 44.5 | 79.9 | 80.9 | 118.6 | 10.3 | 45.6 | 83.4 |
| [*o*-Coum] | 78.5 | 113.6 | 12.9 | 45.2 | 81.3 | 82.3 | 121.9 | 8.4 | 45.4 | 84.9 |
| [*m*-Coum] | 81.8 | 115.5 | 14.2 | 47.1 | 82.7 | 85.1 | 123.2 | 9.9 | 46.4 | 86.7 |
| CAFA | 74.3 | 121.1 | 1.2 | 32.7 | 89.7 | 77.6 | 126.0 | -0.4 | 34.0 | 91.6 |
| SA | 74.2 | 116.0 | 6.2 | 41.5 | 80.7 | 77.0 | 121.9 | 3.1 | 41.7 | 83.3 |
| FA | 81.2 | 119.2 | 9.9 | 39.6 | 89.6 | 84.5 | 125.0 | 7.4 | 40.6 | 91.9 |
| *p*-CA | 80.9 | 124.3 | 4.7 | 37.7 | 91.3 | 84.2 | 130.0 | 2.2 | 38.6 | 93.6 |
| *o*-CA | 81.3 | 127.3 | 2.0 | 37.8 | 91.5 | 84.5 | 133.1 | -0.6 | 38.1 | 94.3 |
| *m*-CA | 83.4 | 129.5 | 2.0 | 42.9 | 88.5 | 85.8 | 135.1 | -1.2 | 43.2 | 90.7 |

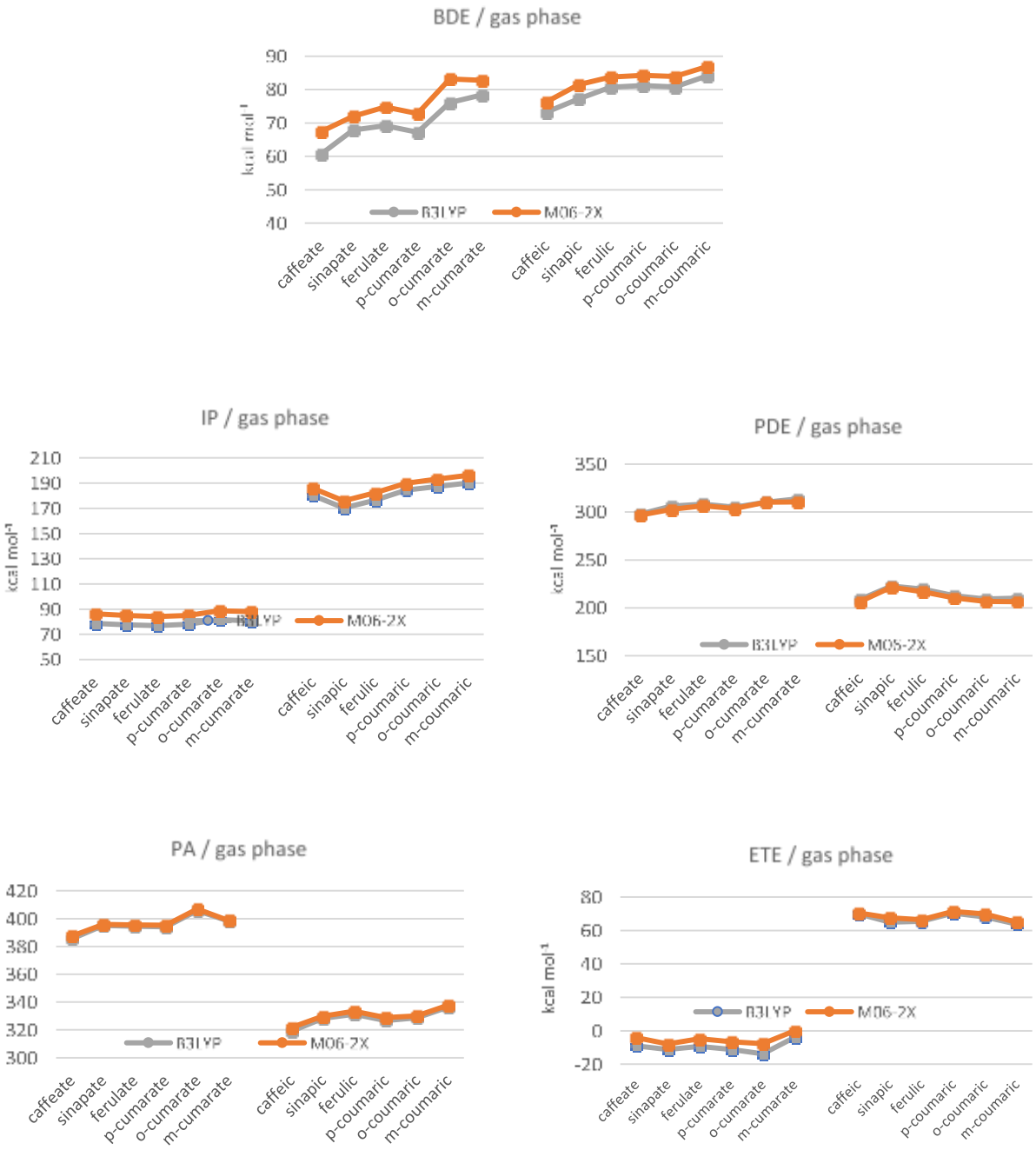


**Figure 3.3** BDE, PA, ETE, IP, PDE values, calculated at the UB3LYP/6-311++G(d,p) or M06-2X/6-311++G(d,p) levels of theory in gas phase for the hydroxycinnamates (left side in each frame) and corresponding acids (right side in each frame).


**Figure 3.4** BDE, PA, ETE, IP, PDE values, calculated at the UB3LYP/6-311++G(d,p) or M06-2X/6-311++G(d,p) levels of theory with PCM solvent model in water for the hydroxycinnamates (left side in each frame) and corresponding acids (right side in each frame).


**Figure 3.5** BDE, PA, ETE, IP, PDE values, calculated at the UB3LYP/6-311++G(d,p) or M06-2X/6-311++G(d,p) levels of theory with PCM solvent model in ethanol for the hydroxycinnamates (left side in each frame) and corresponding acids (right side in each frame).

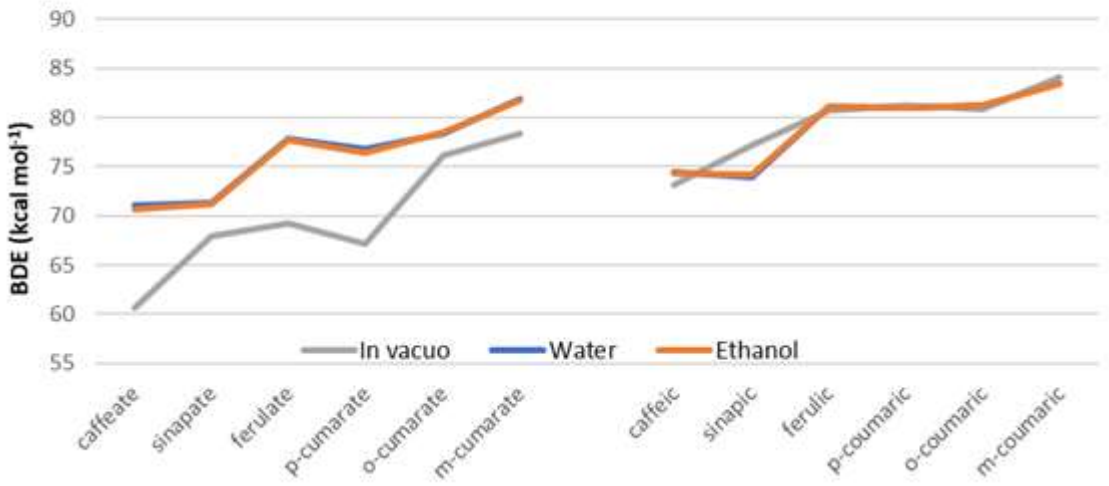


**Figure 3.6** BDE values, calculated at the UB3LYP/6-311++G(d,p) level of theory either in gas phase or with PCM solvent model for water or ethanol for the hydroxycinnamates (left) and corresponding acids (right). The compounds are reported according to their DPPH antioxidant trend.

increase, while for other (SA, *p*-CA, *m*-CA) there is a small decrease. Therefore, while for other compounds[27] it was observed that the O-H dissociation energy increases on going from gas phase to polar media, this cannot be generalized for the undissociated acids in this class of compounds. For both HCAs- and HCAs, the BDE values in PCM for caffeate and sinapate are lower than those of the other compounds, in agreement with the antioxidant trend observed in DPPH assay, and the same is true for the corresponding acid. We note that the BDE values for ferulate and ferulic acid do not follow the antioxidant trend.

As can be noted in Table 3.4, the bond dissociation energy of $HCAs^-$ is always lower than that of the corresponding acidic form in both solvents. A similar trend was observed by Amić et al.[35] in water for the dihydrocaffeic and dihydroferulic acids. These data correlate well with the higher antioxidant activity profile experimentally observed for choline salts.

The correlation observed between the experimental results and the calculated BDE values suggests that in the presence of the radical DPPH, both $HCA^-$s and HCAs can react with a single step mechanism of the HAT type. Furthermore, the BDEs values indicate that the HAT mechanism is thermodynamically more favoured for $HCA^-$s when compared with the corresponding HCAs.

### *3.4.6 IP, PDE and SET-PT mechanism*

As illustrated in Table 3.2, the first step of SET-PT involves the loss of one electron and it is

therefore related to the ionization potential (IP) which quantifies the electron donor capability of a molecule. Molecules with lower IP are more susceptible to the electron transfer and this facilitates reactivity through SET-PT mechanism. The values reported for the coumaric derivatives (Table 3.4) indicate that the -OH group in *para* position shows the lowest IP values due to the best effect of stabilization of the radical by resonance in the phenylpropenoic structure, as already observed be Szeląg et al.[27] for other compounds.

To assist with the analysis of the data in Table 3.4, the IP values are also plotted in Figure 3.7.

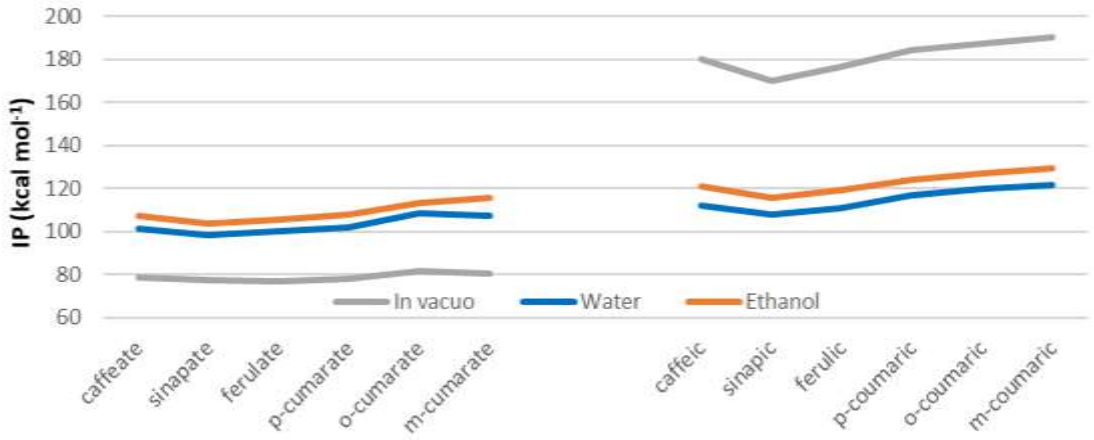


**Figure 3.7** IP values, calculated at the UB3LYP/6-311++G(d,p) level of theory either in gas phase or PCM solvent model for water or ethanol for the hydroxycinnamates (left) and corresponding acids (right). The compounds are reported according to their DPPH antioxidant trend.

The results show that *in vacuo* IP values for $HCAs^-$ (ranging between 76.9 and 81.7 kcal $mol^{-1}$) are significantly lower than that in polar media (ranging from 98.2 to 115.5 kcal $mol^{-1}$), thus indicating that single electron abstraction is easier in absence of the solvent. An opposite behaviour is observed for HCAs showing *in vacuo* IPs higher than in water or ethanol (170.1÷190.1 kcal $mol^{-1}$ *vs* 108.0÷129.5 kcal $mol^{-1}$). The different behaviour between HCAs and $HCAs^-$ can be reasonably explained by the stabilization of ionic species by polar solvents. Comparison of the IP of the same species in water and ethanol indicates that this index decreases with the surrounding medium polarity. This behaviour is observed for both HCAs and $HCAs^-$; however, the largest differences among solvents are observed for the acids. For HCA, with the exception of the caffeic acid, the calculated IPs follow the oxidative trend observed in

the DPPH assay both in solvent and in gas phase. For $HCAs^-$, the DPPH trend is not followed at all by the IP values in gas phase, while in the presence of solvents a better correlation is observed. In the considered solvents, comparison of the data of HCAs with those of $HCAs^-$ shows that the IP is generally lower for the salts. This is not surprising since the electron transfer from an anion is expected to be easier than that from a neutral molecule. This suggests that SET-PT mechanism should be favoured for $HCA^-$ when compared to HCA compounds.

For both $HCA^-$ and HCA compounds, the calculated IP values are significantly larger than the corresponding BDE values, thus indicating that the HAT mechanism is thermodynamically more favoured than the first step of SET-PT. It is worth noting that, although the trends obtained with B3LYP and M06-2X are the same, the IP values for HCAs- and HCAs computed with the M06-2X method are significantly higher by ca 8-10 kcal $mol^{-1}$ for most $HCAs^-$ and ca 5-6 kcal $mol^{-1}$ for HCAs compared to the corresponding ones obtained with B3LYP.

The second and last step of the SET-PT mechanism is the loss of a proton from the radical formed in the first step (Table 3.2), thus it is correlated to the PDE. In gas phase PDE values are significantly higher than in polar media, which suggests that the proton loss is greatly enhanced by the presence of a solvent (Table 3.4 and Figure 3.8) With PCM solvent, the PDE values are much lower than the IPs, therefore the first step of the SET-PT process is to be considered the rate limiting step. We noted that, somehow counterintuitively, the less polar solvent (ethanol) leads to lower PDE values than the most polar solvent (water). This result is in agreement with the findings obtained with calculations performed at the B3LYP/6-311++g(d,p) theory level by of Chen *et al.* on similar compounds, that found for several natural phenolic acids a proton dissociation ability slightly stronger in ethanol than in water.[21] It is worthwhile noting that this result is confirmed also at the M06-2X theory level, although the PDEs are smaller than those calculated with B3LYP by about 4-6 kcal mol-1 for $HCAs^-$ and 2-3 kcal $mol^{-1}$ for HCAs.

Among the studied compounds, the lowest PDEs are obtained for HCAs in ethanol, with values ranging between 1.2 and 9.9 $kcal.mol^{-1}$. Regardless the presence or nature of the solvent, the second step is always favoured for the HCA compounds.

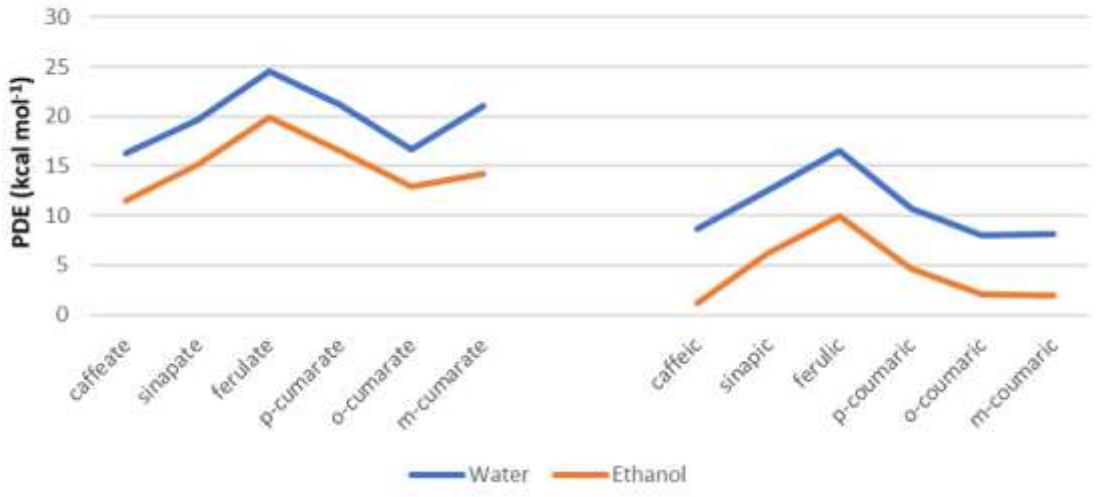


**Figure 3.8** PDE values, calculated at the UB3LYP/6-311++G(d,p) level of theory with PCM solvent model for water or ethanol for the hydroxycinnamates (left) and corresponding acids (right). The compounds are reported according to their DPPH antioxidant trend.

### *3.4.7 PA-ETE and SPLET mechanism*

I have investigated also the possibility of having a sequential proton loss-electron transfer mechanism by analysing the proton affinity and the electron transfer enthalpies.

As can be seen in Table 3.4 and Figure 3.9, the PA values of all studied compounds obtained in gas phase are significantly higher than the ones obtained in water and ethanol. As already discussed for IP values, such a difference can be explained considering the ion stabilizing effect of polar solvents. The $HCA^-$ compounds show higher PA values compared to their parent acids in all three environments studied, indicating that this step is more favourable for the acids. This trend is rationalized considering that the loss of a proton from a negatively charged species, leading to a dianion, is less likely than from a neutral species. The PAs calculated in water and ethanol for both $HCAs^-$ and HCAs are lower than the BDEs and IPs, revealing that in polar solvents the first step of SPLET mechanism is thermodynamically favoured over HAT and the first step of SET-PT. Differently from what observed for the other TPs, no systematic difference among the values obtained with the two functional is observed (Figure 3.3-3.6).

The second step of the SPLET mechanism is associated with the ETE descriptor. ETE values calculated in water and ethanol for both HCAs and $HCAs^-$ are much higher than those of PA (Table 3.4 and Figure 3.10). Thus, the electron transfer is the rate limiting step of SPLET in polar solvents. The ETEs calculated in gas phase are lower than those in both polar solvents, and

for the $HCAs^-$ are

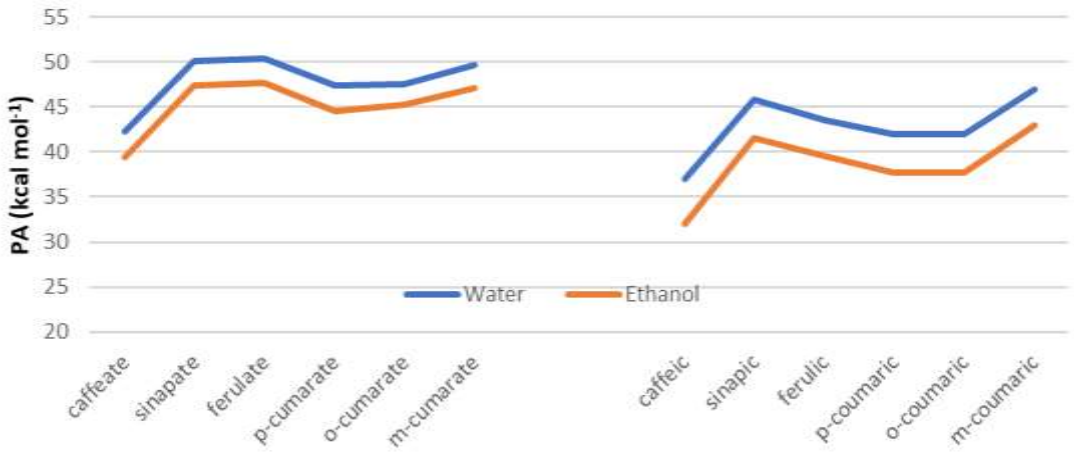


**Figure 3.9** PA values, calculated at the UB3LYP/6-311++G(d,p) level of theory with PCM solvent model for water or ethanol for the hydroxycinnamates (left) and corresponding acids (right). The compounds are reported according to their DPPH antioxidant trend.

even negative; this is due to the lack of stabilization of the dianion in absence of solvent, which in turns makes the electron transfer very favourable. In polar solvents, ETEs of $HCAs^-$ are lower than those of HCAs because the single electron transfer process from an anion requires lower energy than from a neutral form. Therefore, $HCAs^-$ are more susceptible to the second step of SPLET mechanism than HCA compounds.

By comparing the BDE and the ETE values, we can draw some conclusions concerning the overall possible mechanism of radical scavenging. In ethanol, the HAT mechanism is more favoured than the SPLET for both acids and the corresponding anions. However, such a preference seems to be higher for the undissociated acids, while for the anions the BDE and HAT values are comparable for some compounds, i.e. sinapate and ferulate. In water, the SPLET mechanism may be favoured for the hydroxycinnamates, with exception for the caffeate, since their ETE values are lower than BDEs. For the acids, the HAT mechanism is in general favoured;[21,23] however, it should be noted, that the BDE and ETE values for some compounds are not very different, and therefore both mechanisms seem to plausible.

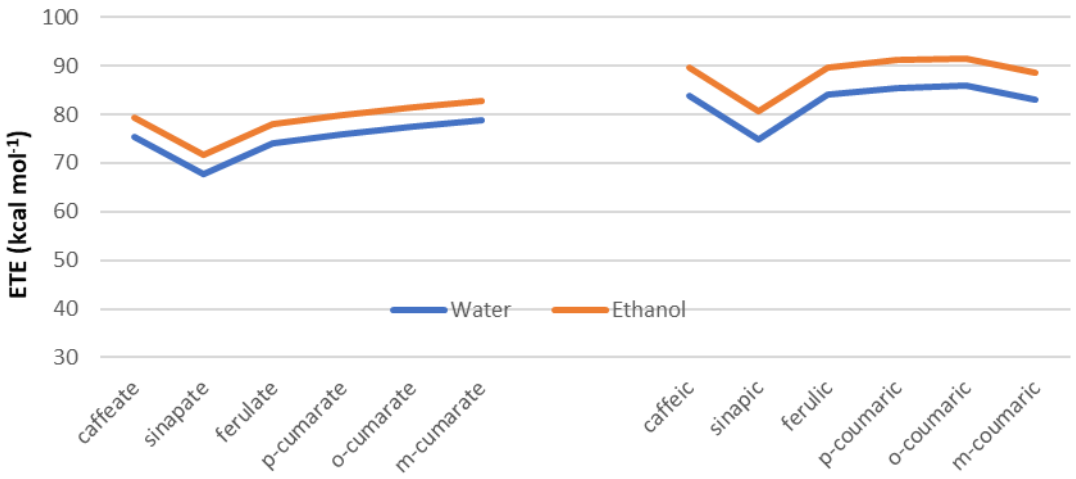


**Figure 3.10** ETE values, calculated at the UB3LYP/6-311++G(d,p) level of theory with PCM solvent model for water or ethanol for the hydroxycinnamates (left) and corresponding acids (right). The compounds are reported according to their DPPH antioxidant trend.

## 3.5 Conclusions

[Cho][HCA] ILs were screened for their antioxidant activity by using experimental DPPH assay and theoretical calculation (DFT) and for their citoxocity by MTT assay. An improvement in the antioxidant activity was observed for all cholinium salts compared to HCAs. Only the pairs of compounds *m*-CA/[Cho][*m*-Coum] and *o*-CA/[Cho][*o*-Coum] showed weak antioxidant activity. The same order of scavenging activity was observed for both acids and salts. The MTT results pointed out the safety of all the salts. Only [Cho][Caff] exhibited marginal cytotoxicity.

DFT calculations performed on all the intermediates of the considered oxidation paths (HAT, SET-PT and SPLET) allowed to rationalize the experimental trends of the antioxidant activity observed for DPPH assay for both classes of $HCAs^-$ and HCAs. Comparison of the calculated TPs typically associated with the above-mentioned mechanism (BDE, IP, PDE, PA and ETE) with the experimental findings indicated that:

- for all HCAs, the HAT mechanism is favored over SPLET and SET-PT in ethanol. A similar result is obtained in water solvent only for CAFA, *o*-CA and *p*-CA. Differently, for SA, FA and *m*-CA the thermodynamic parameters for HAT and SPLET are similar, thus indicating that both mechanisms are plausible. A similar finding was reached by Chen et al. on several phenolic acids;
- for all $HCAs^-$, the ethanol solvent favors the HAT mechanism, while water solvent favors

the SPLET;

- the energies of the intermediates involved in the radical scavenging mechanism are found to be generally lower for $HCAs^-$ compared to the parent acids, thus explaining their improved antioxidant capability;
- the TPs calculated for the SET-PT mechanism clearly revealed that this mechanism is to be excluded for both the hydroxycinnamate and their parent acid.
- The computational results obtained using the 6-311++G(d,p) basis set, with the widely employed density functional B3LYP and those obtained with the more recently developed M06-2X functional lead to the same conclusions. In particular, the TPs values followed the same trends when comparing different compounds or different solvents or when comparing HCA- with the parent acid.

Overall, the promising antioxidant properties proved by both experimental and theoretical analysis together with the evidence of no cytotoxicity suggest that [Cho][HCA] ILs are valid candidates as an alternative to HCAs in pharmaceutical field.

## 3.6 Experimental section

### *3.6.1 Antioxidant activity*

The antioxidant activity of HCAs and [Cho][HCA] ILs was measured by 1,1-diphenyl-2-picrylhydrazyl (DPPH) assay. The principle of the method is based on the color change of the DPPH solution when the radical is quenched by the antioxidant. Namely, when DPPH solution is mixed with an antioxidant substance, the reduced form of DPPH is obtained, and the violet solution turns to be yellow. This color change was monitored at 515 nm using an UltroSpec 2100 pro (Amersham Bioscience, Milan, Italy). The scavenging activity of HCAs and [Cho][HCA] ILs on the DPPH radical was determined following the method described by Huang et al.[22] Briefly, 700 μL of a DPPH ethanol solution (25 mg/L) was mixed with 300 μL of a stock solution (with a known concentration) of each compound at different concentrations. The assay was performed in triplicates. A corresponding blank solution was prepared by mixing 700 μL of a DPPH aqueous solution and 300 μL of distilled water. The samples were incubated for 30 min in the dark at room temperature and then the absorbance at 515 nm was measured. The radical scavenging activity (RSA) was calculated as a percentage of DPPH discoloration using the equation:

$$\% \text{ RSA} = [(A_{DPPH} - A_S)/A_{DPPH}] \times 100$$

where $A_S$ is the absorbance of the solution when the compound is added at a particular level and $A_{DPPH}$ is the absorbance of the blank solution. The concentration providing 50% of radical scavenging activity (EC50) was calculated from the graph of RSA percentage against concentration by semilog regression analysis in GraphPad PRISM v8 (GraphPad software, San Diego, CA, USA) software.

### *3.6.2 DFT calculations*

The structure of all of the studied HCAs, $HCAs^-$, and the intermediate species involved in the studied mechanisms were optimized by means of DFT calculations. In details, geometry optimization was performed employing the unrestricted B3LYP functional as implemented in the commercially available suite of programs GAUSSIAN 16,[36] using the 6-311++G(d,p) basis set for all atoms. The same level of theory was used to perform the vibrational analysis on all of the optimized structures in order to verify the character of the stationary points (no imaginary frequencies were found) and to compute the thermodynamic parameters at 298.15 K. For each compound and oxidation state, the global minimum *in vacuo* was identified through a relaxed potential energy scan performed around all of the rotatable bonds, with steps of 180°. Spin contamination in the radicals was low, always under 0.8 and in all of the optimizations the annihilation of the first spin contaminant lead to the value 0.75.

All PCM calculations were carried out at 298.15 K, and the molecular cavity was constructed using the default procedure in which the radii of the spheres placed around each atom are derived from the UFF force field and scaled by a factor of 1.1. The same calculations were performed using the relatively recent Minnesota hybrid meta exchange- correlation functionals M06-2X of Zhao & Trulhar[37], which is increasingly used in the study of antioxidant compounds. Graphics of molecular models were generated using GaussView6.[38]

### *3.6.3 Cell line and culture conditions*

B16-F10 murine melanoma cells were obtained from the Interlab Cell Line Collection (ICLC) (IRCCS Azienda Ospedaliera Universitaria San Martino – IST Istituto Nazionale per la Ricerca sul Cancro Genova, Italy). 3T3 murine fibroblast cell line was kindly provided by Dr. A. Diana, University of Cagliari. Subcultures of cell line were grown in 75-$cm^2$ culture flask in phenol red-free Dulbecco's modified Eagle's medium (DMEM, Invitrogen, USA) with high glucose, supplemented with 10% fetal bovine serum (FBS), 2 mM L-Glutamine, penicillin (100U/ml) and streptomycin (100µg/ml) at 37° C in 5% $CO_2$.

### *3.6.4 In vitro cytotoxicity*

The cytotoxic effect of [Cho][HCA] ILs was evaluated in B16-F10 and 3T3 cells by using the 3-(4,5-dimethylthiazol-2-yl)-2,5-diphenyltetrazolium bromide (MTT) assay, based on the cleavage of the tetrazolium salt by mitochondrial dehydrogenases in viable cells. In brief, $3 \times 10^4$ and $3 \times 10^5$ cells/mL B16-F10 and 3T3 cells respectively, in 100 mL of medium were seeded into a 96-well plate and incubated for 24 h at 37 C°. After 48 h incubation, various concentrations ranging from 6.2-200 µM of each salt were added to cultures and incubated for additional 24 h at 37 C°. Then, an 8 µL portion of MTT solution (5 mg/mL in $H_2O$) was added and left for 4 h at 37 °C. The cells were lysed with 100 µL of DMSO and color development was measured at 570 nm with an Infinite 200 auto microplate reader (Infinite 200, Tecan, Austria). The absorbance was proportional to the number of viable cells.

### *3.6.5 Statistical analysis*

All the experiments were carried out in triplicate. The results were expressed as means ± SD and evaluated by analysis of variance (ANOVA) followed by Bonferroni post-test carried out on GraphPad PRISM v8 (GraphPad software, San Diego, CA, USA) software. Differences were considered significant at $p < 0.05$.

## References


1. Robbins, R. J. (2003). Phenolic Acids in Foods : An Overview of Analytical Methodology. Journal of Agricultural and Food Chemistry, **51**, 2866–2887.
2. Soobrattee, M. A., Neergheen, V. S., Luximon-Ramma, A., Aruoma, O. I. and Bahorun, T. (2005). Phenolics as potential antioxidant therapeutic agents: Mechanism and actions. Mutation Research/Fundamental and Molecular Mechanisms of Mutagenesis, **579**, 200–213.
3. Rocha, L. D., Monteiro, M. C. and Teodoro, A. J. (2012). Anticancer Properties of Hydroxycinnamic Acids -A Review. Cancer Clinical Oncology, **1**, 109–121.
4. Macoy, D. M., Kim, W. Y., Lee, S. Y. and Kim, M. G. (2015). Biosynthesis, physiology, and functions of hydroxycinnamic acid amides in plants. Plant Biotechnology Reports, **9**, 269–278.
5. Duthie, G. G., Gardner, P. T. and Kyle, J. A. M. (2021). Plant polyphenols: are they the new magic bullet ? Proceedings of the Nutrition Society, **62**, 599–603.
6. Gaspar, A., Garrido, E. M., Esteves, M., Quezada E., Milhazes N., Garrido, J. and Borges,

F. (2009). New insights into the antioxidant activity of hydroxycinnamic acids: Synthesis and physicochemical characterization of novel halogenated derivatives. European Journal of Medicinal Chemistry, **44**, 2092–2099.

7. Molyneux, P. (2004). The use of the stable free radical diphenylpicryl- hydrazyl ( DPPH ) for estimating antioxidant activity. Journal of Science and Technology, **26**, 211–219.
8. Grimme, S. and Schreiner, P. R. (2018). Computational Chemistry: The Fate of Current Methods and Future Challenges. Angewante Chemie - International Edition, **57**, 4170–4176.
9. McArdle, S., Endo, S., Aspuru-Guzik, A., Benjamin, S. C., and Yuan, X. (2020). Quantum computational chemistry. Reviews of Modern Physics, 92(1), 015003.
10. Catlow, C. R. A., Buckeridge, J., Farrow, M. R., Logsdail, A. J., and Sokol, A. A. (2017). Quantum Mechanical/Molecular Mechanical (QM/MM) Approaches. Handbook of Solid State Chemistry, 647-680.
11. Kryachko, E. S. and Ludeña, E. V. (2014). Density functional theory: Foundations reviewed. Physical Report, **544**, 123–239.
12. LaPointe, S. and Weaver, D. (2007). A Review of Density Functional Theory Quantum Mechanics as Applied to Pharmaceutically Relevant Systems. Current Computer - Aided Drug Design, **3**, 290–296.
13. Sun, Y., Hao, Q., Lu, L., Wang, X. and Yang, X. (2010).Vibrational spectroscopic study of o - , m - and p -hydroxybenzylideneaminoantipyrines. Spectrochimica Acta Part A. Molecular and Biomolecular Spectroscopy, **75**, 203–211.
14. Leopoldini, M., Russo, N. and Toscano, M. (2011). The molecular basis of working mechanism of natural polyphenolic antioxidants. Food Chemistry, **125**, 288–306.
15. Zheng, Y., Deng, G., Liang, Qin., Chen, D., Guo, R. and Lai, R. (2017). Antioxidant Activity of Quercetin and Its Glucosides from Propolis : A Theoretical Study. Scientific Reports 1–11.
16. Anouar, E., Calliste, C. A., Košinová, P., Di Meo, F., Duroux, J. L., Champavier, Y., Marakchi, K. and Trouillas, P. (2009). Free Radical Scavenging Properties of Guaiacol Oligomers : A Combined Experimental and Quantum Study of the Guaiacyl-Moiety Role. Journal of Physical Chemistry A, **114**, 13881–13891.
17. Speybroeck, V. Van and Johan, R. (2010). The calculation of thermodynamic properties of molecules. Chemical Society. Reviews, **39**, 1764–1779.
18. Galano, A., Mazzone, G., Marino, T., Ra, J. and Russo, N. (2016). Food Antioxidants : Chemical Insights at the Molecular Level. Annual Review of Food Science and

Technology, 335–352.

19. Rice-Evans, A. C., Miller, N. J.and Paganga, G. (1996). Structure antioxidant activity relationships of flavonoids and phenolic acids. Free Radical Biology Medicine, **20**, 933–956.
20. Foti, M. (2015). Use and Abuse of the DPPH • Radical. Journal of agricultural and food chemistry, **63**, 40, 8765–87769.
21. Chen, Y., Xiao, H., Zheng, J. and Liang, G. (2015). Structure-thermodynamics-antioxidant activity relationships of selected natural phenolic acids and derivatives: An experimental and theoretical evaluation. PLoS One, **10**, 1–20.
22. Xue, Y., Zheng, Y., An, L., Dou, Y. and Liu, Y. (2014). Density functional theory study of the structure – antioxidant activity of polyphenolic deoxybenzoins. Food Chemistry, **151**, 198–
23. Mazzone, G., Russo, N. and Toscano, M. (2016). Antioxidant properties comparative study of natural hydroxycinnamic acids and structurally modified derivatives: Computational insights. Computational Theorethical Chemistry, **1077**, 39–47.
24. Chen, J., Yang, J., Ma, L., Li, J., Shahzad, N. and Kim, C. K. (2020). Structure-antioxidant activity relationship of methoxy , phenolic hydroxyl , and carboxylic acid groups of phenolic acids. Scientific Reports, **10**, 2611.
25. Urbaniak, A., Molski, M. and Szelag, M. (2012). Quantum-chemical Calculations of the Antioxidant Properties of trans - p -coumaric Acid and trans -sinapinic Acid. Computational METHODS and Science Technology **18**, 1–12.
26. Lithoxoidou, A. T. and Bakalbassis, E. G. (2004). Liquid-Phase Theoretical Antioxidant Activity Trend of Some Cinnamic Acid Antioxidants. Journal of American Oil Chemistry Society, **81**, 799.
27. Szeląg, M., Urbaniak, A. and Bluyssen, H. A. R. (2015). A theoretical antioxidant pharmacophore for natural hydroxycinnamic acids. Open Chemistry. **13**, 17–31.
28. E. Cancès and B. Mennucci. Analytical derivatives for geometry optimization in solvation continuum models. (1998). *J*ournal of Chemical Physics, **109**, 249–259.
29. Cossi, M., Barone, V., Mennucci, B. and Tomasi, J. (1998). Ab initio study of ionic solutions by a polarizable continuum dielectric model. Chemical Physics Letters. **286**, 253–260
30. Rimarcik, J; Lukeš, V.; Klein, E.; Ilin, M. (2010). Study of the solvent effect on the enthalpies of homolytic and heterolytic N-H bond cleavage in p-phenylenediamine and tetracyano-p-phenylenediamine. Journal of Molecular StructureTHEOCHEM, **952**, 25–30.

31. Bartmess, J. E. Thermodynamics of the Electron and the Proton. (1994). Journal of Physical Chemistry, 98, 6420–6424.
32. Marković, Z., Tošović, J., Milenković, D. and Marković, S. (2015). Revisiting the solvation enthalpies and free energies of the proton and electron in various solvents. Computational Theorethical Chemistry, **1077**, 11-17.
33. Marenich, A. V., Cramer, C. J. and Truhlar, D. G. (2009). Universal Solvation Model Based on Solute Electron Density and on a Continuum Model of the Solvent Defined by the Bulk Dielectric Constant and Atomic Surface Tensions. Journal of Physical Chemistry, 6378–6396.
34. Ahamed, T. K. S., Rajan, V. K., Sabira, K. and Muraleedharan, K. (2019). DFT and QTAIM based investigation on the structure and antioxidant behavior of lichen substances Atranorin, Evernic acid and Diffractaic acid. Computational Biological Chemistry. **80**, 66–78.
35. Amić, A., Marković, Z., Klein, E., Dimitrić Marković, J. M. and Milenković, D. (2018). Theoretical study of the thermodynamics of the mechanisms underlying antiradical activity of cinnamic acid derivatives. Food Chemistry, **246**, 481–489.
36. Frisch, M. J., Trucks, G. W., Schlegel, H. B.; Scuseria, G. E., Robb, M. A., Cheeseman, J. R., Scalmani, G.; Barone, V., Petersson, G. A., Nakatsuji, H., Li, X., Caricato, M., Marenich, A. V., Bloino, J., Janesko, B. G., Gomperts, R., Mennucci, B., Hratchian, H. P., Ortiz, J. V., Izmaylov, A. F., Sonnenberg, J. L., Williams-Young, D., Ding, F., Lipparini, F.; Egidi, F., Goings, J., Peng, B., Petrone, A., Henderson, T., Ranasinghe, D., Zakrzewski, V. G.; Gao, J., Rega, N., Zheng, G., Liang, W., Hada, M., Ehara, M., Toyota, K., Fukuda, R.; Hasegawa, J.; Ishida, M.; Nakajima, T.; Honda, Y.; Kitao, O.; Nakai, H.; Vreven, T.; Throssell, K., Montgomery, Jr., J. A., Peralta, J. E., Ogliaro, F., Bearpark, M. J., Heyd, J. J.; Brothers, E. N., Kudin, K. N. Staroverov, V. N., Keith, T. A., Kobayashi, R., Normand, J., Raghavachari, K., Rendell, A. P., Burant, J. C., Iyengar, S. S., Tomasi, J., Cossi, M., Millam, J. M., Klene, M., Adamo, C., Cammi, R., Ochterski, J. W., Martin, R. L., Morokuma, K., Farkas, O., Foresman, J. B. and Fox, D. J. Gaussian 16, revision A.03; Gaussian, Inc.: Wallingford CT, **2016**. Gaussian 16.
37. Zhao, Y. and Truhlar, D. G. (2008). The M06 suite of density functionals for main group thermochemistry, thermochemical kinetics, noncovalent interactions, excited states, and transition elements. Theorethical Chemistry Accounts. **120**, 215–241.
38. Dennington, R., Keith, T. A. and Millam, J. M. (2016).GaussView, Version 6, Semichem Inc., Shawnee Mission, KS.

# 4

# Anti-tyrosinase and anti-melanogenic activities of [Cho][Caf], [Cho][Fer] and [Cho][*p*-Coum]

## 4.1 Introduction

Besides their multiple beneficial effects, many HCAs have been described in the literature as inhibitors of tyrosinase (Ty). Tyrosinase (EC 1.14.18.1) or polyphenoloxidase (PPO) is a copper-containing monooxygenase catalysing the o-hydroxylation of monophenols to the corresponding catechols (mono-phenolase or cresolase activity), and the oxidation of catechols to the corresponding o-quinones (diphenolase or catecholase activity)[1] (Figure 4.1).

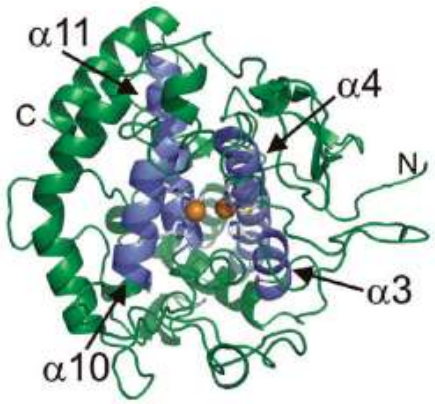


**Figure 4.1**. Crystal Structure of *Agaricus bisporus* Mushroom Tyrosinase. (figure from Ismaya, W. T., Rozeboom, H. J., Weijn, A., Mes, J. J., Fusetti, F., Wichers, H. J., & Dijkstra, B. W. (2011). Biochemistry, 50 (24), 5477-5486)

Tys are widespread in nature[2,1] whereabout they are often referred to as phenolases, phenol oxidases, polyphenol oxidases, catechol oxidases, depending on the particular source. The properties of Ty vary depending upon the oxidation states of the two copper atoms in the active site. Native Ty occurs mainly as met-tyrosinase in which a hydroxyl ion is bound to the two copper ions. The enzyme is commonly found as a tetrameric protein with a molecular mass of 120 kDa, composed of two subunits of ~43 kDa (H subunit) and two subunits of~14 kDa (L subunit).[3] Phenols bind to met-tyrosinase but are not oxidized by this form of the enzyme. Catechols, however, are oxidized by met-tyrosinase that in the process is reduced to deoxy-tyrosinase in which both coppers are now in the Cu(I) oxidation state. Deoxy-tyrosinase rapidly binds dioxygen to give oxy-tyrosinase in which the two oxygen atoms are held between the copper ions in the active site. Oxy-tyrosinase is the primary oxidizing form of the enzyme and oxidizes phenols by a monooxygenase mechanism and oxidizes catechols by an oxidaze mechanism (Figure 4.2). Thus, in the presence of dioxygen both phenols and catechols are

oxidized by oxy-tyrosinase to ortho-quinones by quite separate oxidative cycles. During the catecholic cycle a catechol is occasionally treated as a phenol and oxidized by oxy-tyrosinase by a monooxygenase mechanism leading to the irreversible formation of deact-tyrosinase[4] in which one.

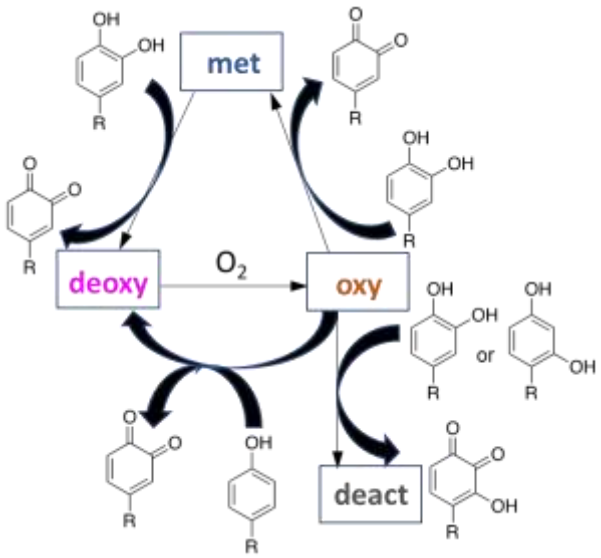


**Figure 4.2** The inter-relationship of the four discrete oxidation states of tyrosinase. Readapted from ref. 4.

Ty plays a rate-limiting enzyme in the synthesis of melanin and constitutes the primary cause for undesired browning of fruits and vegetables as well as diseases resulting from overproduction of melanin.[2] Melanins, the main pigment primarily responsible in the skin, hair and eyes pigmentation of human, are produced by melanocytes through melanogenesis. Melanogenesis and skin pigmentation are the most important photoprotective factor in response to ultraviolet radiation damaging from the sun and skin photocarcinogenesis.[5] The abnormal loss of melanin and depigmentation can be a serious facial esthetic and dermatological problem among humans.[6] On the contrary, the increased melanin synthesis and accumulation of these pigments occur in many types of skin disorders.[7] Due to the critical role of Ty in the melanogenesis and browning process, controlling the activity of enzyme by tyrosinase inhibitors is an essential endeavor for treating hypopigmentary disorders of mammals and enzymatic browning of fruits and fungi.[8] For this reason, the use of Ty inhibitors has applications both in cosmetics and pharmaceutical field for preventing hyperpigmentation due to the overproduction of melanin in the epidermis, and in

food industry to counteract the browning responsible of loss of nutritional and market values of foods.[9] Another area of application of tyrosinase inhibitors is cancer research. Indeed, in melanocytes, Ty is overexpressed during tumorigenesis.[10] Previous studies have suggested that inhibition of upregulated tyrosinase enzyme in melanoma cells might inhibit cell proliferation of melanoma cells.[11] Involved in the biosynthetic pathways of the melanin pigment, the immunogenic enzyme tyrosinase is recognized as a sensitive marker for melanoma.[10] Despite overexpression of Ty is usually associated with melanoma tumorigenesis, the inhibition of melanogenesis by direct interaction on tyrosinase doesn't interfere with the expression of the involved transcription factors.[12] Therefore, the melanoma cells can still proliferate but the tyrosinase produced are not functional.

The compounds recognized as Ty inhibitors may act in different ways, in particular as specific Ty inactivators and inhibitors, o-dopaquinone scavengers, alternative enzyme substrates, nonspecific enzyme inactivators and denaturants.[2] Only specific tyrosinase inactivators and reversible inhibitors actually bind to the enzyme as "true inhibitors" and really inhibit its activity. Generally, the mode of inhibition by "true inhibitors" is one of these four types: competitive, uncompetitive, mixed type (competitive/uncompetitive), and noncompetitive. A competitive inhibitor can bind to a free enzyme and prevents substrate binding to the enzyme active site.[13] An uncompetitive inhibitor binds only to the complex formed between the enzyme and the substrate (E-S complex). As the name suggest, the mixed type inhibitors can act both as a competitive inhibitor for the active site or can bind the complex E-S. The noncompetitive inhibitors are structurally different from substrates and hence bind enzymes at sites distinct from substrate binding site and reduce the enzyme activity by locking or causing changes in the active site. (i.e. no competition with substrate).[14] They can bind to both the enzyme and E-S complex. Since Ty is a metalloenzyme, copper chelators such as many aromatic acids, phenolic and poly-phenolic compounds, a few non-aromatic compounds, can inhibit tyrosinase competitively by mimicking the substrate of tyrosinase.[1,15,16]

To date, numerous effective Ty inhibitors have been identified and developed for use in medical and cosmetic products,[6] food bioprocessing, and agricultural and environmental industries.[2] Although in medicine Ty inhibitors are a class of important clinical antimelanoma drugs, only a few compounds are known to serve as effective and safe Ty inhibitors.[15]

One of the most investigated and efficient natural Ty inhibitors is kojic acid (KA)[17] (Figure 4.3). KA is widely used in cosmetics as a depigmenting agent. Nevertheless, it is also

considered as an harmful agent because of its undesirable side effects such as cytotoxicity, skin cancer, and dermatitis.[18] Therefore, there is a need of new natural occurring or synthetic compounds with high anti-tyrosinase activity, low toxicity, and adequate skin absorption properties.[19]

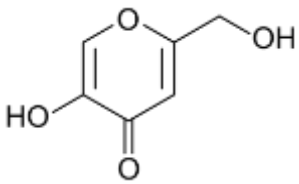


**Figure 4.3** Kojic Acid

*p*-CA, CAFA, and FA are the most common hydroxycinnamic acids widely distributed in fruit and vegetables. Their interaction with tyrosinase has been the object of many investigations. [20] *p*-CA is a very selective and more potent inhibitor toward human and murine tyrosinases than toward mushroom tyrosinase (MT).[21] It inhibited human and murine tyrosinases ~100 and ~10 times more strongly than KA respectively, although the inhibitory effects against MT are comparable. CAFA can be enzymatically oxidized by mushroom tyrosinase acting as a substrate.[22] Nevertheless, CAFA and its ester derivative n-nonyl caffeate were also explored for their catalytic inactivation efficiency on the enzyme MT in presence of L-DOPA through spectrophotometric methods.[23] The coniugation product of CAFA with dihydrolipoic acid also proved to have inhibitory activity on both mushroom and human tyrosinase.[24] FA inhibits melanin formation through competitive inhibition of tyrosinase and, if incorporated in a topical formulation containing 5% vitamin C and 1% vitamin E, showed a double photo-protection activity against the damages of long-term UV radiation.[25,26]

A part of my PhD thesis was dedicated to evaluate [Cho][HCA] ILs also for their effect on tyrosinase *in vitro*. Due to the well known anti-tyrosinase activity of CAFA, *p*-CA, and FA, only cholinium salts derived from these HCAs were investigated. In particular, I evaluated the activity of these compounds on Ty extracted from the champignon mushroom *Agaricus bisporus* (MT). Despite the different composition of MT compared to human Ty (HT) in terms of the amino acid sequence, MT is often used as a suited model for studies on melanogenesis, mainly because it is commercially available in a purified form. Furthermore, the cytotoxicity and the antimelanogenic

effects of cholinium salts were examined in MNT-1 human melanoma cells, using Kojic acid as a reference compound.

## 4.2 Effects of [Cho][HCA]ILs on the activity of mushroom tyrosinase

The kinetic mechanism of inhibition of MT by CAFA and [Cho][Caf], used as substrates, was investigated according to the Michaelis-Menten model that describes the rate of enzyme-catalyzed reactions and their dependence on enzyme and substrate concentrations for many enzymes. This model postulates that an enzyme (E) and its substrate (S) bind reversibly to form an enzyme-substrate complex (ES), which dissociates to yield the free enzyme and product (P):

$$E + S \rightleftharpoons ES \rightarrow E + P$$

The Michaelis-Menten equation for this system is written as:

$$v = \frac{V_{max}\,[S]}{K_M + [S]} \qquad (1)$$

where $V_{max}$ is the maximum reaction velocity, [S] is the substrate concentration and, $K_M$, known as the Michaelis constant, is defined as the substrate concentration at which the rate of product formation is half its maximum value . Estimates of $K_M$ and $V_{max}$ can be easly obtained by a double reciprocal plot (Lineweaver-Burk), solved for $K_M$ and $V_{max}$ according to the following equation:

$$(1/V_0) = (K_M/V_{max})(1/[S]) + 1/V_{max} \qquad (2)$$

Fit to a linear model allows extraction of the slope ($=K_M/V_{max}$), y-intercept ($1/V_{max}$), and x-intercept ($= - 1/K_M$). Since $K_M$ is a measure of binding affinity of the substrate to the enzyme, large values are indicative of weaker binding between enzyme and substrate, while low values indicate that only a small amount of substrate is needed to saturate the enzyme, thus a high affinity for substrate. Since $V_{max}$ reflects how fast the enzyme can catalyze the reaction, this

point is reached when there are enough substrate molecules to completely fill (saturate) the enzyme's active sites. The lower is $V_{max}$, the faster that point is reached.

The capability of MT to oxidize CAFA and [Cho][Caf], used as substrates, to *o*-quinone was analysed spectrophotometrically by following the changes in the UV–Vis spectrum of solutions at increasing concentration of the inhibitors and at a constant concentration of the enzyme (see Experimental section). Due to the low solubility of CAFA in water, a 10% (v/v) ethanol stock solution of this compound was prepared and then diluted with phosphate buffer solution up to the desired concentration of the substrate. In the case of [Cho][Caf], in order to evaluate the impact of the solvent on the rate of the enzymatic reaction of MT, two different stock solutions were prepared: a) 100% aqueous solution and b) 10% (v/v) ethanol solution.

As can be seen in Figure 4.4A, under the experimental conditions adopted in this study, the oxidation reaction of CAFA and [Chol][Caf] by MT followed Michaelis–Menten kinetics. Kinetic parameters were determined by Lineweaver–Burk plots, all data sets being reasonably well described by a linear fit with $R^2 > 0.99$ (Figure 4.4B). The results are summarized in Table 4.1. The order of the Michaelis constant ($K_M$) values was as follows: CAFA > $[Cho][Caf]_{ethanol}$ > $[Cho][Caf]_{water}$ with the maximum value seven times greater than the minimum.The same order was observed for the maximum reaction velocity ($V_{max}$), evidencing that the substrate with the lowest and highest affinity were CAFA and $[Cho][Caf]_{water}$, respectively. The calculated values of $V_{max}/K_M$ showed the enzyme catalytic efficiency, i.e. the specificity of substrates toward mushroom tyrosinase. The order of the $V_{max}/K_M$ values for the three substrates was as follows: $[Cho][Caf]_{water}$ > $[Cho][Caf]_{ethanol}$ > CAFA. Therefore, the most suitable substrate for mushroom tyrosinase was [Cho][Caf] in a aqueous solution.

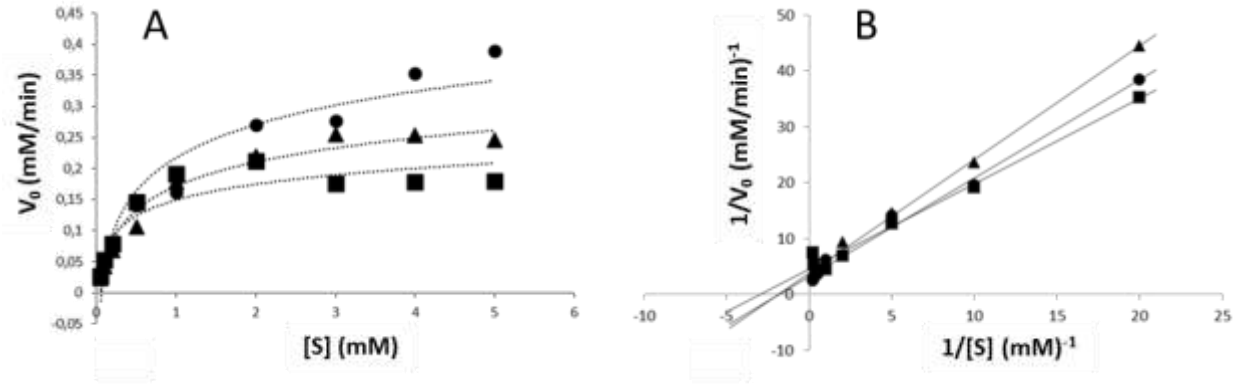


**Figure 4.4** A) Michaelis–Menten and B) Linewaver-Burk plots for MT assay at varied concentrations of substrate ranging from 0.05 to 5 mM of: ●, CAFA in ethanolic solution ; ▲, [Cho][Caf] in ethanolic solution; ■, [Cho][Caff] in aqueous solution.

**Table 4.1** Kinetic parameters of mushroom tyrosinase for the oxidation of [Chol][Caf] and CAFA.

| **Substrate (solvent)** | **$V_{max}$** | **$K_M$** | **$V_{max}/K_m$** |
|---|---|---|---|
| CAFA (4% EtOH) | 0.48 ± 0.04 | 1.6 ± 0.4 | 0.3 |
| [Chol][Caf] (4% EtOH) | 0.30 ± 0.01 | 0.71 ± 0.09 | 0.42 |
| [Chol][Caf] (Water) | 0.20 ± 0.01 | 0.24 ± 0.07 | 0.83 |

The effects of [Cho][Fer], [Cho][*p*-Coum], and their acid precursors (FA and *p*-CA) on the tyrosinase activity were evaluated by analyzing their inhibitory action for the oxidation of TBC-ADA catalyzed by MT. Similarly to [Cho][Caf] and CAFA, the stock solution of HCA was prepared in 10% ethanol solution, while two stock solutions were preprared for the cholium salt, in water ad 10% etanol solution, respectively. As shown in Figure 4.5, all compounds were found to inhibit tyrosinase activity in a concentration-dependent manner. As their concentrations increased, the enzyme activity was rapidly decreased but not completely suppressed. Both [Cho][HCA] ILs exhibited an inhibitory effect stronger compared to their acidic parents, with the highest effect observed in aqueous solution, thus evidencing that [Chol][Fer] and [Cho][*p*-Cum] were more potent inhibitors than FA and *p*-CA

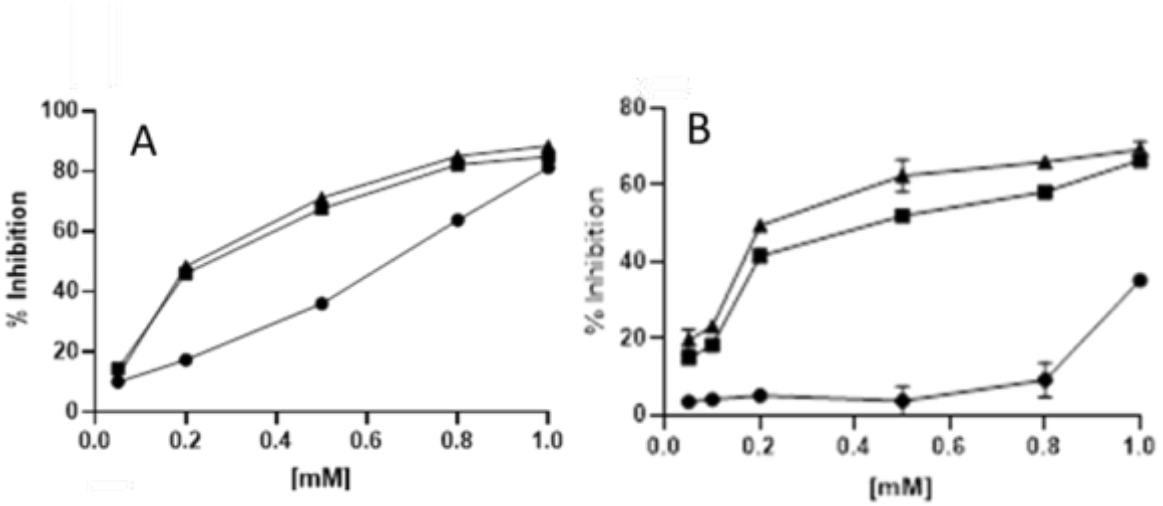


**Figure 4.5** Inhibitory effect of A) FA (●), [Cho][Fer] in 4% ethanolic solution (■), and [Chol][Fer] in aqueous solution (▲)and B) *p*-CA (●), [Cho][*p*-Coum] in 4% ethanolic solution (■), and [Cho][*p*-Coum] in aqueous solution (▲).

## 4.3 Cytotoxicity of [Cho][HCA] ILs on MNT-1 cell line

FA and *p*-CA acids have been reported for their various cytotoxic mechanism in several types of cells[27] and for their antityrosinasic activity in human and murine melanoma cells.[21,9] Antitumor efficacy of CAFA was previously evaluated on human cutaneous melanoma SK-Mel-28 cell line wherein CAFA showed a decreasing in cell viability and induced apoptosis. The antiproliferative effect of CAFA was also attributed to his role in cell cycle modulation, inhibition of colony formation, and changes in the expression of caspases.[27]

The three [Cho][HCA] ILs and KA, used as reference compound, were assessed for their cytotoxicity in MNT-1 human melanoma cells, which are known to have an overexpression of tyrosinase. Melanocyte viability was measured at different concentrations of compounds in the range of 10–1000 mM and at two different exposure times (24 and 48 h). As can be seen in Figure 4.6, compared to control (non-treated cells), KA didn't exhibit significant cytotoxicity at any of the investigated concentrations after 24 hours of exposition, while a significant reduction in cell viability was observed after 48 hours of exposure in all range of concentrations. Similarly, KA has been reported to be nontoxic at doses below 100 mg/mL in B16-F10 murine melanoma.[28]As to [Cho][HCA] ILs, our results suggested [Chol][Fer] and [Chol][*p*-Coum] as more promising compounds than [Chol][Caff]. Indeed, [Chol][Fer] and [Chol][*p*-Coum]

displayed low cytotoxicity, even at very highest doses and after 48 hours exposition time, while [Chol][Caf] showed significant cytotoxicity at both exposition times, reaching the maximum at 1000 and 500 µM after 24 and 48 hours, respectively. The behavior of [Chol][Caf] is in good agreement with the findings of cytotoxicity obtained for this IL on B16-F10 murine melanoma cells.

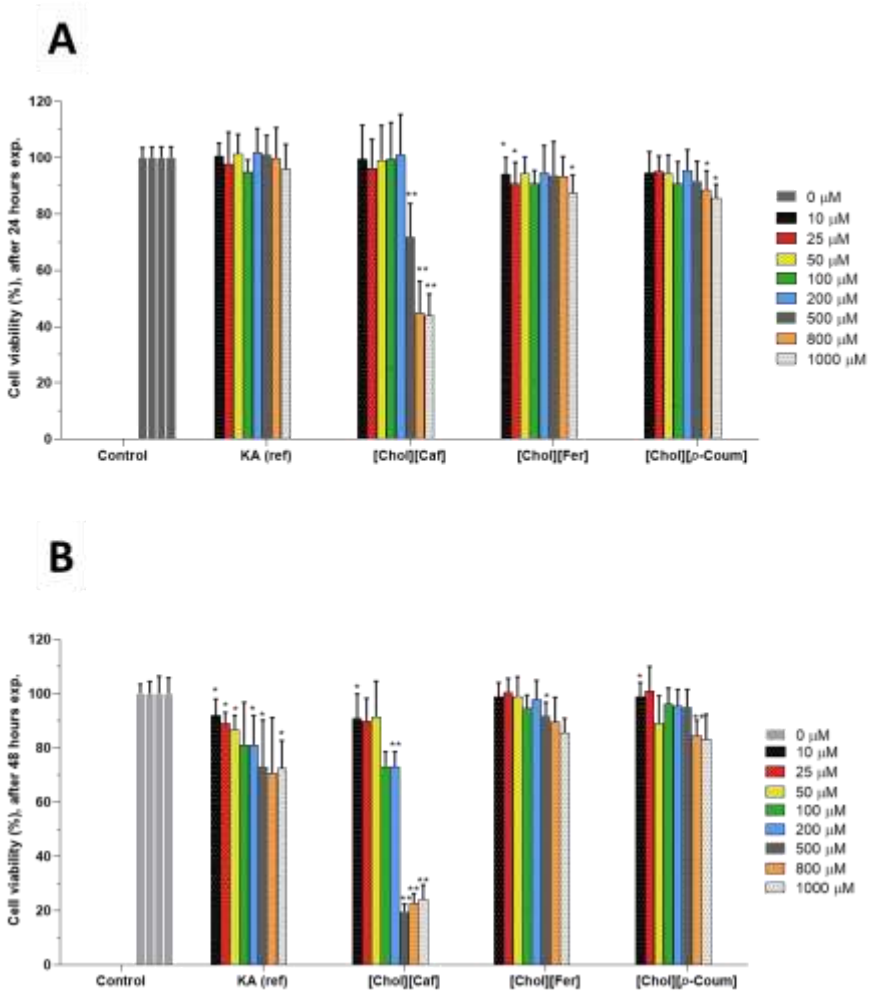


**Figure 4.6** Cell viability of human MNT-1 melanoma cell line after a) 24 and b) 48 h of exposure to different concentrations of [Cho][HCA] ILs. KA was used as a reference compound. Cell viability was assayed with MTT test. Data are expressed as the percent of cell viability (means ± S.E.M. of three independent experiments). Asterisk denotes the statistical significance between control (non-treated) and treated cells: * $p < 0.001$, ** $p < 0.05$ in the Student's t test.

## 4.4 Depigmenting activity of [Cho][HCA] ILs in MNT-1 cell line

To investigate the effect [Cho][HCA] ILs on melanogenesis, MNT-1 cells were incubated for

48 h at a compound concentration of 200 μM. Since MNT-1 cells are highly pigmented melanoma cells [29], α-MSH (α-melanocyte-stimulating hormone) was not added to this assay system.The results are depicted in Figure 4.7 where melanin contents, expresses as percentage of controls, are reported for each studied system. The results showed that KA, used as reference compound, and all [Cho][HCA] ILs inhibited melanogenesis activity. The strongest effect was observed for [Cho][*p*-Coum] that reduced the melanin production to 77.65%, followed by KA (78.25%), [Chol][Fer] (82.82%), and [Chol][Caff] (89.29%). The high antimelanogenic effect of [Cho][*p*-Coum] agrees with the high efficiency observed for *p*-coumaric acid in murine melanoma cells and human epidermal melanocytes, compared to other natural hydroxycinnamic acids.[30,31] Furthermore, it's interesting to note that, oppositely to the order of efficacy observed for the mushroom tyrosinase inactivation of [Cho][*p*-Coum] and [Cho][Fer] , the anti-melanogenic effect of [Cho][*p*-Coum] was stronger than that [Chol][Fer]. This different trend could be ascribed to the difference composition between mushroom and human tyrosinase in terms of amino acid sequence. Additionally, the effects in melanin production of [Chol][Caf] and of KA might be altered also by the (even slight) cytotoxic effect measured in MTT assay at the same conditions of dose (200 mM) and time of exposition (48 h).

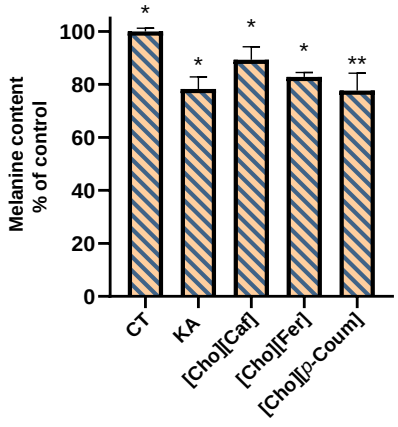


**Figure 4.7** Melanin contents of MNT-1 human melanoma cells after 48 h of incubation with [Chol][HCA] ILs and KA, used as a reference. The test compound concentration was at 200 μM. The results are expressed as percentages of the control and are mean ± S.D. of three separate experiments. Asterisk denotes the statistical significance between control (non-treated cells) and treated cells: * $p < 0.001$, ** $p < 0.05$ in the Student's t test.

## 4.5 Conclusions

It is well-documented that some HCAs possess inhibitory effects against tyrosinase. Although this property makes HCAs very promising agent in different fields such as food, cosmetic and pharmaceutical industries, their low solubility in water limits their applications. In this study, I attempted to evaluate the effect of [Cho][Caf], [Cho][Fer], and [Cho][*p*-Coum] on MT activity and the melanogenesis in human melanoma cells. The results indicate that treatment of MT with these compounds led to a higher decrease in tyrosinase activity than that induced by the corresponding acid precursors. [Cho][Caf] demonstrated to be a better substrate than CAFA ($V_{max}$ 0.20 ± 0.01 and $K_M$ 0.24 ± 0.07 vs. $V_{max}$ 0.48 ± 0.04 and $K_M$ 1.6 ± 0.4), while the highest tyrosinase inhibition was showed by [Cho][Fer] with a reduction of the enzymatic activity of 88.3% ± 0.9.

Concerning the inhibition of cholinium salts on the melanogenesis in MNT-1 cells, [Cho][*p*-Coum] exhibited the best depigmenting effect, even overcoming the reference compound KA. Although the biologic impact of [Cho][Caf], [Cho][Fer], and [Cho][*p*-Coum] in human melanogenesis deserves further investigations, in the light of the present results, these compounds may be potential chemicals to treat dermatological diseases. Thus, the importance of these three HCA derivatives as new agents for skin disease worths to be elucidated in future studies.

## 4.6 Experimental section

### *4.6.1 Chemicals and reagents*

All commercially available solvents and reagents were used without further purification. *p*-CA, CAFA were FA, were purchased from Sigma-Aldrich (Milan, Italy). Mushroom tyrosinase (MT) was purchased from Worthington. [Cho][HCA] ILs were synthesized as previously described (Chapter 2).

### *4.6.2 Mushroom Tyrosinase assays*

A stock solution of MT was freshly made by dissolving 10 mg of MT in 5 mL (1800 EU/ml) of 100 mM phosphate buffer solutions (pH 6.5). A tyrosinase unit was defined as the amount of MT increasing the absorbance at 280 nm by 0.001 per minute at pH 6.5 and 25 °C in a 3 mL

reaction mix containing L-tyrosine.

The MT activity was measured spectrophotometrically using [Cho][Caf] and CAFA as substrates. After the addition of 775 mL of distilled water or hydroalcolic solution, 100 mL of 100 mM phosphate buffer (pH 6.5), 100 mL of aqueous or hydroalcoholic substrate solution, and 25 mL of tyrosinase solution (45 EU) into a cuvette, the formation of *o*-caffeoquinone was immediately monitored for 2 min by measuring the absorbance at 480 nm (the maximum absorbance in the UV-Vis scan of the conversion of CAFA in o-caffeoquinone) with an Ultrospec 2100 Pro UV-vis (Amersham Biosciences). The reaction was carried out at 25°C. Three repetitions of each experiment were made. A control reaction in absence of the enzyme was also conducted.

The inhibitory actions of [Cho][Fer], [Cho][*p*-Coum], FA, and CA on MT were evaluated spectrophotometrically by tracking the adduct formation between 4-tert-butyl-1,2-benzoquinone (TBC) and 4-amino-N,N-diethylaniline (ADA) at 625 nm ($e_{625}$ = 11120 $M^{-1}$ $cm^{-1}$) [32]. In this assay, 650 mL of distilled water, 100 mL of phosphate buffer 100 mM (pH 6.5), 100 mL of aqueous or hydroalcoholic substrate solution, and 20 mL of tyrosinase solution (diluited1:10; 3,6 EU) were placed into a cuvette and the solution was immediately monitored for 10 min. The percentage of inhibition (I %) of the enzyme activity was calculated according to the equation I%=(DA - DB)/ DA × 100, where DA is the difference in the absorbance of the control sample when the absorbance increased linearly and DB is the difference in the absorbance of the test sample calculated in the same range of time.[32] Inhibition activity assay was performed at [Cho][HCA] ILs and HCA concentrations of 1, 0.8, 0.5, 0.2, 0.1, 0.05 mmol $L^{-1}$. Three repetitions of each experiment were made.

### *4.6.3 Cell culture*

MNT-1 cells were kindly provided by Dr. Manuela Gaspar (iMed.ULisboa, Portugal). MNT-1 were cultured in Dulbecco's modified Eagle's medium (DMEM) supplemented with 10% fetal bovine serum (FBS) and 1% l-glutamine, penicillin–streptomycin and fungizone (Life Technologies, Grand Island, NY, USA). Cells were incubated in a humidified atmosphere at 37 °C and 5% $CO_2$. Cell morphology was observed using an inverted microscope Nikon Eclipse 80i (Nikon, Tokyo, Japan).

### *4.6.4 Cell Viability assay*

The cytotoxic effect of [Cho][HCA] ILs and KA was assayed by using 3-[4,5-dimethylthiazol-2-yl]-2,5-diphenyltetrazolium bromide (MTT).[33] Briefly, MNT-1 cells were seeded in 96-well plates and allowed to adhere. After adhesion, cells were incubated for 24 and 48 h ($4\times 10^5$ and $2.5 \times 10^5$ cells/ml, respectively) and treated with a range of 10 concentrations of KA and [Cho][HCA] ILs (10–1000 mM), at 37 °C in 5% $CO_2$. Upon exposure, 50 mL MTT solution (1 mg/mL in PBS, pH 7.2) was added to each well. After 4 h of incubation, the medium was replaced with 150 μL dimethyl sulfoxide (DMSO) to dissolve the formazan crystals. The plate was shaken for about 2 h protected from light. Cell viability was measured by the optical density of reduced MTT at 570 nm using a microplate reader (Synergy HT from BioTeK Instruments Inc., Winooski, VT, USA). The percentage of viable cells was determined as the ratio between the absorbance of treated versus control (non-treated) cells.

### *4.6.5 Compound toxicity on MNT-1 human melanoma cell lines*

To obtain safe doses to be used in subsequent experiments on cells, the cytotoxic effect of the three salts [Chol][Fer], [Chol][*p*-Coum] and [Cho][Caf] was assayed also on MNT-1 human melanoma cell line. Briefly, MNT-1 cells were seeded in 96-well plates and allowed to adhere. After adhesion, cells were incubated for 24 and 48 h ($4\times 10^5$ and $2.5 \times 10^5$ cells/ml, respectively) and treated with a range of 10 concentrations of KA and [Cho][HCA] ILs (10–1000 mM), at 37 °C in 5% $CO_2$. Upon exposure, 50 mL MTT solution (1 mg/mL in PBS, pH 7.2) was added to each well. After 4 h of incubation, the medium was replaced with 150 μL dimethyl sulfoxide (DMSO) to dissolve the formazan crystals. The plate was shaken for about 2 h protected from light. Cell viability was measured by the optical density of reduced MTT at 570 nm using a microplate reader (Synergy HT from BioTeK Instruments Inc., Winooski, VT, USA). The percentage of viable cells was determined as the ratio between the absorbance of treated versus control (non-treated) cells.

### *4.6.6 Melanin production assay in human MNT-1 melanoma cells*

MNT-1 melanoma cells were grown in T-75 culture flasks at a density of $9 \times 10^5$ cells/mL in 10 mL of medium for 24 h. The cells were then treated with the non-cytotoxic concentration of 200 mM (in medium solution) for 48 h. This concentration was selected based on the MTT

viability results, presented below, causing a small reduction in cell viability (~15–20%) in 48 hours. After incubation, the cell culture medium (supernatant) was removed and transferred to a fresh tube and read directly at 465 nm with using a microplate reader (Synergy HT from BioTeK Instruments Inc., Winooski, VT, USA). The adherent MNT-1 cells were washed with PBS and detached from the flask using 0.05% trypsin-EDTA. The cells were collected in a test tube and washed twice with PBS. The cellular melanin was then extracted and measured as previously described.[34]

## References


1. Rescigno, A., Sollai, F., Pisu, B., Rinaldi, A. and Sanjust, E. (2002). Tyrosinase inhibition: General and applied aspects. Journal of Enzyme Inhibition and Medicinal Chemistry, **17**, 207–218.
2. Zolghadri, S., Bahrami, A., Khan, M. T. H., Munoz-Munoz, J., Garcia-Molina, F., Garcia-Canovas F, and Saboury, A. A. (2019) A comprehensive review on tyrosinase inhibitors, Journal of Enzyme Inhibition and Medicinal Chemistry, **34**, 279-309.
3. Ismaya W.T., Rozeboom H.J, Schurink M, Boeriu, C. G. and Dijkstraet B. W. (2011). Crystallization and preliminary X-ray crystallographic analysis of tyrosinase from the mushroom Agaricus bisporus. Crystallization Communications, **67**, 575–578.
4. Ramsden, C. A. and Riley, P. A. (2014). Tyrosinase : The four oxidation states of the active site and their relevance to enzymatic activation, oxidation and inactivation. Bioorganic and Medicinal Chemistry, **22**, 2388–2395.
5. Lin, J. Y. and Fisher, D. E. (2007). Melanocyte biology and skin pigmentation. Nature, **445**, 843–850.
6. Burger, P., Landreau, A., Azoulay, S., Michel, T. and Fernandez, X. (2016). Skin whitening cosmetics: Feedback and challenges in the development of natural skin lighteners. Cosmetics, **3**, 36.
7. Tomita, Y. and Suzuki, T.(2004). Genetics of Pigmentary Disorders. (2004). Genetics of pigmentary disorders. American. Journal of Medical Genetics, **131**, 75–81.
8. Zolghadri, S., Bahrami, A., Tareq, M., Khan, H. and Saboury, A. A. A comprehensive review on tyrosinase inhibitors. Journal of Enzyme Inhibition and Medicinal Chemistry, **34**, 279–309 (2019).

9. Taofiq, O., González-Paramás, A. M., Barreiro, M. F., Ferreira, I. C. F. R. and McPhee, D. J. (2017). Hydroxycinnamic acids and their derivatives: Cosmeceutical significance, challenges and future perspectives, a review. Molecules, **22**, 281.
10. Buitrago, E., Hardré, R., Haudecoeur, R., Jamet, H., Belle, C., Boumendjel, A., Bubacco, L. and Réglier, M. (2016). Are Human Tyrosinase and Related Proteins Suitable Targets for Melanoma Therapy? Current Topic in Medicinal Chemistry, **16**, 3033–3047.
11. Vad, N. M., Kandala, P. K., Srivastava, S. K. and Moridani, M. Y. (2010), Structure-toxicity relationship of phenolic analogs as anti-melanoma agents: An enzyme directed prodrug approach. Chemico- Biological Interactions, **183**, 462–471.
12. Eisenhofer, G., Tian, H., Holmes, C., Matsunaga, J., Roffler-Tarlov, S. and Hearing, V.J. (2003), Tyrosinase: a developmentally specific major determinant of peripheral dopamine. The FASEB Journal, **17**, 1248-1255.
13. Price, N. C. (1980). What is meant by 'competitive inhibition? Trends in Biochemical Science, **5**, 11.
14. Blat, Y. (2010). Non-Competitive Inhibition by Active Site Binders. Chemical Biology & Drug Design, **75**, 535-540.
15. Loizzo, M.R., Tundis, R. and Menichini, F. (2012). Natural and Synthetic Tyrosinase Inhibitors as Antibrowning Agents: An Update. Comprehensive Reviews in Food Science and Food Safety, **11**, 378-398.
16. Parvez, S., Kang, M., Chung, H.-S. and Bae, H. (2007). Naturally occurring tyrosinase inhibitors: mechanism and applications in skin health, cosmetics and agriculture industries. Phytotherapy Research, **21**, 805-816.
17. Noh, J. M., Kwak, S.Y., Seo, H.S., Seo, J.H., Kim. B.G. and Y.S. Lee. (2009). Kojic acid-amino acid conjugates as tyrosinase inhibitors. Bioorganic Medicinal Chemistry Letters. **19**, 5586–5589
18. Burdock, G. A., Soni, M. G. and Carabin, I. G. (2001). Evaluation of health aspects of kojic acid in food. Regulatory Toxicology and Pharmacology, **33**, 80–101.
19. Hsu, KD., Chen, HJ., and Wang, CS. (2016). Extract of Ganoderma formosanum Mycelium as a Highly Potent Tyrosinase Inhibitor. Scientific Reports, **6**, 32854.
20. Gülçin, I. (2006). Antioxidant activity of caffeic acid (3,4-dihydroxycinnamic acid). Toxicology **217**, 213–220.
21. An, S. M., Koh, J. S. and Boo, Y. C. (2010). *p*-coumaric acid not only inhibits human

tyrosinase activity in vitro but also melanogenesis in cells exposed to UVB. Phythoterapy Research, **24**, 1175–1180.

22. Thalmann, C. R. and Lötzbeyer, T. (2002). Enzymatic cross-linking of proteins with tyrosinase. European Food Research and Technology, **214**, 276–281.
23. Garcia-Jimenez, A. Teruel-Puche, J. A., Garcia-Ruiz, P. A., Saura-Sanmartin, A., Berna, J., Rodríguez-López, J. N. and Garcia-Canovas, F. (2017). Action of tyrosinase on caffeic acid and its n-nonyl ester. Catalysis and suicide inactivation. International Journal of Biological Macromolecules, **107**, 2650–2659.
24. Micillo, R.; Sirés-Campos, J.; García-Borrón, J.C.; Panzella, L.; Napolitano, A.; Olivares, C. (2018). Conjugation with Dihydrolipoic Acid Imparts Caffeic Acid Ester Potent Inhibitory Effect on Dopa Oxidase Activity of Human Tyrosinase. International Journal of Molecular Sciences, **19**, 2156.
25. Liang, C. P., Chang, C. H., Liang, C. C., Hung, K. Y. and Hsieh, C. W. (2014), In vitro Antioxidant activities, free Radical Scavenging Capacity, and Tyrosinase inhibitory of Flavonoid compounds and Ferulic Acid from Spiranthes sinensis. Molecules**, 19**, 4681–4694.
26. Taofiq, O., González-Paramás, A. M., Barreiro, M. F., Ferreira, I. C. F. R. and McPhee, D. J. (2017). Hydroxycinnamic acids and their derivatives: Cosmeceutical significance, challenges and future perspectives, a review. Molecules, **22**, 281.
27. Abotaleb, M., Liskova, A., Kubatka, P. and Büsselberg, D. (2020), Therapeutic potential of plant phenolic acids in the treatment of cancer. Biomolecules, **10**, 1–23.
28. Lajis, A. F. B., Hamid, M. and Ariff, A. B. (2012). Depigmenting effect of kojic acid esters in hyperpigmented B16F1 melanoma cells. Journal of Biomedicine and Biotechnology, **2012**, 1-9.
29. Mikami, M., Sonoki, T., Ito, M., Funasaka, Y., Suzuki, T., & Katagata, Y. (2013). Glycosylation of tyrosinase is a determinant of melanin production in cultured melanoma cells. Molecular Medicine Reports, **8**, 818-822.
30. Lee, N. S., Choi, S., Moon, S.-W. and Boo, Y. (2008), p-Coumaric acid, a constituent of Sasa quelpaertensis Nakai, inhibits cellular melanogenesis stimulated by α-melanocyte stimulating hormone. British Journal of Dermatology, **159**, 292-299.
31. Boo, Y. C. (2019). p-coumaric acid as an active ingredient in cosmetics: A review focusing on its antimelanogenic effects. Antioxidants **8**, 275.

32. Asthana, S. Zucca, P., Vargiu, A.V., Sanjust, E., Ruggerone, P., Rescigno, A., (2015). Structure–Activity Relationship Study of Hydroxycoumarins and Mushroom Tyrosinase. Journal of Agricultural and Food Chemistry, **63**, 7236–7244.
33. Twentyman, P. R. (1987). A study of some variables in a tetrazolium dye (MTT) based assay for cell growth and chemosensitivity. British Journal of Cancer, **56**, 279–285
34. Soddu, G., Sanjust, E., Murgia, S. and Rescigno, A. (2004), Interference of Some Tryptophan Metabolites in the Formation of Melanin In Vitro. Pigment Cell Research, **17**, 135-141.

# 5

# Cell metabolomics: Impact of [Cho][HCA]ILs on the metabolism of human MNT-1 melanoma cells

## 5.1 The metabolomics approach

The word “omics” refers to a class of disciplines aimed at the study of complex biology systems.[1] They include, among the others, genomics, transcriptomics, proteomics, and metabolomics. Whereas genomics, transcriptomics, and proteomics are based on the analysis of the complete genome, gene expression and proteins, respectively, metabolomics is deemed as the end point of the “omics” cascade (Figure 5.1).[2] Metabolomics entails the comprehensive analysis of the inventory of endogenous small molecules (molecular mass < 1500 Da) present in a biological system as a result of intermediary cellular metabolism[3,4]. The general aim of metabolomics is to detect/quantify fluctuations in this inventory, the metabolome, upon a given stimulus/perturbation such as disease, toxicant, pharmaceutical drug, environmental factors or diet. Being the downstream product of gene expression, the metabolome can be regarded as a reliable snapshot of the molecular phenotype of an organism that closely reflects the cell functional status. Hence, the comprehensive description of metabolite changes, through metabolomics, has the potential to reveal unforeseen deviations from homeostasis and to identify new endpoint markers of effect.

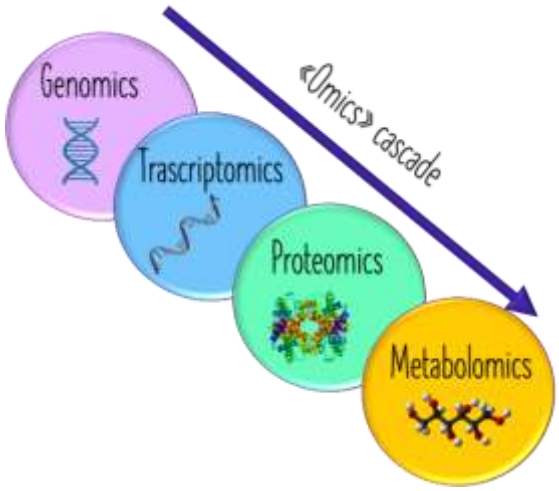


Figure 5.1 “Omics” cascade

Based on the research area of application as well as the specific objective of the analysis, the biological questions addressed in metabolomics research are equally or even more diverse, for instance discovering new diagnostics and therapeutics for diseases, optimizing output from industrial biotechnology, improving food quality, or support health claims of functional foods.

Basically, metabolomics studies can be divided in *targeted* and *untargeted* analyses.[5] Targeted analysis, known also as quantitative metabolomics, is focused on accurate identification and quantitation of a defined set of metabolites in biological samples. Typically, this set of metabolites is predetermined by the scientific question at hand or the size of the metabolite library that is available in the software used for data analysis. Untargeted approaches establish that the significant metabolites are by definition unknown prior to analysis, as are their physico-chemical characteristics, which usually encompass a wide variability range and an exhaustive separation of them from the matrix is usually required for quantification. Untargeted studies are highly interested in the identification of unknown metabolites, especially when they are the biomarkers of a study.[6]

A further differentiation of metabolomics analyses can be done based on the scientific application: *metabolic profiling*, *metabolic fingerprinting*, *metabolic footprinting*, and *metabolomics*.[7] *Metabolic profiling* is the quantitative analysis of a group of pre-defined metabolites, like members of a particular pathway. *Metabolic fingerprinting* mostly uses spectroscopic data and involves sorting datasets into categories so that conclusions can be drawn about the classification of individual samples.[8] The studies of metabolic fingerprinting are focused on the classification of samples by analysing their intracellular metabolome (endometabolome). The term *metabolic footprinting* refers to the study of the extracellular metabolites (exometabolome), i.e., what a cell or system excrete under controlled conditions into the growth media, while *metabolomics* provides an unbiased overview of whole-cell metabolic patterns.[7]

## 5.2 Metabolomics analytical platforms

The main analytical platforms used in metabolomics studies are nuclear magnetic resonance (NMR) spectroscopy and mass spectrometry (MS). These techniques enable the simultaneous detection of tens to hundreds of metabolites in complex mixtures like biofluids and tissue/cell extracts, providing a holistic approach which is clearly more powerful than the measurement of a few pre-established metabolites by classical biochemical methods.[4,9] MS-based methods are generally more sensitive than NMR, enabling the detection of metabolites present at sub-nanomolar concentrations. However, the wider view of the metabolome offered by MS methods does not always translate into a significant gain in biochemical information, as the resulting data

may be extremely complex and difficult to interpret. For this reason, MS is often coupled with chromatographic methods, most commonly gas chromatography (GC) and liquid chromatography (LC) that allow to resolve peak overlap. GC-MS is limited to volatile compounds, while LC-MS is suitable for the analysys of thermal instable metabolites. Despite its inherent sensitivity limitations (measured concentrations in the micromolar to milimolar range), high resolution NMR is a non-destructive technique with an unparalleled analytical reproducibility and the ability to provide unequivocal structural and quantitative information on a wide range of metabolites. Recent progresses have allowed improvements of NMR sensitivity thanks to the use of high field magnets and cryiogenic technology.[10]

It is evident that there is no analytical platform able to analyse alone the metabolome. Although currently most of the metabolomics studies use either NMR or MS separately, a growing number of investigations has been proving that combining NMR and MS analysis is very valuable to a more complete characterization of metabolome.

## 5.3 Multivariate analysis

NMR and MS techniques produce data sets with a number of metabolite features greatly exceeding the number of samples (thousands of variables, while a number of samples ranging from a few tens to a few hundred because of time and cost limits). To overcome the high level of complexity of the data matrix, principally due to the high number of variables, data analysis is typically done through multivariate statistical tools that extract the latent biochemical information in the data set by creating new pseudo-variables that reduce its dimensionality. Basically, these techniques can be grouped into three different approaches:

- *exploratory* methods that provide an overview of all data in order to identify trends, patterns or clustering;

- *classification or discriminant* methods that organize the samples into categories and classes on the basis of common characteristics;

- *regression* methods to create models for prediction of the response.

The most widely used multivariate analysis methods include Principal Component Analysis (PCA) and Partial Least Squares (PLS). Both methods transform the original variables in a

smaller set of new variables tha generally are sufficient to account for the majority variations (e.g., PCA) or to maximise separability (e.g., PLS) of the entire data.

***PCA*** is an unsupervised technique used whereby no a priori information on sample groups is included.[11] This method generates new uncorrelated (orthogonal) variables, called principal components (PCs: PC1, PC2,…PCn) as linear combination of the original variables. In the new space of reduced dimensionality, PCs represent the directions along which the data has maximum variance. Then, PC1 accounts for most of the variance, PC2 for the 2nd largest variance and so on, always obeying the constraint that all PCs are orthogonal to each other. The relationship between variance, PC and information is that the larger the variance carried by a PC, the larger the dispersion of the data points along this direction, and thus the more the information it has. Mathematically, the search for the directions of the new system of coordinates can be traced back to the search for the eigenvalues and eigenvectors of the covariance matrix of the original data set: eigenvectors are the directions of the axes where there is the most variance; eigenvalues are the variances associated with each principal component.

The results of PCA are graphically represented by two plots. The *scores plot* shows the positions of each observation in the new coordinate system of PCs. When investigating *scores plot*, clustering, outliers, time-based patterns can be explored. The *loadings plot* provides an easier visualization on how strongly each original variable influences a principal component: large loadings (positive or negative) indicate that a particular variable has a strong relationship to a particular principal component. Loadings plots provide also information on how variables correlate with one another.

***PLS*** is a multivariate projection method for modelling a linear relationship between independent variables X and dependent variables Y,[12] seeking to find a set of latent features that maximises the covariance between X and Y. This method provides a simple way to deal with missing data giving an actrative connection between two central operations in matrix algebra and statistics. Partial least squares discriminant analysis ***(PLS-DA)*** is a variant of PLS used for a classification and discrimination problems. It is performed by a PLS regression to find a linear relation between a X predictor matrix and a response vector Y that assume discrete values. This means that each sample is assigned a value of 1 or 0 depending on whether or not it belongs to a specific class. Given the very high ratio of variables to samples typically characterising the matrices used in metabolomic studies, both PLS and PLS-DA models are susceptible to over-fitting and thus sample separation in the scores plot does not always correspond to consistent

differences between the groups. The leave- one-out cross-validation is most frequentely used to select the optimal number of components for classification and validate the results found, allowing to estimate predictable Y variation (i.e., $Q^2$): the closer $Q^2$ is to 1 the more robust is the model. To further assess model consistency and performance, a response permutation test can be also applied.[13] In brief, permutation testing compares the original model's goodness of fit with the values obtained after class randomization. Loading plots and Variable importance in the Project (VIP) value are commonly used in PLS-DA for biomarker selection. VIP score is the squared function of the PLS weights counting the amount of explained y variance in each dimension. The higher the VIP scores, the more influential the corresponding variable is. VIP values more than 1.0 are used as a cut off value for variable selection, representing those variables to be most effective ones in the model.

## 5.4 Cell Metabolomics

Metabolomic studies of cultured mammalian cells have been growing exponentially over the last years, with applications reported in diverse areas like drug testing, mechanistic understanding of diseases and toxicology.[14] Compared to metabolomics of animal models or human subjects, *in vitro* cell metabolomics offers several advantages, such as a high control over experimental variables, less stringent ethical issues, lower costs and potentially lower biological variability.[15] On the other hand, the number of studies reported in the literature is still low as compared to the use of metabolomics for the analysis of body fluids (e.g. serum, plasma, urine, etc.) since metabolomic analysis of cultured cells involves specific requirements that can be quite challenging. One critical issue is obtaining reliable and reproducible results that are representative of the *in vivo* situation.[14] Moreover, cell lines tend to have stable phenotypes which do not depend on donor characteristics, unlike primary cells, particularly those of human origin, which are characterised by high phenotypic variability.[14] Another aspect to consider is the number of cells needed to obtain detailed metabolic information. Under common NMR acquisition conditions (500-600 MHz field strength, regular high resolution probe), a minimum of ~3-5 million cells per sample is typically required to detect a few tens of metabolites.[16] Hence, in a study involving several experimental conditions and biological replicates of each condition, growing sufficiently high cell numbers can be a demanding task.

A major requirement for *in vitro* cell studies is to plan an adequate experimental study design, which guarantees the feasibility of the experiment and answers the question of interest. Moreover, different culture pratical aspects may contribute to introduction of variability to the metabolomic data. For instance, the method of detachment from the culture surface when culturing adherent cells. A commonly used method consists of using trypsin to cleave cell adhesion proteins, together with ethylenediaminetetraacetic acid (EDTA) to chelate calcium ions needed for integrin-mediated cell attachment. Although trypsinization is extensively used in routine cell culture, it has been enhanced that it alters the physiological state of cells, changing their metabolic profile.[17] Moreover, depending on the cell type and the time required for trypsinization, this procedure has been shown to cause significant metabolite leakage by increasing cell membrane permeability.[2] Another inconvenience regards the time-consuming steps that follow trypsin addition (washing and centrifugation), which can lead to metabolite modifications and further losses. To overcome this issue, an alternative approach consists of mechanically scraping the cells of the culture surface, after medium removal. In particular, direct scraping in the presence of the extraction solvent has been recommended as the more suitable harvesting procedure that maximises overall metabolite yield and enables rapid metabolism quenching.[17,18] The deactivation (quenching) of cellular metabolic activity at the time of sampling is a crucial step to avoid fluctuations in metabolite levels during sample collection and processing, which could lead to misleading results. There are several ways to quench enzymatic activity, such as addition of ice-cold organic solvents, liquid nitrogen freezing or of quenching buffers.[14] If cell integrity is to be preserved, the use of a cold isotonic saline solution (0.9% NaCl, 0.5 ºC) is favoured.[19]

Given the diverse chemical nature of intracellular metabolites, there is no universal method capable of extracting the whole cellular content. Nevertheless, efforts have been made to establish the most efficient and reproducible extraction procedures which are compatible with the analytical platform to be used. In particular, different solvent mixtures have been extensively tested, including different proportions of water, acids and organic solvents.[18,20] Among the solvent mixtures compared, the one based on methanol, chloroform and water was highlighted as the most suitable for retrieving a higher number of metabolites from adherent mammalian cells and for achieving reliable and robust NMR metabolic profiles.[20] Indeed, this mixture allows the dual-phase extraction of both polar and lipophilic compounds, facilitating their composition to be characterised separately.

## 5.5 Effect of [Cho][HCA] ILs on the metabolome of MNT-1 cells

Cell-based assays play a pivotal role in understanding cell physiology in the presence of pharmaceutical reagents in both healthy and diseased states as well as in drug discovery. The classical assays are based on traditional cell culture methods with the possibility of measuring various functional activities such as proliferation, toxicity, changes in morphology or gene expression. Although studies of cell-based metabolomics are currently still few, the results obtained so far have been showing the potential of this approach as a complementary tool to the study of cell function, offering the closest direct measurement of a cell's physiological activity.

In the light of these considerations and the results of the biological assays performed on [Cho][Caf], [Cho][Fer] and [Cho][*p*-Coum], described in Chapter 4, I have investigated the impact of these compounds on the metabolome of human MNT-1 melanoma cells in order to gain additional information on the potential biological activity of these compounds as new pharmaceutical agents. In particular, possible cellular metabolic changes induced by the action of cholinium salts were explored by NMR-based metabolomics analysis of both the hydrophilic and lipophilic extracts of cells and the aqueous culture medium before and after exposure to ILs. For the sake of comparison, NMR experiments were performed also for cells treated with Kojic acid (KA).

### *5.5.1 Metabolic profile of the aqueous extract of MNT-1 cells and culture medium*

Figures 5.2 and 5.3 show a representative $^{1}$H NMR spectrum of the aqueous extract of human MNT-1 melanoma cells and cell culture medium, respectively. Based on the analysis of 2D NMR spectra recorded for selected samples, literature data[21] and the Human Metabolome Database (https://hmdb.ca), 31 metabolites were identified in the $^{1}$H NMR spectrum of the aqueous extract. These include several amino acids, Krebs cycle intermediate, choline compounds, sugars, and energy related metabolites. The spectrum of cell culture was mainly characterized by the peaks of nutrient substrates including various amino acids and glucose to provide the entire necessary elements for the cellular growth.

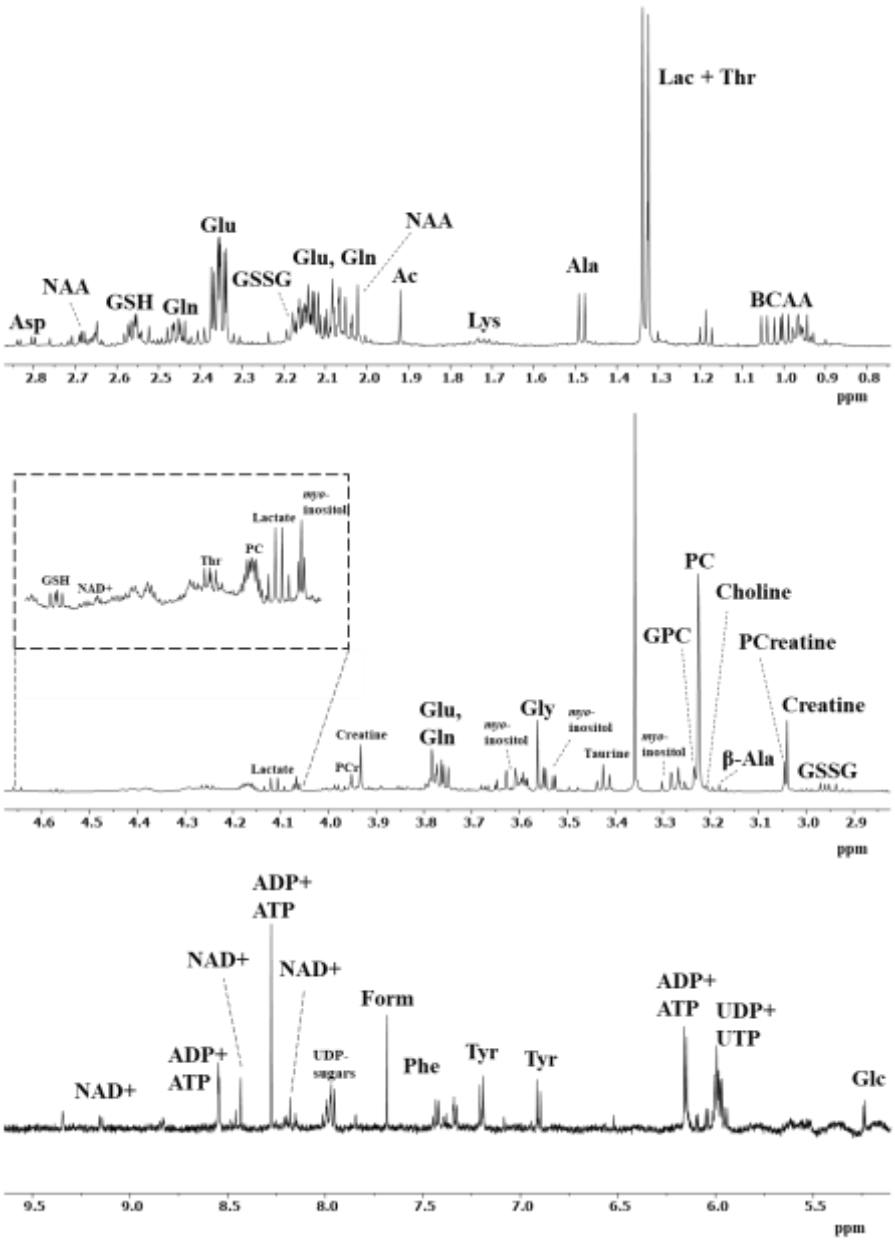


**Figure 5.2** Representative 500 MHz $^{1}$H NMR spectrum of the aqueous extract of human MNT-1 melanoma cells. Abbreviations: Acetate (Ac), Adenosine diphosphate ($ADP^{+}$), Adenosine triphosphate (ATP), Alanine (Ala), Aspartate (Asp), Branched-chain amino acids (BCAA), Formate (Form), Glucose (Glu), Glutamine (Gln), Glutathione disulfide (GSSG), Glycerol phosphorylcholine (GPC), Glycine (Gly), Lactate (Lac), Lysine (Lys), *N*-acetylaspartate (NAA), Nicotinamide Adenine Dinucleotide ($NAD^{+}$), Phosphocholine (PC), Phosphocreatine (PCreatine), Reduced Glutatione (GSH), Taurine (Tau), Threonine (Thr), Tyrosine (Tyr), Phenylalanine (Phe), Uridine diphosphate ($UDP^{+}$), Uridine diphoposphate sugars (UDP-sugars), Uridine triphosphate (UTP),

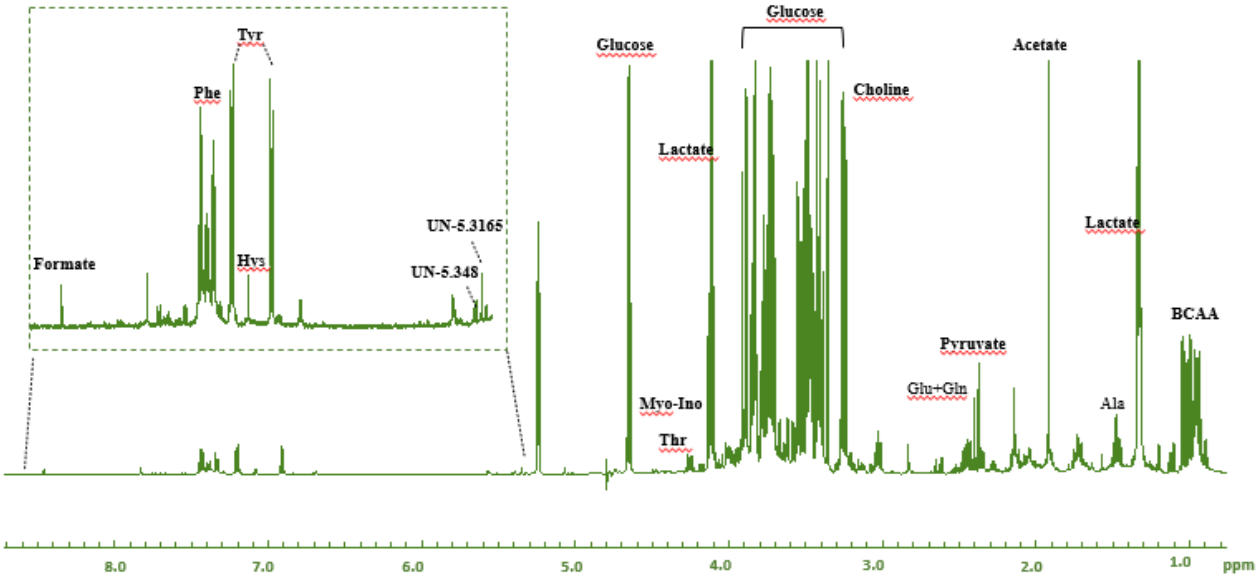


**Figure 5.3** Representative 500 MHz $^{1}$H NMR spectrum of cell culture medium. Abbreviation: Acetate (Ac), Alanine (Ala), Branched-chain amino acids (BCAA), Formate (Form), Glucose (Glu), Glutamine, (Gln), Hystidine (Hys), Lactate (Lac), Phenylalanine (Phe), Tyrosine (Tyr), Unknown (UN).

The whole NMR data set relative to the aqueous extracts from treated and untreated cells was preliminarily examined by PCA. The first two principal components, PC1 and PC2, explained 42.7 and 29.7% of the total variance, respectively. Evaluating the PC1 vs PC2 plot revealed no clear separation of samples either according to the treatment (control vs treated cells) or according to the nature of compounds (Figure 5.4).

In order to obtain better insights on the biochemical consequences occurring upon compound exposure, an unsupervised (PCA) and a supervised (PLS-DA) model were separately built for each treated cell system in a pairwise comparison with controls (Figure 5.5). Only the models constructed to compare KA-incubated samples with controls failed to distinguish the metabolic profiles of treated and untreated cells (data not shown), PLS-DA model exhibiting a predicitive power, $Q^2$, equal to 0.176. Regarding the models built with cells exposed to [Cho][HCA]ILs, all three PCA scores plots showed a reasonable separation between controls and treated samples (Figures 5.5, left side).

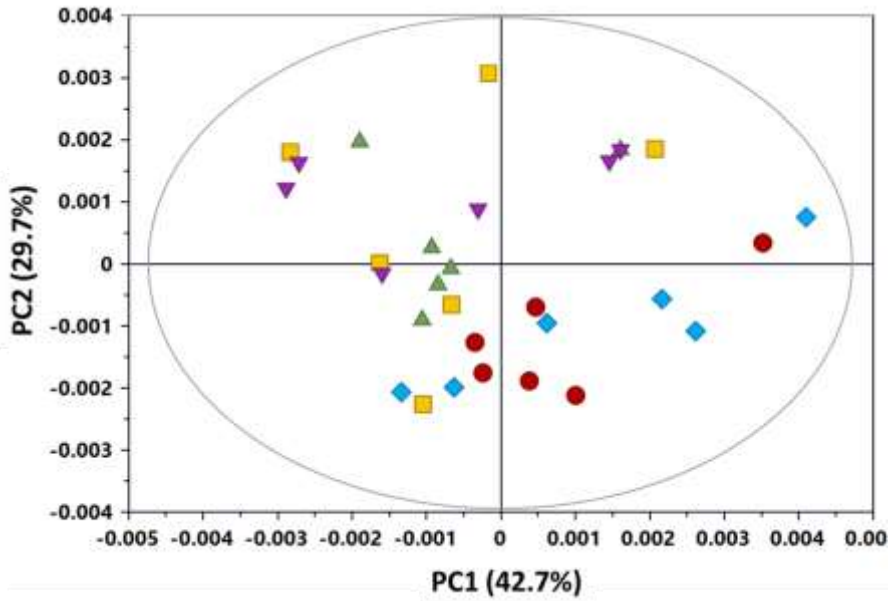


**Figure 5.4** PC1 vs PC2 plot of the PCA model built with the whole $^{1}$H NMR data set of the aqueous extracts of treated and untreated MNT-1 cells: ●, Control; ▲, [Cho][Caf]; ■, [Cho][Fer]; ▼, [Cho][*p*-Coum]; ♦, KA.

Nevertheless, a satisfying discrimination between the two groups ($Q^2 > 0.4$) was achieved only in case of exposure to [Cho][Caff] (Figure 5.5A, center) and [Cho][*p*-Coum] (Figure 5.5B, center). Differentely. the model built with control and [Cho][Fer]-treated samples exhibited a weak predictive power ($Q^2 < 0.386$) (Figure 5.6C, center). Inspection of PLS-DA loadings colored according to the VIP values (Figure 5.5, right side) qualitatively evidenced the metabolites with the most important contribution to sample discrimination, thus providing immediate assessment of the main similarities and differences between the metabolic effects produced by [Cho][HCA]ILs. Hot (cold) color denotes high (low) VIP value and thus a high (low) contribution of the corresponding metabolite for the discrimination of samples. Variables with a VIP value greater than 1 possess significant differences. As can be noted, the most important discriminant features comprised changes in the levels of taurine, choline, branched-chain amino acids, alanine, citrate, glucose, phosphocholine and myo-inositol. Higher level of phosphocholine compare to controls was the only common variation between the three exposure to cholimiun salts.

Complementary information on the effects induced on polar cellular metabolites by exposure to [Cho][HCA]ILs and KA was achieved by univariate statistical analysis of the spectral

integration of individual metabolite peaks (only signals clearly representative of a single compound and not severely overlapped with other peaks were taken into consideration). These results are summarised in the form of heatmap in Figure 5.6, color-coded according to the percentage of variation of each metabolite in treated cells relatively to controls. Only variations with a medium-large magnitude (|ES|>0.5) were considered.

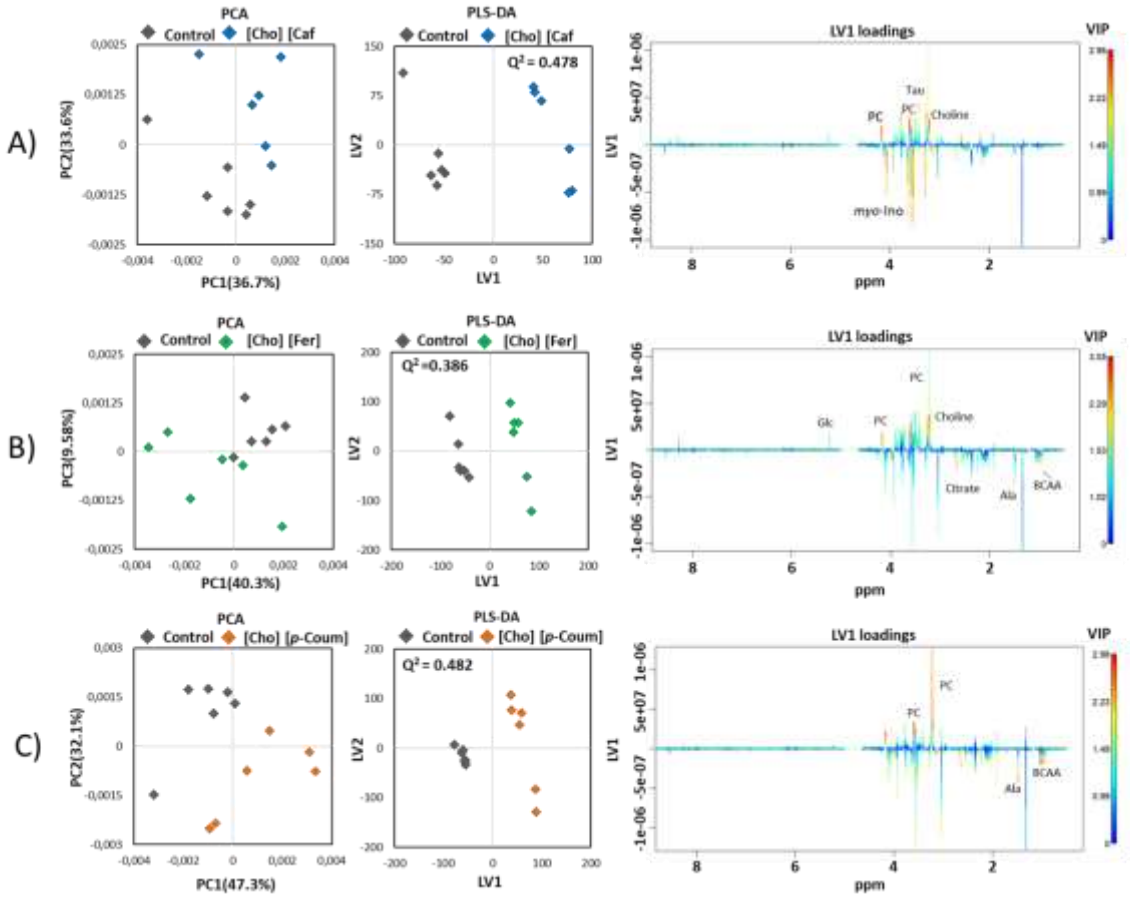


**Figure 5.5** PCA (left) and PLS-DA (center) scores plots of the models built with the $^{1}$H NMR spectra of the aqueous extract of cells treated with [Cho][HCA]ILs. VIP-coded PLS-DA loading plot (right) revealing the metabolites with large intensities responsible for the discrimination of the corresponding score plots. A) [Cho][Caff]; B) [Cho][Fer]; C) [Cho][*p*-Coum]-.Abbreviation: Alanine (Ala), Branched-chain amino acids (BCAA), Glucose (Glu), Phosphocholine (PC), Taurine (Tau), Myo-inositol (Myo-inos).

As can be noted, the effects produced at the intracellular level in aqueous metabolites were more numerous and more pronounced in [Cho][Fer] ILs exposed cells. Indeed, ten were the metabolites whose concentrations were significantly altered by the presence of [Cho][Fer], while

nine were that significally affected by the exposure to [Cho][*p*-Coum]. Only seven metabolites were altered by cell treatment with [Cho][Caf], and four by treatment with KA.

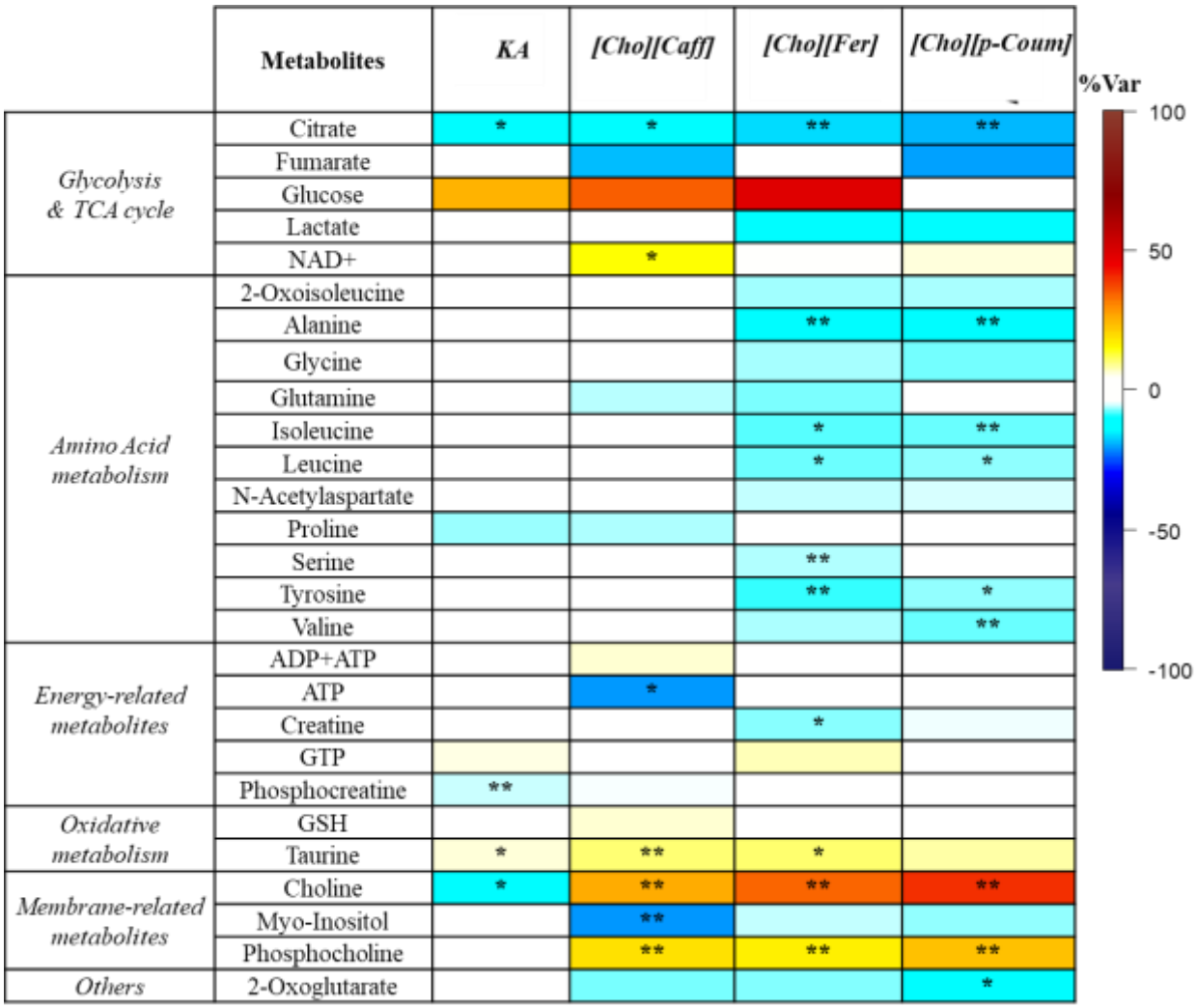


**Figure 5.6** Heatmap showing % variations of the metabolite levels in the aqueous extracts of MNT-1 treated cells compared to control. The color scale represents percentage of variation. Only significant p values are shown: * $p < 0.05$; ** $p < 0.01$. Abbreviations: ADP, adenosine diphosphate; ATP, adenosine triphosphate; GTP, guanosine triphosphate $NAD^+$, nicotinamide adenine dinucleotide; GSH, reduced glutathione.

Analysis of the extracellular metabolites (exometabolome) in the cell culture medium provided complementary information on the metabolic activity of cells. Indeed, comparing the metabolite composition of cell conditioned medium with that of acellular culture medium (incubated under the same conditions but in the absence of cells) allowed to assess the metabolites consumed and

excreted by MNT-1 cells upon treatment. The results relative to the most significant changes observed are depicted in Figure 5.7 where negative variarions denote metabolite consume, while positive variations indicate metabolite excretion. Statistically significant differences respect to controls are denoted with an asterics. Amino acids, carbohydtates, organic acids, choline and myo-inositol are standard components of culture media.

As can be seen in Figure 5.7, some amino acids (AA) present in the culture medium such as branched-chain amino acids (BCAA: valine, leucine, and isoleucine), glutamine and histidine were consumed by both untreated and treated cells. Conversely, others AA such as alanine, glutamate and threonine were excreted by cells. Among the excreted AA, significant variations compared to controls were observed for alanine only upon cell exposure to [Cho][HCA] ILs, levels being significantly lower, while treonine and tyrosine were found to be significantly higher in the presence of KA. Additionally, the most significant differences in term of consumption of AA were observed only in the presence of KA, exhibiting lower absorption of valine, leucine, and histidine.

The analysis of the exometabolome evidenced also a decrease of cholinium (Cho) content in the media of controls and KA-treated cells, while an increase was observed in the presence of [Cho][HCA] ILs, thus evidencing Cho consumption by the first two samples and cellular excretion upon exposure to HCA-derivatives. Similarly to choline, consumption of myo-inositol (MI) occurred also in the media of both untreated and KA-treated cells, without any significant variations between the observed decreased MI content. Differentely, a significant excretion of intercellular MI took place upon cell treatments with cholium salts. The most intense variations in the medium composition were observed for organic acids and carbohydrates, the former increasing and the latter decreasing in both treated and untreated cell compared to the acellular medium. Significant changes compared to controls were observed only for pyruvate and formated in the medium of cells trated with [Cho][Caf].

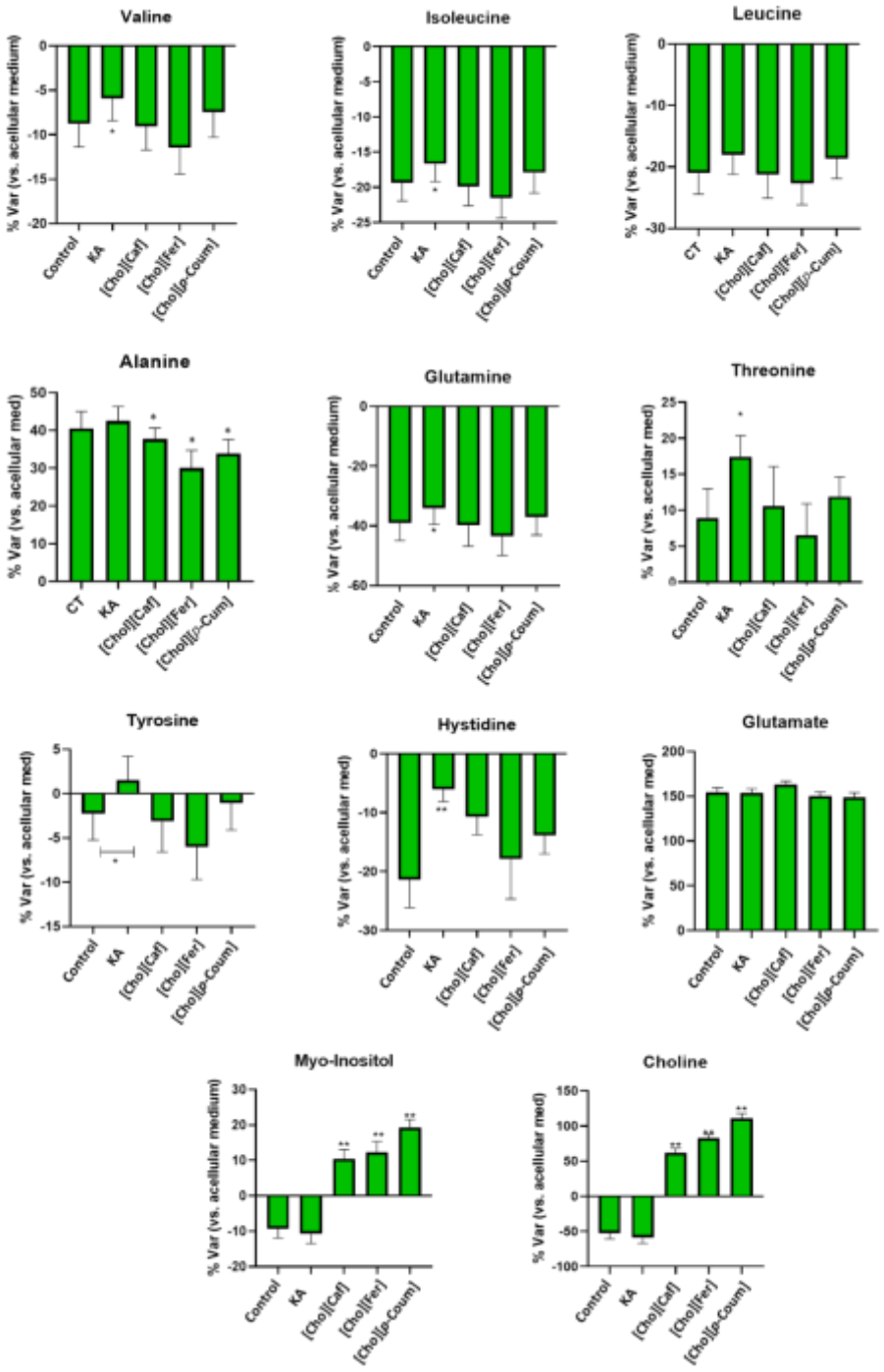


**Figure 5.7** Relative variation of intercellular metabolites in the culture media (n=6) of treated cells and controls compared to unconditioned culture media. Asterics denotes statistically significant differences compared to control: * *p*-value < 0.05; ** *p*-value < 0.01 (To continue)

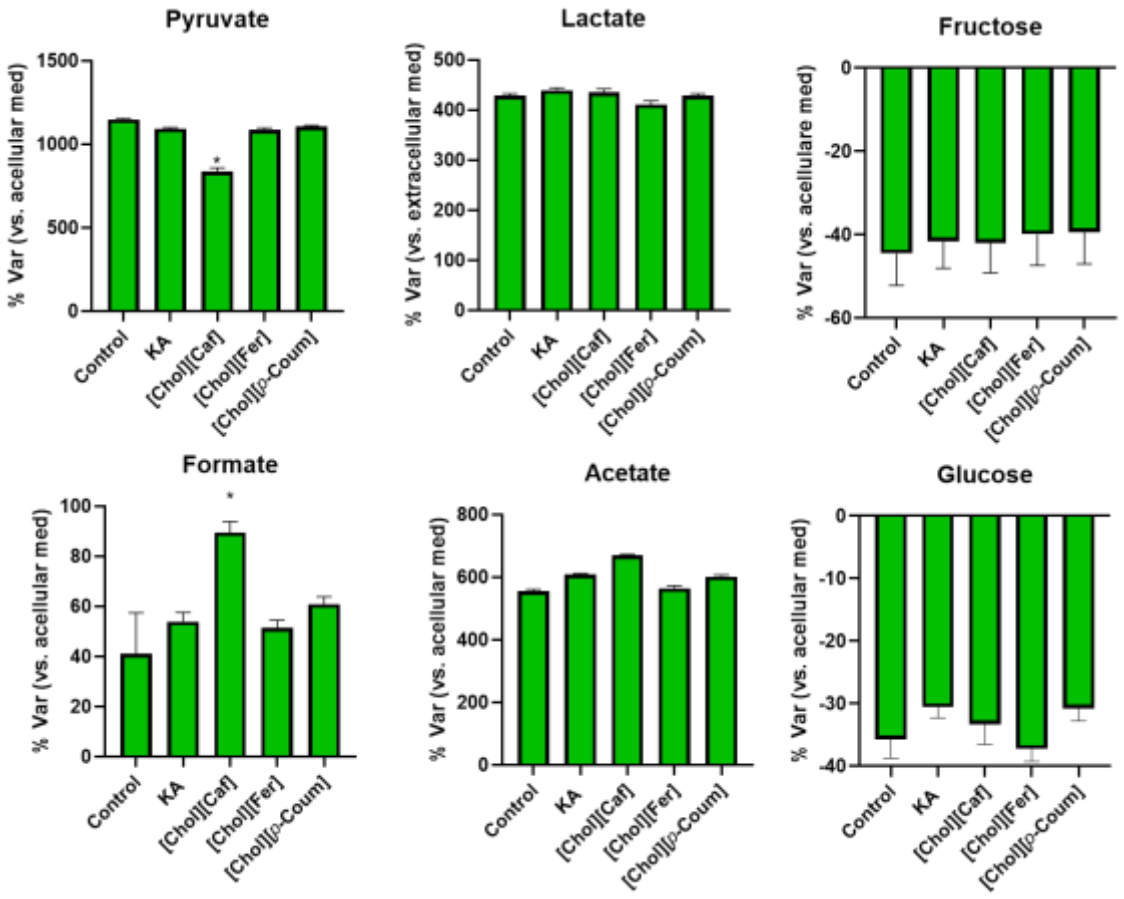


**Figure 5.7** Relative variation of intercellular metabolites in the culture media (n=6) of treated cells and controls compared to unconditioned culture media. Asterics denotes statistically significant differences compared to control: * *p*-value < 0.05; ** *p*-value < 0.01.

### *5.5.2 Metabolic profile of the lipid extract of MNT-1 cells*

Figure 5.8 shows $^{1}$H NMR spectrum of lipophilic extracts from MNT-1 cells. Spectral assignment relied primarily on matching the chemical shift information derived from 1D and 2D spectra to previous literature reports[21] and the Human Metabolome Database (https://hmdb.ca). The main contributors to the lipophilic profile were the signals of cholesterol and phosphatidylcholine (PTC), two major components of cell membranes. Cholesterol was easily identified through its characteristic singlet arising from $CH_3$-18 (0.69 ppm), while PTC was identified through the intense proton signals arising from $N(CH_3)_3$ headgroup (3.30 ppm), $CH_2$-N (3.75 ppm), $CH_2$-OP (4.31 ppm), glyceryl $CH_2$-*sn*3 (3.92 ppm) and CH-*sn*2 (5.29 ppm). Other membrane phospholipids, namely phosphatidylethanolamine (PTE) in both the diacyl and

plasmenyl forms and sphingomyelin (SM), were also identified. A band from an unknown metabolite (UN-3.150 ppm) was found to overlap with peaks of PTE plasmenyl form. Additionally, smaller amounts of neutral lipids, namely cholesterol esters, diglycerides (DG) and triglycerides (TG) were also noticed.

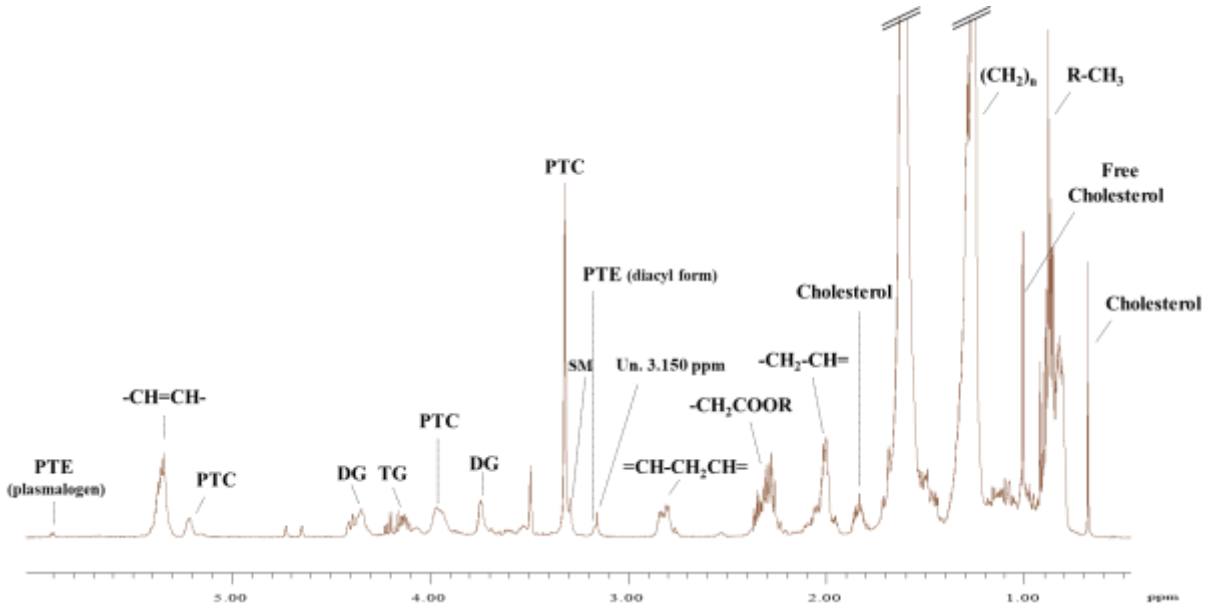


**Figure 5.8** Representative 500 MHz $^{1}H$ NMR spectrum of the lipophilic extract from MNT-1 cells in $CDCl_3$. Abbreviations: Diglycerides (DG), Phosphatidylcholine (PTC), Phosphatidylethanolamine (PTE), Sphingomyelin (SM), Triglycerides (TG).

Comparing the NMR profile of the lipid extracts from treated and untreated cells didn't point out significant changes due to the exposure to cholium salts and KA, except for those summarised in Figure 5.9. As can be seen, one of the most significant variation was the increase in the levels of $CH_3$ fatty acid chains signal upon [Cho][*p*-Coum] treatment, while the other was observed in the presence of [Cho][Caf] and [Cho][Fer] and regarded the above mentioned peak at 3.15 ppm not attributed.

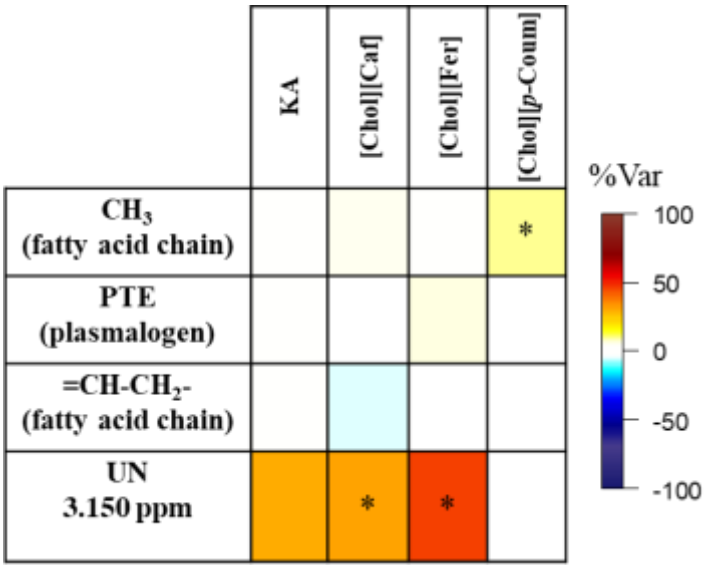


**Figure 5.9** Heatmap showing the most significant % variations observed in the the lipid extracts of treated MNT-1 cells compared to control. The color scale represents percentage of variation. Only significant p values are shown: * $p < 0.05$; ** $p < 0.01$.

### *5.5.3 Discussion*

Cellular metabolism can be viewed as a complex network of chemical reactions, catalysed by enzymes and strictly regulated, which allow organisms to grow and reproduce, maintain their structures, and respond to environmental changes.[22] As represented in Figure 5.10, these reactions are organised into many inter-dependent metabolic pathways.[23]

Besides the dysregulation of glucose metabolism, metabolic reprogramming in cancer cells is characterized by abnormal lipid metabolism, amino acids metabolism, mitochondrial biogenesis, and other bioenergetic metabolism pathways. Investigation on these energy metabolism reprogramming is of fundamental importance to understand the molecular events of malignancy and help to improve the ways to diagnose and treat cancer.[24]

The results of the metabolomics study performed in my PhD thesis showed that the metabolic profiles of human MNT-1 melanoma cells assessed by $^{1}$H NMR spectroscopy are sensibly affected by the exposure to [Cho][HCA]ILs. These variations allowed to gain some important information about the cellular mechanisms affected by these compounds. As summarized in the Venn diagramm in Figure 5.11, the most important changes concerned a down-regulation of

most of the amino acids, and energy related metabolites and an up-regulation of glucose, $NAD^+$, choline and phosphocholine. These results are discussed below in term of the possible altered metabolic pathways.

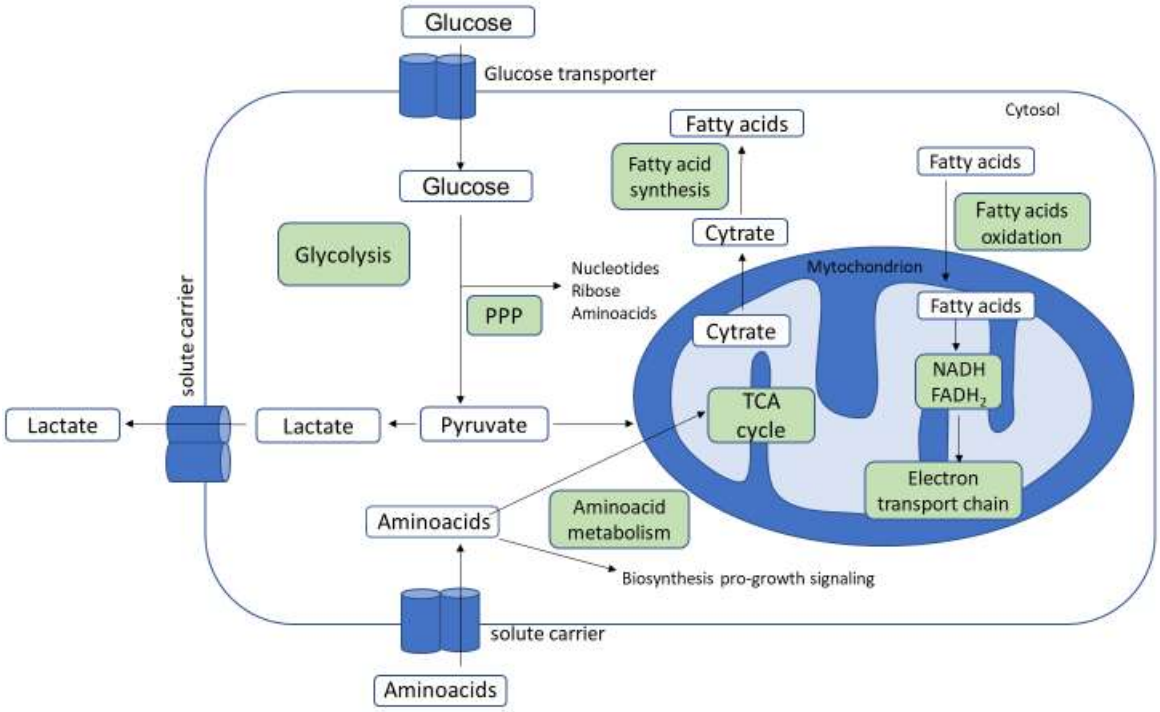


**Figure 5.10.** Diagram illustrating the integration of major metabolic pathways in animal cells. Pyruvate, from glycolysis, is either converted into lactate and released, or used to fuel the tricarboxylic acid (TCA) cycle. The TCA cycle can also be fuelled by several amino acids, which originate acetyl-CoA, pyruvate or cycle intermediates, or by acetyl-CoA resulting from fatty acid oxidation. Citrate, generated in the TCA cycle, and NADPH, from the pentose phosphate pathway (PPP), are then used for fatty acid synthesis. Finally, NADH and FADH2, produced in the TCA cycle and during fatty acid oxidation, contribute for ATP production from the electron transport chain. Readaped from[22]

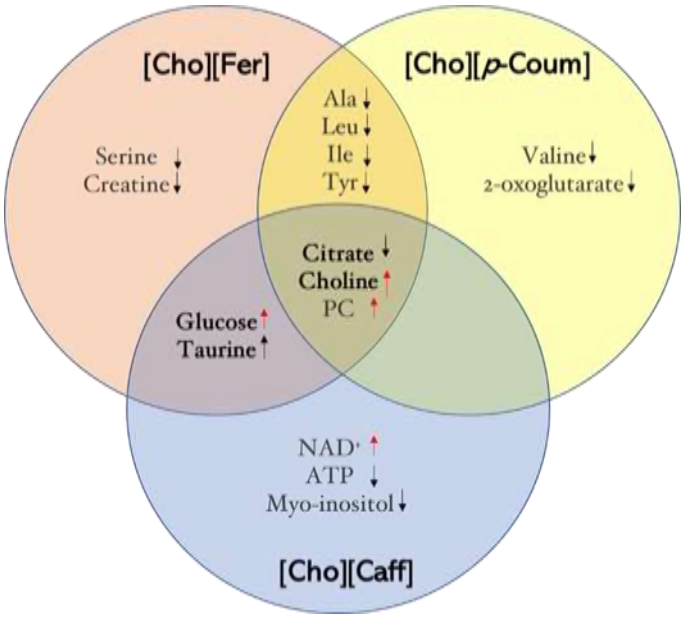


**Figure 5.11** Venn diagram illustrating a summary of the intracellular metabolites most sensibly altered upon treatment with [Cho][HCA]ILs. Bold character denotes metabolites affected also by exposure to Kojic acid. Abbreviation: PC, phosphocholine.

***Glucose metabolism.*** Glucose is the major nutrient to fuel cell growth. Its metabolism contains glycolysis pathway, pentose phosphate pathway (PPP), and serine synthesis pathway (SSP) in the cytoplasm and tricarboxylic acid (TCA) cycle in the mitochondria.

*Glycolysis* is a central pathway of glucose metabolism. It starts with the uptake of extracellular glucose and proceeds within the cell's cytosol. It is a ten-step process by which cells split one glucose molecule into two pyruvate molecules, yielding also two ATP and two NADH molecules. Pyruvate can be converted into lactate as the end product for extracellular secretion, or oxidised to yield the acetyl group of acetyl-coenzyme A, which enters the TCA cycle, as part of cellular respiration. Although glycolysis is not highly efficient in energetic terms (net production of two ATP molecules per each glucose molecule oxidised), it plays essential roles in generating NADH molecules, used as electron carriers in multiple biochemical reactions, and in providing intermediates for biosynthetic purposes. Accordingly, rapidly proliferating cells (such as tumour cells) are often characterised by intense glycolytic activity.[25]

Another important pathway of glucose metabolism is *gluconeogenesis*, defined as the endogenous production of glucose from non-carbohydrate precursors, mainly lactate, certain amino acids and glycerol. These precursors are first converted into pyruvate, either directly (e.g. lactate and alanine) or through TCA cycle intermediates (e.g. oxaloacetate from aspartate) or enter the pathway at later stages (e.g. glycerol converted to dihydroxyacetone phosphate). Gluconeogenesis and glycolysis are usually reciprocally regulated so that one pathway is minimally active while the other is highly active.[26]

The TCA cycle is a series of eight enzyme-catalysed reactions which take place in the mitochondria and form a key part of cellular aerobic respiration.[27] Acetyl-CoA from glycolysis-derived pyruvate, fatty acid oxidation, or amino acid metabolism, enters the TCA cycle by donating its acetyl group to the four-carbon oxaloacetate, forming the six-carbon citrate, in a condensation reaction. Next, in reversible steps, citrate is dehydrated yielding cis-aconitate, which is hydrated to form isocitrate. The oxidative decarboxylation of isocitrate, requiring NAD(P)+ as the electron acceptor, then forms α-ketoglutarate, NAD(P)H and $CO_2$. Another oxidative decarboxylation follows, in which α-ketoglutarate is converted to succinyl-CoA and $CO_2$. In this step, $NAD^+$ also acts as the electron acceptor. Then, succinate is reversibly formed through the hydrolysis of the thioester bond in succinyl-CoA. This reaction has intermediate steps where the enzyme is phosphorylated, and then the phosphoryl group is transferred to ADP/GDP to form ATP/GTP (substrate-level phosphorylation). Succinate is then reversibly oxidised to fumarate, and $FADH_2$ is formed from FAD. Following the reversible hydration of fumarate to malate, the latter is finally oxidised to oxaloacetate, with production of NADH, in a reversible step. NADH and $FADH_2$ are two major products of the TCA cycle, which transfer electrons to molecular oxygen (reducing it to water) in a set of membrane proteins known as the electron transport chain. This leads to the formation of a proton gradient across the inner mitochondrial membrane, which powers the synthesis of ATP. Overall, this process of oxidative phosphorylation generates 26 (or 28) of the 30 (or 32) ATP molecules formed when one glucose molecule is completely oxidised to carbon dioxide and water. Notably, the tight coupling between electron transfer (with recycling of electron donors back to the TCA cycle) and ADP phosphorylation to ATP ensures that the rate of the TCA cycle matches the need for ATP.[28] The TCA cycle also has a role in anabolism, as it provides intermediates for biosynthesis, such as succinyl-CoA for the formation of porphyrins, α-ketoglutarate or oxaloacetate for the synthesis of amino acids, and citrate for the formation of fatty acids. This anabolic role is usually sustained

by replenishment of TCA cycle intermediates by anaplerosis, mainly using amino acids as substrates,[29] in order to keep the cycle operating.

The analysis of the metabolic profiles of the aqueous extract of MNT-1 cells treated with [Cho][HCA]ILs and KA showed that the exposure to these compounds alter the levels of some metabolites involved in glycolysis and TCA cycle (Figure 5.12). The citrate content decreased significantly in the presence of all compounds following the order [Cho][*p*-Coum] > [Cho][Fer] > [Cho][Caf] ≈ KA, suggesting a possible intensification of the TCA cycle. A statistically significant decreases in intracellular lactate content was found only in cells treated with [Cho][*p*-Coum] and [Cho][Fer], probably due to the conversion of lactate into pyruvate and thus the increased demand for pyruvate by increased TCA cycle activity. Additionally, increased levels of $NAD^+$ were observed only in [Cho][Caf] treated cells.

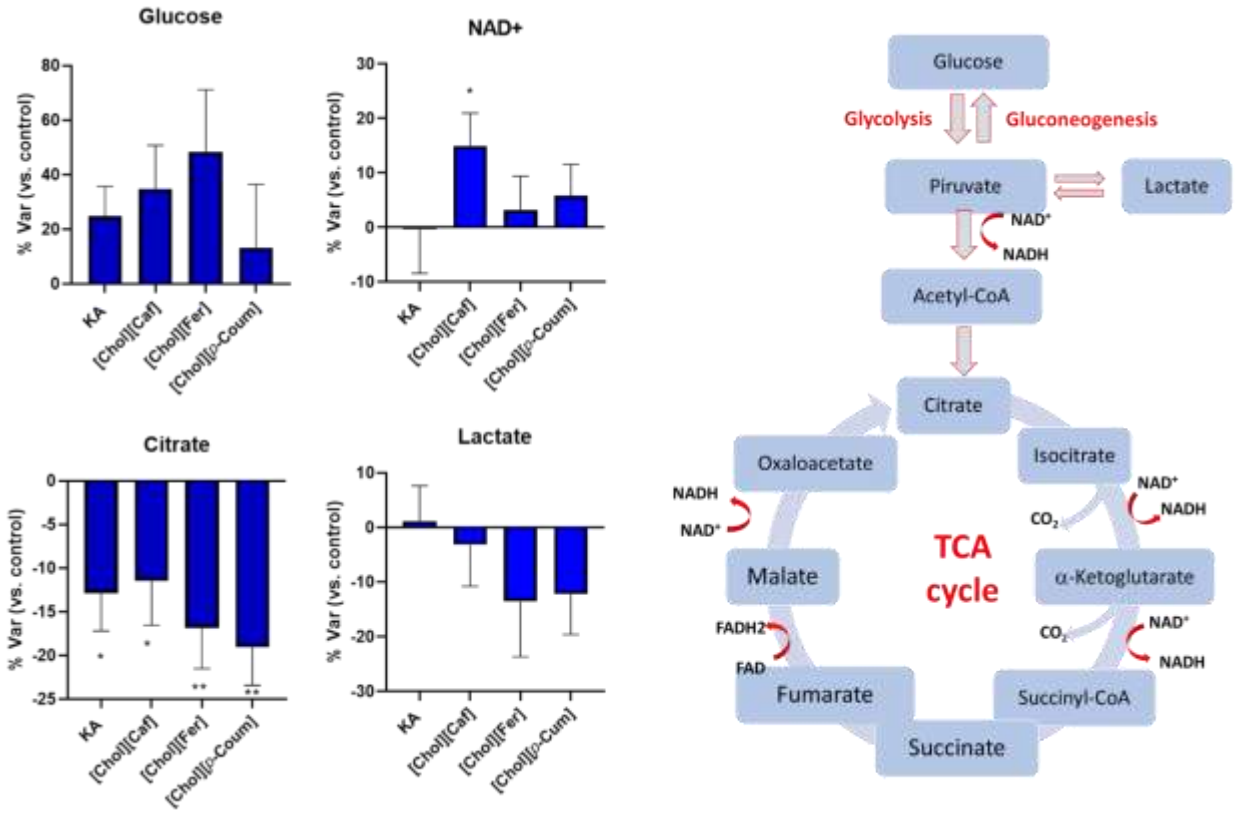


**Figure 5.12** Relative variation of metabolites related to the TCA cycle and glycolysis in the aqueous extract of treated MNT-1 cells compared to controls. Shown are means ± standard deviation (n=6). * *p*-value < 0.05; ** *p*-value < 0.01.

***Amino acid metabolism.*** AA are essential nutrients for the *in vitro* cultivation of cells. They are used as the basic building blocks of proteins as well as for the sysnthesis of non-essential amino acids and other metabolic intermediates. Cancer cells, in particular, have an increased requirement for amino acids to meet their rapid proliferation.

Comparing the content of intracellular amino acids evidence the occurrence of a mild significant decrease (< 20%) of alanine, valine, leucine, isoleucine, serine, and tyrosine only for the cells treated with [Cho][*p*-Coum] and [Cho][Fer] (Figure5.13). BCAAs play an important role in energy homeostasis and nutrient signaling as well as nitrogen balance.[30,31] Several recent studies have found BCAA metabolism to have an important role in cancer metabolism depending on both the tissue-of-origin and the cancer genetics.

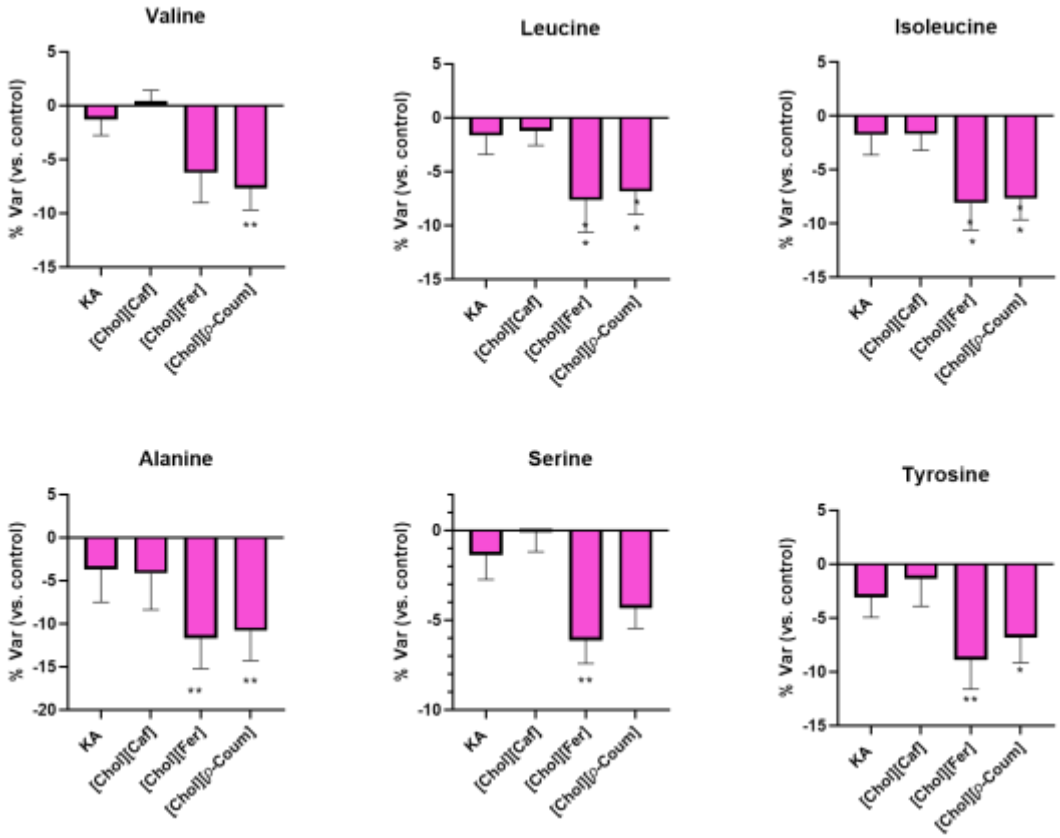


**Figure 5.13**. Relative variation of amino acids in the aqueous extract of treated MNT-1 compared to respective controls. Shown are means ± standard deviation (n=6). **p*-value < 0.05; ***p*-value < 0.01.

Of note is the significant decrease in intracellular serine levels occurring upon exposure to [Cho][Fer]. Serine has a central role for the biosynthesis of many molecules, including

sphingolipids and phospholipids, and is a precursor of the nonessential amino acids glycine and cysteine and headgroup precursor of membrane phospholipids. Cells can obtain serine by either import from the extracellular environment or intracellular synthesis from glucose. Serine metabolism is frequently dysregulated in cancers and its increased biosynthesis is one of many metabolic changes that have been reported in cancer cells.[32] It is therefore likely that the lower serine content in cells treated with [Cho][Fer] compared to controls indicates the involvement of this compound in the related metabolic pathway.

***Choline metabolism.*** Choline (Cho) is an essential nutrient that is derived from the diet. It is the precursor of phosphocholine (PC) that, in turn, is both a precursor and a breakdown product of phosphatidylcholine which forms the characteristic bilayer structure of cellular membranes and regulates membrane integrity. Abnormal Cho metabolism is reported as a common feature in different types of cancer, with consequent alterations in the levels of cho-derivatives compounds, including PC.[33] Being elevate in tumoral cells, both Cho and PC are being exploited for non-invasive detection in cancer diagnosis by using magnetic resonance spectroscopy (MRS) or positron emission tomography (PET)[34] as well as for monitoring the therapeutic response of tumours since treatment with conventional chemotherapeutic agents results in a decrease of total Cho levels. Nevertheless, despite the substantial progresses made in understanding the molecular mechanisms responsible of the aberrant choline metabolic profile associate to cancer, a comprehensive understanding has not been reached yet.

Under the present experimental conditions, two sources of Cho are present: the cell culture media whose ChoCl is a standard component, and the HCA-derivatives, cholinium being used as cation in the formulation. Compared to controls, a significant increase in both intracellular Cho and PC was observed in all [Cho][HCA][ILs] treated cells (Figure 5.14). Differentely, in the presence of KA, the levels of Cho significantly decreased, while that of PC didn't significantly change. Considering that cancer is characterized by an elevation of total choline-containing compounds, the down-regulation of intracellular level of Cho upon cell treatment with KA could be taken as an indication of reduced cell proliferation. Accordingly, the up-regulation of Cho and PC following exposure to [Cho][HCA] ILs may suggest an adaptive response of cells to continue proliferating, likely due to an increased absorption of Cho through the cellular membrane promoted by a higher Cho concentration in the medium.

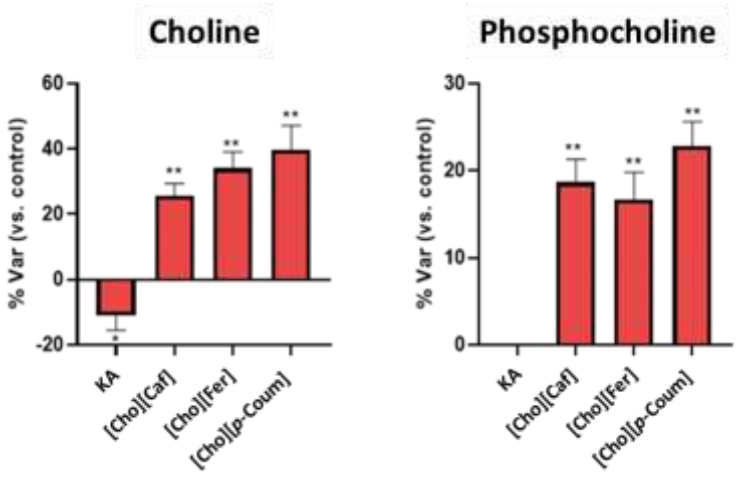


**Figure. 5.14** Relative variations of intracellular choline and phosphocholine in the aqueous extracts of treated MNT-1 cells compared to controls (untreated cells). Shown are means ± standard deviation (n=6). * *p*-value < 0.05; ** *p*-value < 0.01.

However, it is worth mentioning that variations in phospholipids concentration can also indicate changes of cell membrane composition and permeability, and thus an alteration of the normal physiological functions of cells.[35] Therefore, given the role of PC as constituent of membrane phospholipids, it can not be excluded that the increase of PC observed upon cell tratments with [Cho] [HCA] ILs may be a consequence of membrane degradation.

***Myo-inositol and taurine.*** Myo-inositol (MI) is an essential growth factor for both normal and malignant human cells, playing different important functions. Its increased requirements in proliferating cells has been suggested to be due to greater phospholipid bio-synthesis for increased membrane production. In addition, in the free state, MI behaves as an osmolyte like taurine (Tau), a known osmoregulatory amino acid associated with maintaining cell redox homeostasis[36]

The intracellular content of MI exhibited a significant decrease compared to controls only upon exposure to cholinium-salts. In parallel, an opposite trend was followed by Tau (Figure 5.15). Intracellular MI depletion was observed to be associated with intracellular osmotic stress: an increase in intracellular osmolarity induces MI release, thus leding to intracellular MI depletion.[37] Therefore, being both MI and Tau key organic osmolyets, it is likely that the inverse

relationship observed between their intracellular trends in the presence of [Cho][HCA] ILs is an indication of possible osmotic alterations.

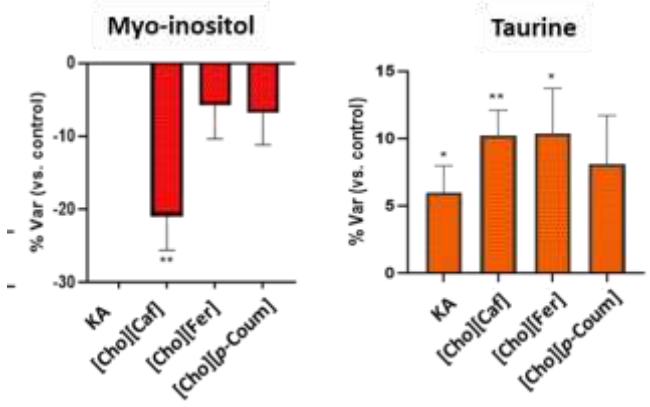


**Figure. 5.15** Relative variations of intracellular myo-inositol and taurine in the aqueous extracts of treated MNT-1 cells compared to controls (untreated cells). Shown are means ± standard deviation (n=6). * *p*-value < 0.05; ** *p*-value < 0.01.

***Creatine metabolism.*** Creatine metabolism is intimately connected with ATP requirements.[38] Creatine, along with its metabolic derivatives, forms an important system for efficient energy buffering during times of high ATP demand of rapidly growing cells, such as malignant cells. Phosphorylation of creatine by creatine kinase generates phosphocreatine which can be used in the reverse direction to phosphorylate ADP to ATP, Thus, phosphocreatine accumulation serves as a high-energy carrier to regenerate levels of ATP.

The analysis of cellular metabolome evidenced that the exposure to [Cho][HCA]ILs modulated the levels of energy-carrying molecules (Figure 5.16). In particular, a decrease of both ATP and phosphocreatine was observed only in the presence of [Cho][Caf], Differently, in the presence of [Cho][Fer] and [Cho][*p*-Coum] only creatine was reduced and upon KA exposure only phosphocreatine decreased suggesting a possible involvement of the phosphocreatine−creatine kinase shuttle system in the bioenergetic shift of malignant cells.

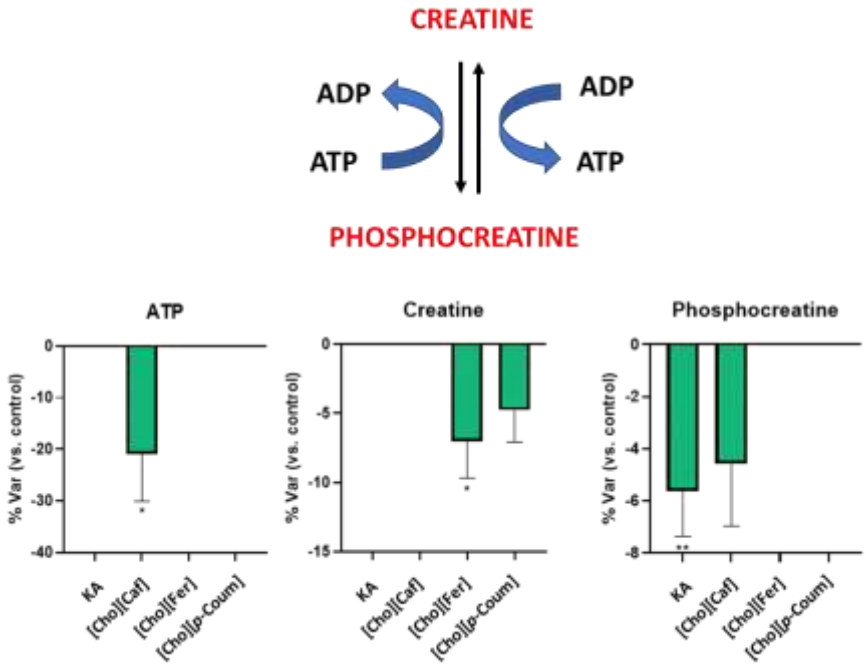


**Figure 5.16** Relative variation of metabolites related to creatine metabolism in the aqueous extract of treated MNT-1 cells compared to controls. Shown are means ± standard deviation (n=6). * *p*-value < 0.05; ** *p*-value < 0.01.

## 5.6 Conclusions

Overall, the $^{1}$H NMR analysis of the aqueous and lipid extracts of MNT-1 cells and culture medium evidenced the occurrence of cell metabolic modulations upon exposure of [Cho][HCA] ILs, although to a different extent depending on the nature of the hydroxycinnamate. Various were the effects observed in the presence of ILs compared to controls and KA-treated cells: (i) the enhancement of Cho and PC contents, likely reflecting a shift of choline metabolism; ii) an opposite trends for myo-inositol and taurine, suggesting possible osmotic alterations; iii) a marked decrease in lactate and citrate levels, indicative of an intensification of the TCA cycle; iv) a lower concentration of intracellular amino acids. No important alterations of the cell lipid composition were observed in the presence of any compounds. While this metabolomics study at the present stage does not offer a complete mechanistic picture of the cellular adaptation to the action of cholinium-based hydroxycinnamate ILs, the evidence that [Cho][HCA] ILs have a measurable influence on the metabolomic profile

of the MNT-1 cell line provides bases for the development of future investigations to improve the current understanding of the biological activity of these compounds.

## 5.7 Experimental section

### *5.7.1 Cell culture*

Human MNT-1 melanoma cells were kindly provided by Dr. Manuela Gaspar (iMed.ULisboa, Portugal). MNT-1 were cultured in Dulbecco's modified Eagle's medium (DMEM) supplemented with 10% fetal bovine serum (FBS) and 1% l-glutamine, penicillin–streptomycin and fungizone (Life Technologies, Grand Island, NY, USA). Cells were incubated in a humidified atmosphere at 37 °C and 5% $CO_2$. Cell morphology was observed using an inverted microscope Nikon Eclipse 80i (Nikon, Tokyo, Japan).

### *5.7.2 Cell Exposure for Metabolomics Assays*

MNT-1 cells were seeded at a density of 2.5 × 105 cells/ml onto 10 cm diameter Petri dishes and allowed to adhere for 24 h. Then, the medium was replaced by fresh complete medium containing [Chol][Caf], [Chol][Fer], [Chol][p-Coum] or the reference compound KA at a final concentration of 200 μM. This concentration was selected based on the MTT viability results (Chapter 4), causing a small reduction in cell viability (~15–20%) in 48 hours. Fresh medium was added to control cells. In all cases, medium and cell extract samples were collected after 48 h incubation period. Three independent assays were typically performed for each exposed substance.

### *5.7.3 Cell culture supernatants*

Medium aliquots were collected from each petri-dish (including medium without cells incubated under the same conditions) and centrifuged at 1000 xg for 10 min. The supernatants were then collected and stored at -80ºC. To remove interfering proteins, thawed supernatants were then subjected to a protein-precipitation protocol described by Kostidis.[42] Briefly, 600 mL of cold methanol 100% (v/v) at -80ºC were added to 300 mL of supernatant (1:3 proportion). The aliquots were then kept at -20ºC for 30 min, after which they were centrifuged at 13000 x g

for 20 min. The supernatant was then transferred to another vial, vacuum dried (SpeedVac, Eppendorf) and stored at -80ºC until NMR acquisition.

At the time of analysis, the dried samples were resuspended in 600 mL of deuterated phosphate buffer (PBS 100 mM, pH 7) containing 0.1 mM 3-(trimethylsilyl) propanoic acid (TSP-d4), and 550 mL of each sample were then transferred to 5 mm NMR tubes.

### *5.7.4 Cell extracts*

To collect cell samples, the remaining medium was discarded from each dish and the cells washed 4 times with 10 mL of cold PBS. The intracellular metabolites were then extracted using a biphasic extraction protocol with methanol:chloroform:water (1:1:0.7). After adding1 mL of cold methanol (80% v/v) to quench metabolic activity of the cells, cells were scraped off the dish, transferred to a glass vial with 150 mg of glass beads (to aid in cell disruption) and vortexed for 2 min. Next, 400 mL of cold chloroform (-20 ºC) was added to the tube and vortexed (2 min), followed by addition of 400 mL of chloroform and 360 mL cold milli-Q water. The samples were vortexed, allowed to rest on ice for 20 min and centrifuged at 3000 xg for 10 min. The lower organic phase was transferred to an amber glass vial and the remaining sample subjected to another chloroform addition (400 mL) and centrifugation. The resulting organic phase was then added to the previous amber vial, while the top aqueous phase was transferred to a microcentrifuge tube. Finally, the polar extracts were vacuum dried, and lipophilic extracts were dried under a nitrogen flow, after which they were stored at -80ºC. At the time of NMR analysis, the dried samples of the polar phases were resuspended in 600 mL of deuterated phosphate buffer (PBS 100 mM, pH 7) containing 0.1 mM TSP-d4, and 550 mL of each sample were then transferred to 5 mm NMR tubes. A summarized schematic representation of the experimental protocol used can be found in Figure 5.17.

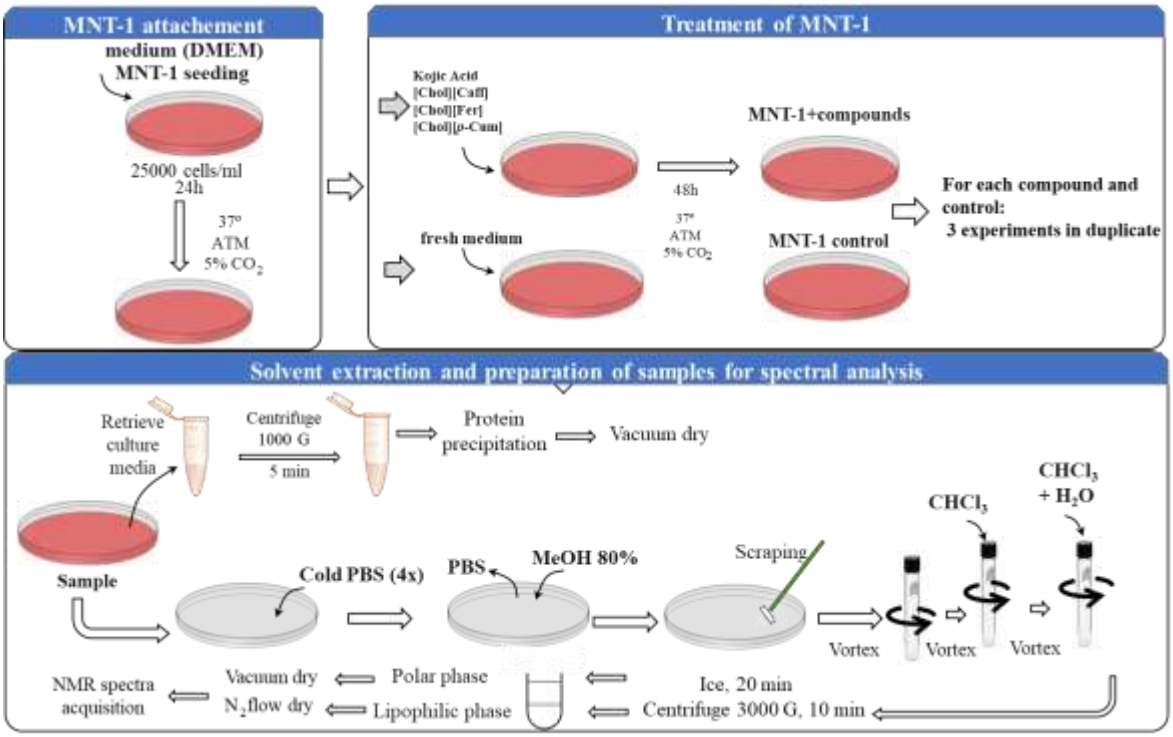


**Figure 5.17** Cells treatment, extraction and preparation of dry extract samples for metabolomics

### *5.7.5 $^{1}H$ NMR Spectroscopy*

All samples were analyzed in a Bruker Avance III HD 500 NMR spectrometer (University of Aveiro, PT National NMR Network) operating at 500.13 MHz for 1H observation, at 298 K. Standard 1D 1H spectra with water presaturation (pulse program 'noesypr1d', Bruker library) were recorded with 32k points, 7002.801 Hz spectral width, a 2 s relaxation delay and 512 scans (for media/ polar extracts, respectively). Two-dimensional NMR spectra were also recorded for selected samples to aid metabolite identification, namely $^{1}$H-$^{1}$H TOCSY, J-resolved and $^{1}$H-$^{13}$C HSQC spectra. Metabolite assignment was based on matching 1D and 2D spectral information to reference spectra available in Chenomx, BBIOREFCODE-2–0–0 (Bruker Biospin, Rheinstetten, Germany) and HMDB.192,193

Spectral processing was carried out using TopSpin 4.0.3 (Bruker Biospin, Rheinstetten, Germany). Each FID was multiplied by a cosine function (with a shift sine bell, ssb, value of 2), zero filled to 64k data points and Fourier-transformed. The resulting spectra were then manually phased, baseline corrected and calibrated to the TSP (δ 0 ppm) or the glucose (δ 5.235 ppm) signals, in media or polar extracts spectra, respectively.

### *5.7.6 Multivariate analysis of spectral data*

After processing, the spectra were visualized and prepared for multivariate analysis in Amix Viewer 3.9.15 (Bruker Biospin, Rheinstetten, Germany). Each spectrum was normalized by its total area, excluding the water-suppression region and some contaminant signals, such as chloroform, ethanol and methanol. The normalized data were then organized into matrices ('bucket tables'), containing the information on the signals intensity (variables) at each chemical shift in the different spectra (observations).

Data matrices were uploaded into SIMCA-P 11.5 (Umetrics, Umeå, Sweden), where PCA (Principal Component Analysis) and PLS-DA (Partial Least Squares- Discriminant Analysis) were applied. After testing different scaling types, unit-variance scaling (UV), in which each column (containing the intensities at a particular chemical shift) is divided by its respective standard deviation, was chosen. This procedure gives equal variance to all variables, allowing for variations in less abundant metabolites to have the same weight in multivariate models as more intense signals. The results were then visualized through factorial coordinates ('scores') and factorial contributions ('loadings') colored according to variable importance to projection (VIP). For PLS-DA models, $Q^2$ and $R^2$ values, respectively reflecting predictive capability and explained variance, obtained from sevenfold internal cross validation, were used to assess the robustness of class discrimination.

### *5.7.7 Spectral integration and univariate analysis*

Spectral integration of selected signals was carried out in Amix-Viewer 3.9.15 (Bruker Biospin, Rheinstetten, Germany), to provide a quantitative measurement of metabolic variations. Signals representative of each metabolite that were found to be relatively free of overlap were integrated and normalized by the total spectral area. For each metabolite, the percentage of variation in treated samples was calculated relative to respective controls, along with the effect size (ES) and the statistical significance (p-value, as determined by the t-student test). The variations with medium-large magnitude ($|ES|>0.5$) were expressed in heatmaps colored as a function of % of variation, using the R-statistical software

## References


1. Berry, D. P.; Meade, K. G.; Mullen, M. P.; Butler, S.; Diskin, M. G.; Morris, D.; Creevey, C. J. (2011). The integration of 'omic' disciplines and systems biology in cattle breeding. Animals, **5**, 493–505.
2. Dettmer, K. and Hammock, B. D. Metabolomics - A new exciting field within the 'omics' sciences. (2004). Environmental and Health Perspective, **112**, 396–397.
3. Fiehn, O. (2002). Metabolomics - The link between genotypes and phenotypes. Plant Molecular Biology, **48**, 155–171.
4. Nicholson, J. K., Lindon, J. C. and Holmes, E. (1999). 'Metabonomics': Understanding the metabolic responses of living systems to pathophysiological stimuli via multivariate statistical analysis of biological NMR spectroscopic data. Xenobiotica, **29**, 1181–1189
5. Fernández-Peralbo, M. A. and Luque de Castro, M. D. (2012). Preparation of urine samples prior to targeted or untargeted metabolomics mass-spectrometry analysis. TrAC - Trends Analytical Chemistry, **41**, 75–85.
6. Bingol, K. (2018). Recent Advances in Targeted and Untargeted Metabolomics by NMR and MS/NMR Methods. High-Throughput, **7**, 9.
7. Oldiges, M. et al. (2007). Metabolomics: Current state and evolving methodologies and tools. Applied Microbiology and Biotechnology, **76**, 495–511.
8. P. Krishnan, N. J. Kruger, R. G. Ratcliffe, (2005). Metabolite fingerprinting and profiling in plants using NMR, Journal of Experimental Botany, 56, 410, 255–265.
9. Lenz, E. M. and Wilson, I. D. (2007). Analytical Strategies in Metabonomics. Journal of Proteome Research, **6**, 443–458
10. Markley, Joh L; Brüschweiler, Rafael; Edison, Arthur S; Eghbalnia, Hamid R; Powers, Robert; Raftery, Daniel; Wishart, David S. (2017). The future of NMR-based metabolomics. Current Opinion in Biotechnology, **43**, 34–40.
11. Wold, S., Esbensen, K. and Geladi, P. (1987). Principal Component Analysis. Chemometrics and intelligent laboratory systems, **2**, 37–52.
12. Henningsson, M., Sundbom, E., Armelius, B. and Erdberg, P. (2001). PLS model building: A multivariate approach to personality test data. Scandinavian Journal of Psychology, **42**, 399-409.
13. Golland, P., Liang, F., Mukherjee, S. and Panchenko, D. (2005). Permutation Tests for

Classification. Lecture Notes in Computer Science, Springer, Berlin, Heidelberg. **3559**, 501–502.

14. León, Z., García-Cañaveras, J. C., Donato, M. T. and Lahoz, A. (2013). Mammalian cell metabolomics: Experimental design and sample preparation. Electrophoresis **34**, 2762–2775.
15. Čuperlović-Culf, M., Barnett, D. A., Culf, A. S. and Chute, I. (2010). Cell culture metabolomics: Applications and future directions. Drug Discovery Today, **15**, 610–621.
16. Duarte, I. F., Lamego, I., Rocha, C. and Gil, A. M. (2009). NMR metabonomics for mammalian cell metabolism studies. Bioanalysis, **1**, 1597–1614.
17. Teng, Q., Huang, W., Collette, T. W., Ekman, D. R. and Tan, C. (2009). A direct cell quenching method for cell-culture based metabolomics. Metabolomics, **5**, 199–208
18. Dettmer, K., Nürnberger, N., Kaspar, H. et al. (2011). Metabolite extraction from adherently growing mammalian cells for metabolomics studies: Optimization of harvesting and extraction protocols. Analytical and Bioanalytical Chemistry, **399**, 1127–1139.
19. Dietmair, S., Timmins, N. E., Gray, P. P., Nielsen, L. K. and Krömer, J. O. (2010). Towards quantitative metabolomics of mammalian cells: Development of a metabolite extraction protocol. Analytical Biochemistry, **404**, 155–164
20. Martineau, E., Tea, I., Loaëc, G., Giraudeau, P. and Akoka, S. (2011). Strategy for choosing extraction procedures for NMR-based metabolomic analysis of mammalian cells. Analytical and Bioanalytical Chemistry, **401**, 2133–2142.
21. Santana-Filho, A. P. De et al. (2017). NMR metabolic fingerprints of murine melanocyte and melanoma cell lines: Application to biomarker discovery. Scientific Reports, **7**, 1–9
22. Neill, L. A. J. O., Kishton, R. J. and Rathmell, J. (2016). A guide to immunometabolism for immunologists. Nature Reviews Immunology.
23. Kanehisa, M., Sato, Y., Kawashima, M., Furumichi, M. and Tanabe, M. (2016). KEGG as a reference resource for gene and protein annotation. Nucleic Acid Research. **44**, 457–462.
24. Li, C., Zhang, G., Zhao, L., Ma, Z. and Chen, H. (2016). Metabolic reprogramming in cancer cells: Glycolysis, glutaminolysis, and Bcl-2 proteins as novel therapeutic targets for cancer. World Journal of Surgical Oncology, **14**, 1–7.
25. Mazurek, S. (2007). Tumor Cell Energetic Metabolome. In Molecular System

Bioenergetics, V. Saks (Ed.).

26. Zhang, X., Yang, S., Chen, J. and Su, Z. Unraveling the Regulation of Hepatic Gluconeogenesis. Frontiers in Endocrinology, **9**, 1–17 (2019).
27. Raimundo, N., Baysal, B. E. and Shadel, G. S. (2011). Revisiting the TCA cycle : signaling to tumor formation. Trends in Molecular Medicine, **17**, 641–649.
28. Bonora, M. Patergnani, S., Rimessi, A., Marchi, E., Suski, J. M., Bononi, A., Giorgi, C., Marchi, S., Missiroli, S., Poletti, F., Wieckowski, M. R. and Pinton, P. (2012). ATP synthesis and storage. Purinergic Signal, **8**, 343–357.
29. Papers, J. B. C., Owen, O. E., Kalhan, S. C. and Hanson, R. W. (2002). The Key Role of Anaplerosis and Cataplerosis for Citric Acid Cycle Function. Journal of Biological Chemistry, **277**, 30409–30412.
30. Conway, M. E. and Hutson, S. M. (2016). BCAA Metabolism and NH3 Homeostasis. Advances in neurobiology, **13**.
31. Yoon, M. S. (2016). The emerging role of branched-chain amino acids in insulin resistance and metabolism. Nutrients, **8**. 405.
32. Mattaini, K. R., Sullivan, M. R. and Vander Heiden, M. G. (2016). The importance of serine metabolism in cancer. Journal of Cell Biology **214**, 249–257
33. Glunde, K., Jacobs, M. A. and Bhujwalla, Z. M. (2006). Choline metabolism in cancer : implications for diagnosis and therapy. Expert Review of Molecular Diagnostic, **6**, 821–829.
34. Glunde, K., Bhujwalla, Z. M. and Ronen, S. M. (2011). Choline metabolism in malignant transformation. Nature Review Cancer, **11**, 835–847
35. Zong, L., Xing, J., Liu, S., Liu, Z. and Song, F. (2018). Cell metabolomics reveals the neurotoxicity mechanism of cadmium in PC12 cells. Ecotoxicology and Environmental Safety, **147**, 26–33.
36. Schaffer, S., Takahashi, K. and Azuma, J. (2000). Role of osmoregulation in the actions of taurine. Amino Acids **19**, 527–546.
37. Croze, M. L. and Soulage, C. O. (2013). Potential role and therapeutic interests of myo - inositol in metabolic diseases. Biochimie, **95**, 1811–1827
38. Bessman, S. (1985). The Creatine-Creatine Phosphate Energy Shuttle. Annual Review of Biochemistry, **54**, 831–862.
39. Salih J. Wakil, James K. Stoops, A. and Joshi, V. C. (1983). Fatty acid synthesis and its

regulation. Annual Review of Biochemistry, **53**, 537–579.

40. Salati, L. M. and Goodridge, A. G. (1996). Fatty acid synthesis in eukaryotes. Biochemistry of Lipids, Lipoproteins and Membranes **31**, (Elsevier Masson SAS).
41. Hopperton, K. E., Duncan, R. E., Bazinet, R. P. and Archer, M. C. (2014). Fatty acid synthase plays a role in cancer metabolism beyond providing fatty acids for phospholipid synthesis or sustaining elevations in glycolytic activity. Experimental Cell Research, **320**, 302–310
42. Kostidis, S., Addie, R. D., Morreau, H., Mayboroda, O. A. and Giera, M. (2017). Quantitative NMR analysis of intra- and extracellular metabolism of mammalian cells: A tutorial. Analitica Chimica Acta, **980**, 1–24.

# 6

# General Conclusions

## 6.1 Conclusions and perspectives

The main purpose of this thesis was to obtain hydroxycinnamic derivatives with improved water solubility properties compared to the acid parents without losing the antioxidant properties and their safety for their possible use in the pharmaceutical or cosmetic field.

In general terms, the results obtained were very satisfactory.

By using a simple neutralization reaction, in line with the principles of the green chemistry, six cholinium hydroxycinnamates were obtained in quantitative yields and with high purity confirmed by IR, NMR spectroscopy and elemental analysis.

By virtue of the appropriate combined measurements of UV spectrophotometry and potentiometry, it was possible to ascertain an improvement of solubility which even exceeded those of the starting acid compounds by 300 times suggesting that synthesis of [Cho][HCA] ILs could be a useful method to overcome the solubility problems of HCAs. The improvement of solubility and the satisfactory stability of salts implies the possibility to develop HCA derivatives with higher bioavailability and good shelf-life.

The six [Cho][HCA] ILs have been studied for their thermal properties and although they proved to be less stable to heat than the starting acids, they still managed to preserve values above 100 °C which are compatible for their incorporation and use in pharmaceutical and cosmetic forms.

[Cho][HCA] ILs were screened for their antioxidant activity by using experimental DPPH assay and theoretical calculation (DFT). The experimental results showed a slight improvement in the antioxidant activity for all cholinium salts compared to HCAs. The same order of scavenging activity was observed for both acids and salts.

DFT calculations performed on all the intermediates of the considered oxidation paths (HAT, SET-PT and SPLET) allowed to rationalize the experimental trends of the antioxidant activity observed for DPPH assay for both classes of $HCAs^-$ and HCAs. Comparison of the calculated thermodynamic parameters typically associated with the above-mentioned mechanism (BDE, IP, PDE, PA and ETE) with the experimental findings indicated that for all $HCAs^-$ and HCAs, the HAT mechanism is favored over SPLET and SET-PT in ethanol. A similar result is obtained in water solvent only for CAFA, o-CA and *p*-CA. Differently, for SA, FA and *m*-CA the thermodynamic parameters for HAT and SPLET are similar, thus indicating that both

mechanisms are plausible. In water solvent for all $HCAs^-$, SPLET mechanism is thermodynamically favored.

The thermodynamic parameters for $HCAs^-$ are found to be generally lower compared to the parent acids, thus explaining their improved antioxidant capability.

The computational results obtained using the 6-311++G(d,p) basis set, with the widely employed density functional B3LYP and those obtained with the more recently developed M06-2X functional lead to the same conclusions.

The cytotoxic effects of [Cho][HCA] ILs were evaluated by MTT assay. The MTT results pointed out the safety of all the salts. Only [Cho][Caf] exhibited marginal cytotoxicity at the highest dose.

The promising antioxidant properties proved by both experimental and theoretical analysis together with the absence or low cytotoxicity suggest that are valid candidates as an alternative to HCAs in pharmaceutical field.

The effects on mushroom tyrosinase activity and the melanogenesis in human melanoma cells of [Cho][Caf], [Cho][Fer] and [Cho][*p*-Coum] were evaluated and compared with the effects of CAFA, FA and *p*-CA. Although HCAs are reported to modulating the tyrosinase enzyme their low solubility in water represent a limit for their applications in food, cosmetic and pharmaceutical fields. The findings indicate that the exposition of MT with [Cho][Caf] led to improved kinetics parameters compared with CAFA while a higher decrease in tyrosinase activity is induced by [Cho][Fer] and [Cho][p-Coum] than the corresponding acid precursors.

Concerning the effects of cholinium ILs on the melanogenesis in MNT-1 cells, [Cho][*p*-Coum] exhibited the best depigmenting effect, even overcoming the reference compound KA.

Although the biologic impact of [Cho][Caf], [Cho][Fer] and [Cho][*p*-Coum] in human melanogenesis deserves further investigations, in the light of the present results, these compounds may be potential chemicals to treat dermatological diseases. Thus, the importance of these three HCA derivatives as new agents for skin disease worths to be elucidated in future studies.

In order to deeply investigate on the biological effects at molecular level of [Cho][Caf], [Cho][Fer] and [Cho][p-Coum] I choose the NMR based cell metabolomic as a complementary tool. Compared to conventional cytotoxicity studies typically based on a single pre-established endpoint, this achievement has great potential for providing new mechanistic insights.

The effects induced by [Cho][HCA] ILs exposure on cellular metabolism were explored by $^{1}$H NMR analysis of the aqueous and lipid extracts of MNT-1 cells and culture medium. The results evidenced the occurrence of significant metabolic alterations in treated cells compared to controls at a different extent depending on the nature of the hydroxycinnamate. In general, the changes in the Cho and PC contents suggested alteration in membrane constituent metabolism, while modifications in the myo-inositol and taurine levels pointed out possible osmotic alterations. The marked decrease in lactate and citrate levels could reflect an intensification of the TCA cycle, while lower concentrations of intracellular amino acids could be ascribed to an inhibition in their synthetic pathways. No significant alterations of the cell lipid composition were observed in the presence of any compounds. The metabolomics study in the present thesis can be viewed as an initial step in the quest for mechanistic answers, which should be followed by more targeted investigations to confirm the hypotheses generated. On the other hand, one should be aware that metabolite levels reflect pools resulting from the interplay between different biochemical processes. The evidence that [Cho][HCA] ILs have a measurable influence on the metabolomic profile of the MNT-1 cell line provides bases for the development of future investigations to improve the current understanding of the biological activity of these compounds chosen after careful dose-response.

## List of pubblications

### Published/accepted for Publication

I. *Theoretical and Experimental Study of the Excess Thermodynamic Properties of Highly Nonideal Liquid Mixtures of Butanol Isomers + DBE*. Leon de Villiers Engelbrecht, Riccardo Farris, Tudor Vasiliu, Monica Demurtas, Alessandra Piras, Flaminia Cesare Marincola, Aatto Laaksonen, Silvia Porcedda and Francesca Mocci. Journal of Physical Chemistry B, 2021; 125:587-600.

II. *Cholinium-based Ionic Liquids from hydroxycinnamic acids as new promising bioactive agents: a combined experimental and theoretical investigation*. Monica Demurtas, Valentina Onnis, Paolo Zucca, Antonio Rescigno, Joanna Izabela Lachowicz, Leon Engelbrecht, Mariella Nieddu, Guido Ennas, Alessandra Scano, Francesca Mocci and Flaminia Cesare Marincola. ACS Sustainable Chemistry & Engineering 2021; 9, 7: 2975-2986.

III. *Benzofuran hydrazones as potential scaffold in the development of multifunctional drugs: Synthesis and evaluation of antioxidant, photoprotective and antiproliferative activity*. Monica Demurtas (first co-author), Anna Baldisserotto, Ilaria Lampronti, Davide Moi, Gianfranco Balboni, Silvia Verturani, Stefano Manfredini and Valentina Onnis. European Journal of Medicinal Chemistry. 2018; 156: 118-125.

IV. *Indole derivatives as multifunctional drugs: Synthesis and evaluation of antioxidant, photoprotective and antiproliferative activity of indole hydrazones*. Monica Demurtas, Anna Baldisserotto, Ilaria Lampronti, Davide Moi, Gianfranco Balboni, Silvia Verturani, Stefano Manfredini and Valentina Onnis. Bioorganic Chemistry. 2019; 85: 568-576.

V. *Synthesis and evaluation of antioxidant and antiproliferative activity of 2-arylbenzimidazoles*. Monica Demurtas (first co-author), Anna Baldisserotto, Ilaria Lampronti, Massimo Tacchini, Davide Moi, Gianfranco Balboni, Silvia Verturani, Stefano Manfredini and Valentina Onnis. Bioorganic Chemistry. 2020; 94: 103396.

VI. *In-Vitro Evaluation of Antioxidant, Antiproliferative and Photo-Protective Activities of Benzimidazolehydrazone Derivatives*. Monica Demurtas (first co-author), Anna Baldisserotto, Ilaria Lampronti, Massimo Tacchini, Davide Moi, Gianfranco Balboni, Silvia Verturani, Stefano Manfredini and Valentina Onnis. Pharmaceuticals. 2020; 13(4), 68.

**Manuscript in preparation**

VII. *Cholinium—based Ionic Liquids from hydroxycinnamic acids: anti-tyrosinase and anti-melanogenic activities and impact on the metabolome of human MNT-1 melanoma cells*. Demurtas et. Al (in preparation)